Aus dem Institut für Kardiogenetik

der Universität zu Lübeck

Direktorin: Prof. Dr. rer. nat. J. Erdmann

Expression of Human CAD-Associated Risk Genes in Blood of Hypercholesterolemic Zebrafish (*Danio rerio)*

Inauguraldissertation
zur Erlangung der Doktorwürde
der Universität zu Lübeck
- aus der Sektion Medizin -

Vorgelegt von

KARIM HEINZ FREDERIC

TARHBALOUTI

Aus Guangzhou, V.R. China

Lübeck 2020

1. Berichterstatterin/Berichterstatter: Prof. Dr. rer. nat. Jeanette Erdmann

2. Berichterstatterin/Berichterstatter: Priv.-Doz. Dr. med. Mahdy Ranjbar

Tag der mündlichen Prüfung: 21.4.2021

Zum Druck genehmigt. Lübeck, den 21.4.2021

Promotionskommission der Sektion Medizin

This thesis is dedicated

to my grandfather Haj Brahim Tarhbalouti

Abbreviation and Units

°C	Degree Celsius
ALT	Alanin-Aminotransferase
AP1	Activating Protein 1
APO	Apolipoprotein
ATF3	Activating transcription factor 3
BMI	Body Mass Index
BODIPY	Boron-dipyrromethene
bp	Base pair
bpm	Beats per minute
bZip	Basic region/leucine zipper
CAD	Coronary Artery Disease
Cal/d	Calories per day
CD14+	Cluster of differentiation 14 positive
cDNA	Complementary DNA
cDNA	Complementary DNA
CONT	Control diet
CREB	cAMP responsive element binding
CRISPR/CAS9	Clustered Regularly Interspaced Short Palindromic Repeats 9
Ct	Cycle threshold
CV	Caudal vein
CVD	Cardiovascular disease
DA	Dorsal aorta
DNase	Desoxyribonuclease
dNTP	Nucleoside triphosphate
dpf	Days post fertilization
EDTA	Ethylenediaminetetraacetic acid
EF1α	Elongation factor 1 alpha
ELISA	Enzyme-linked immunosorbent assay
ENU	Ethyl-nitrosurea
EZRC	European zebrafish resource center
GWAS	Genome wide association study
h	Hour
H&E	Hematoxylin Eosin Staining
HBEGF / HB-EGF	Heparin binding epidermal growth factors
HCD	High Cholesterol Diet
HDL	High density lipoprotein
HEK293	Human embryonic kidney 293
hpf	Hours post fertilization
HUVEC	Human umbilical vein endothelial cell
IFN-ϒ	Interferon gamma
IL	Interleukin
K	Control Diet
kb	Kilobase
l	Liter
LDL	Low density lipoprotein
LDL-C	LDL-cholesterol
ldlr	LDL receptor
LPS	Lipopolysaccharide
M	molar
mA	milliampere
M-CSF	Macrophage colony stimulating factor
mg	milligram
MI	Myocardial Infarction
min	minute
ml	milliliter
mm	millimeter
mmHg	millimeter mercury

mRNA	Messenger RNA
MS-222	Tricaine mesylate
$NaCHO_3$	Sodium bicarbonate
NF-kB	nuclear factor 'kappa-light-chain-enhancer' of activated B-cells
ng/µl	Nanogram per liter
nm	nanometer
NPC1L1	Niemann-Pick C1-Like 1
ORO	Oil Red O
osc./sec	Oscillation per second
oxLDL	Oxidized LDL
p	probability value
PBS	Phospate-buffered saline
PCR	Polymerase chain reaction
PCSK9	Proproteinkonvertase Subtilisin/Kexin Type 9
PCV	Posterior cardinal vein
PFA	Paraformaldehyde
pH	Potential Hydrogen
qPCR	Quantitative Polymerase Chain Reaction
RNA	Ribonucleic acid
RNase	Ribonuclease
RT-qPCR	Real Time quantitative PCR
S	svedberg
SD	Standard deviation
siRNA	Small interfering RNA
SNP	Single nucleotide polymorphism
SORL1	Sortilin-related receptor 1
SORT1	Sortilin 1
TAG	Triacylglycerol
TALEN	Transcription activator-like effector nuclease
TBE	Tris/Borate/EDTA
TLR	Toll like receptor
TNF-α	Tumor necrosis factor alpha
u	unit
UNG	Uracil-DNA glycosylase
UV	Ultraviolet
V	volt
VLDL	Very low-density lipoprotein
VPS-10p	Vacuolar Protein Selector 10
W	watt
w	weeks
WGD	Whole-genome duplication
WHO	World Health Organization
ZF	Zebrafish
ZFIN	Zebrafish information network

Gene / Protein Nomenclature

Human	*ATF3* / ATF3
Mouse	*Atf3* / Atf3
Zebrafish	*atf3* / atf3

Table of Content

1. **INTRODUCTION** **11**

1. 1. **MI AND CAD, MAJOR PUBLIC HEALTH CONCERNS WITH GROWING GENETIC UNDERSTANDING** **11**

1. 1. 1. MI and CAD, cardiovascular conditions on an epidemic rise *11*

1. 1. 2. Hypercholesterolemia, a preventable major risk factor for CVDs *11*

1. 1. 3. Atherosclerosis, an inflammatory deterioration of arterial walls *12*

1. 1. 4. Positive family history suggests a genetic basis for CAD and MI *13*

1. 1. 5. Selected human genes of interest linked to CAD *14*

1. 2. **THE ZEBRAFISH, A NOVEL MODEL ORGANISM IN CARDIOVASCULAR RESEARCH** **19**

1. 2. 1. General characteristics on the zebrafish *19*

1. 2. 2. Outlines in zebrafish anatomy and physiology *20*

1. 2. 3. Experimental usage of zebrafish in cardiovascular research *24*

1. 3. **HYPOTHESIS AND AIM OF THIS WORK** **27**

2. **MATERIALS AND METHODS** **28**

2. 1. **MATERIALS** **28**

2. 1. 1. Ethical approval for animal experimentation *28*

2. 1. 2. Adult and larval zebrafish wild type lines *28*

2. 1. 3. Zebrafish husbandry and larval nursing *28*

2. 1. 4. Equipment and instruments *28*

2. 1. 5. Chemicals, reagents, diet and kits *30*

2. 1. 6. Genomic database and primer design tools *32*

2. 1. 7. Primer sequences *32*

2. 2. **METHODS** **34**

2. 2. 1. Aquaculture *34*

2. 2. 2. Histological study of vascular lipid accumulation *37*

2. 2. 3. CAD associated risk gene expression in zebrafish blood *39*

2. 2. 4. Statistical data analysis *45*

3. **RESULTS** **46**

3. 1. **VASCULAR LIPID ACCUMULATION IN LARVAE UNDER HCD** **46**

3. 1. 1. Descriptive study of ORO whole-mount stained larvae *46*

3. 1. 2. Lipid covered surface quantification in major tail vessels *48*

3. 2. CHOLESTEROLEMIC, VASCULAR AND GENETIC RESPONSE TO HCD IN ADULT ZEBRAFISH **53**

3. 2. 1. High Cholesterol Diet effects on blood lipid levels in zebrafish adult vasculature *53*

3. 2. 2. Vascular histology of adult zebrafish tail sections *54*

3. 3. EXPRESSION ANALYSIS OF *ATF3*, *SORT1* AND *HBEGF* IN HCD-FED ZEBRAFISH BLOOD **56**

3. 3. 1. RNA degradation check in whole fish sample *56*

3. 3. 2. Validation of primers for genes *57*

3. 3. 3. qPCR analysis of hypercholesterolemic zebrafish blood *58*

4. DISCUSSION **67**

4. 1. 4%-HCD LEADS TO LIPID ACCUMULATION IN LARVAL VASCULAR STRUCTURES **67**

4. 2. 4%-HCD LEADS TO A HYPERCHOLESTEROLEMIC RESPONSE IN ADULT ZEBRAFISH **70**

4. 3. 12 WEEKS OF 4%-HCD POINTS TOWARDS FATTY STREAKS FORMING IN ADULT ZEBRAFISH AORTAS **72**

4. 4. CAD-RELATED GENE ORTHOLOGUES INDICATE REGULATION CHANGES IN ZEBRAFISH BLOOD TISSUE IN RESPONSE TO 4%-HCD **74**

4. 4. 1. 12 weeks of 4%-HCD upregulates atf3 expression in zebrafish blood *74*

4. 4. 2. 12 weeks of 4%-HCD leads to opposite responses of both hbegf paralogues *75*

4. 4. 3. sort1a is expressed in blood of 12 weeks 4%-HCD-fed zebrafish, not in control *76*

4. 4. 4. General limitations on employed methods *77*

5. CONCLUSION AND OUTLOOK **80**

6. ABSTRACT (DEUTSCH) **82**

7. APPENDIX **84**

8. REFERENCES **86**

9. POSTERS AND PUBLICATIONS **102**

10. ACKNOWLEDGMENTS **108**

11. CURRICULUM VITAE (DEUTSCH) **109**

List of figures

Figure 1.1.1 Sortilin 1 dependent endocytosis of LDL lipoproteins 17

Figure 1.1.2 Paracrine mechanisms of HB-EGF in cell migration and proliferation ..18

Figure 2.2.1 Experimental set-up for HCD-feeding in Larvae.....36

Figure 2.2.2 Experimental set-up for HCD-feeding in adult zebrafish with following blood analysis and histology. 37

Figure 2.2.3 Blood extraction method by centrifugation in adult Zebrafish 39

Figure 3.1.1 Microscopy images of Oil red O whole-mount stained larvae of HCD- and control-groups at 5, 15 and 25 days of diet (100x). 47

Figure 3.1.2 Lipid deposit coverage in major tail vasculature of zebrafish larvae at 5 days HC and control diet.....49

Figure 3.1.3 Lipid deposit coverage in major tail vasculature of zebrafish larvae at 15 days HC and control diet.....50

Figure 3.1.4 Lipid deposit coverage in major tail vasculature of zebrafish larvae at 25 days HC and control diet.....51

Figure 3.1.5 Vascular lipid deposit evolution in larvae fed 5, 15 and 25 days HCD. 52

Figure 3.2.1 Total cholesterol concentrations measured in adult zebrafish blood fed up to 12 weeks HCD and control diet with subsequent 2-week reversal. 53

Figure 3.2.2 Tail vasculature in a hematoxylin and eosin stained of adult zebrafish (20x and 400x) 54

Figure 3.2.3 Visualizations of ORO and hematoxylin stained dorsal aortas of adult zebrafish after 4, 8 and 12 weeks of HCD and control diet (1000x)..... 55

Figure 3.3.1 UV-imaged agarose-gel of whole adult zebrafish extracted mRNA.. 56

Figure 3.3.2 Results of primer validation for *sort1a.* 57

Figure 3.3.3 Relative expression of *atf3* in blood extracted from 4-, 8- and 12 weeks-fed adult zebrafish..... 60

Figure 3.3.4 Relative expression of the *hbegfa* paralogue in blood extracted from 4-, 8- and 12 weeks-fed adult zebrafish.. 63

Figure 3.3.5 Relative expression of the *hbegfb* paralogue in blood extracted from 4-, 8- and 12 weeks-fed adult zebrafish.. 63

Figure 7.1 Analysis example of ORO-stained lipids covering the surface of a dorsal aorta in a 15 days HCD-fed larva. 84

Figure 7.2 Primer validation for *hbegfa* . 84

Figure 7.3 Primer validation for *hbegfb* . 85

Figure 7.4 Primer validation for *atf3* 85

List of tables

Table 2.1.1 Aquarium water storage.....28

Table 2.1.2 Zebrafish husbandry facility.28

Table 2.1.3 Adult Zebrafish mating tanks28

Table 2.1.4 Zebrafish larvae nursing.....29

Table 2.1.5 Tricaine MS-222 production.29

Table 2.1.6 Histology 29

Table 2.1.7 Microscopes, optics and software 29

Table 2.1.8 Adult zebrafish facility for cholesterol feeding experiments. 29

Table 2.1.9 Materials for blood collection in adult zebrafish 29

Table 2.1.10 Centrifuges, photometers and storage equipment 30

Table 2.1.11 Equipment for Reverse Transcription, RT-qPCR and electrophoresis.....30

Table 2.1.12 Aquarium water components 30

Table 2.1.13 Zebrafish adult and larvae food.....30

Table 2.1.14 Sedative production.....30

Table 2.1.15 Histological dies, fixers and chemicals.....31

Table 2.1.16 Anticoagulants employed in blood extraction procedures 31

Table 2.1.17 Cholesterol measurement in zebrafish plasma.....31

Table 2.1.18 mRNA extraction reagents .31

Table 2.1.19 RT-qPCR reagents and kit ..31

Table 2.1.20 Gel electrophoresis 32

Table 2.1.21 Software and databases..... 32

Table 2.1.22 Genes of interest and house-keeping gene primer sequences 33

Table 2.2.1 Stain protocol for whole mount histology of larvae 37

Table 2.2.2 Hematoxylin & Eosin stain protocol for adult fish tails..... 38

Table 2.2.3 Oil red O stain protocol for adult fish tails..... 38

Table 2.2.4 Reverse Transcription master-mix 42

Table 2.2.5 Reverse transcription steps .. 42

Table 2.2.6 RT-qPCR reaction master-mix 43

Table 2.2.7 7900HT RT-qPCR steps..... 43

Table 3.3.1 UV-visualization of agarose-gel electrophoresis for qPCR amplification of *atf3* in adult zebrafish blood at 4, 8 and 12 weeks of feeding. 59

Table 3.3.2 UV-visualization of agarose-gel electrophoresis for qPCR amplification of *hbegfa* in adult zebrafish blood at 4, 8 and 12 weeks of feeding. 61

Table 3.3.3 UV-visualization of agarose-gel electrophoresis for qPCR amplification of *hbegfb* in adult zebrafish blood at 4, 8 and 12 weeks of feeding. 62

Table 3.3.4 UV-visualization of agarose-gel electrophoresis for qPCR amplification of *sort1a* in adult zebrafish blood at 4, 8 and 12 weeks of feeding. 65

1. Introduction

1.1. MI and CAD, major public health concerns with growing genetic understanding

1.1.1. MI and CAD, cardiovascular conditions on an epidemic rise

Myocardial infarction (MI) is the acute consequence of a cardiac embolic event and the most dreaded complication of atherosclerosis in the heart's coronary arteries, a condition medically termed as coronary artery disease (CAD) (Sager et al. 2017).

Atherosclerosis, from the Greek words *atheros*=gruel and *sclerosis*=hardening, initially creates stenosis of the coronary artery's lumen by the accumulation of lipids in the arterial wall and is followed by an inflammation of the resulting plaque. The shrinking of the vessel's inner diameter decreases the blood flow towards the myocardium, resulting in a mismatch of its actual need and its effective oxygen supply, setting its vitality in danger (Sager et al. 2017; Herold 2018). A complete arterial occlusion can occur once the atherosclerotic plaque ruptures, leading to the formation of an intraluminal thrombus with the consequence of ischemia in the myocardial tissue. CAD can manifest itself in patients through chest pain and often morbidly advances into an acute coronary syndrome or sudden cardiac death (Herold 2018).

CAD adds itself to a variety of atherosclerotic diseases summed under the term of cardiovascular diseases (CVD). These include, among others, peripheral artery disease, mesenteric ischemia or stroke (Herold 2018). CVDs are a leading cause of death, accounting for 31% of deaths worldwide (Mendis et al. 2011; WHO 2017). Within CVD-related deaths, CAD alone accounts for 46% of male and 38% of female cases (WHO 2018). CVDs are a major public health concern with its impact reaching today beyond societies of industrial nations. Indeed, the burden of cardiovascular diseases is foreseen to critically surge in low and middle-income countries for the years to come, accounting already today for 75% of all worldwide recorded CVD-related deaths (Finegold et al. 2013; WHO 2017).

1.1.2. Hypercholesterolemia, a preventable major risk factor for CVDs

Often enough, the development of CVDs is promoted by pre-conditions such as hypercholesterolemia, diabetes or hypertension that can further complicate the patient's outcome (Herold 2018). To date, the development of atherosclerosis and its related diseases is linked to a string of major risk factors that can be categorized, primarily for therapeutic purposes, into modifiable and non-modifiable elements as presented in Table 1.1 (Torpy et al. 2009).

The discerning of these individual cardiovascular risk factors began in 1948 with the today still

ongoing Framingham Heart Study (Mahmood et al. 2014). Hypercholesterolemia was singled out among the major metabolic risk factors leading to CAD, as patients presented low HDL and elevated LDL levels in blood (Mahmood et al. 2014). Additionally, the Seven Country Study of Cardiovascular Diseases indicated already in the 1950s factors such as ethnicity and diet to be influential in the developing of CVDs, as higher mortality rates were recorded in northern Europe and North America compared to Japan or the Mediterranean (Menotti & Puddu, 2015). Based upon these findings, public health programs with the intention to curb cardiovascular mortality were first implemented by the WHO in 1972 with the North Karelia Project in Finland, which at the time accounted for the worldwide highest mortality rate for MI (Puska et al. 2002). Targeted prevention programs, primarily based on dietary habit changes through reduction of cholesterol intake, successfully led to a significant decrease of cardiovascular mortality in high risk groups (Puska et al. 2002).

Nowadays, consensus states that most patients developing CVDs present several moderate yet synergetic risk factors, while a vast minority sees its pathology retraced to a single and distinctive strong component (Puska et al. 2009).

Table 1.1 Preventable and non-preventable risk factors for CAD-formation (from Herold 2018 and Torpy 2009)

Preventable risk factors	➢ LDL-cholesterol >160mg/dl and HDL<40mg/dl ➢ Arterial hypertension >140/90mmHg ➢ Smoking ➢ Diabetes mellitus ➢ Abdominal fat accumulation and obesity ➢ Physical inactivity
Non-preventable risk factors	➢ Age above 45 for males and 55 for females ➢ Male gender ➢ Positive family history in first degree relative or genetic predisposition

1. 1. 3. Atherosclerosis, an inflammatory deterioration of arterial walls

Atherosclerosis lies at the basis of a variety of CVD-related pathologies. It is characterized by the inflammation of large and medium sized arterial walls in response to lipid deposits, resulting in their fibrosis and hardening (Davis 2005). Atherosclerosis' earliest manifestations can come in the form of fatty streaks, presenting themselves as yellow linear thickenings of the intima. These usually form in arteries larger than 2-3mm in diameter in the human body, particularly at vascular branching sites where hemodynamic stress and turbulence occurs more frequently (Davis 2005). Streaks have no initial clinical significance and can be found in any human

population age and group. They can develop, inflame and increase in size though into more serious atheromatous plaques (Underwood, 2010; Davis 2005). Such deposits are principally a result of enduring high LDL levels in the blood, which might lead to its accumulation and retention in the extracellular matrix of the arterial wall (Maxfield & Tabas, 2005). Phospholipids of trapped lipoproteins become oxidized and provoke the endothelium to attract monocytes through chemokine signaling and adhesion receptors (Maxfield & Tabas, 2005). The immune cells differentiate into macrophages, oxidized LDL particles are phagocytized and unload their inner content into the cytoplasm (Maxfield & Tabas, 2005). Cholesterol ester ingesting macrophages accumulate and transform into so-called foam cells. In advanced atheromatous plaques, the cholesterol is found to de-esterify and provoke foam cell apoptosis and necrosis from within the atheroma's core (Maxfield & Tabas, 2005). On the luminal side of the plaque lies a thin layer of smooth muscle cells synthetizing collagens and elastase, allowing the plaque's surface to remain stable above the lipid core (Finn et. al. 2010). Additional T-lymphocytes invade the atheroma's core and secrete Interferon-gamma (IFN-ϒ), inhibiting together with Tumor Necrosis Factor-alpha (TNF-α) and Macrophage-Colony Stimulating Factor (M-CSF) the overlying smooth muscle cells to maintain the fibrous cap's stabilizing extracellular matrix (Finn et al. 2010). T-lymphocytes residing in the lipid core stimulate foam cells to produce proteases, accelerating the fibrous cap's collagens deterioration (Finn et. al. 2010). As the necrotic tissue grows underneath, the cap thins out and eventually ruptures. Thrombogenic inner content is then exposed to the blood stream, triggering platelet activation and the formation of a local thrombus that can immediately grow and effectively occlude the arterial lumen. Depending on the event's location, resulting complications can be myocardial infarctions accompanied by arrhythmia or cardiac failure, cerebrovascular accidents or peripheral vascular disease with subsequent loss of the limb (Underwood 2010; Davis 2005)

1. 1. 4. Positive family history suggests a genetic basis for CAD and MI

As mentioned in Table 1.1, a positive family history is a major risk factor linked to the development of atherosclerosis and cardiovascular diseases. Data collected from offspring of the first Framingham Heart Study illustrate higher odds for developing CVDs if the patients' parents presented the same condition as well (Lloyd-Jones et al. 2004). Strong suggestion that hereditary factors play an intricate role in CVD-pathomechanisms is fortified by evidence indicating increased incidence in affected twin siblings and CAD-manifestations accumulating in certain large families (Marenberg et al. 1994; Mayer et. al. 2007; Samani et al. 2007; CARDIoGRAM 2013). Genome wide association studies (GWAS) on patients admitted for

percutaneous coronary intervention (PCI) under MI-suspicion first suggested 9p21.3 as a prime locus harboring SNPs associated with the development of CAD and infarction (Samani and Schunkert 2008; Schunkert et al. 2008). SNPs encompassed on the 9p21.3 locus alone appear to be wide spread within the european population, as the prospect of carrying one mutation within this ethnicity lies at 50% and two at 25%. Presence of such SNPs were shown to increase the odds for developing MI (Erdmann et al. 2010). Further GWA studies followed identifying more loci associated with higher susceptibility to the formation of CAD (Erdmann et al. 2009, 2011; Schunkert et al. 2011). Remarkably, only a minority of these genes could be associated with classic metabolic risk factors (Table 1.1). The number of loci that become associated with CAD or MI are subject to a constant growth. To date, more than 150 of them have been identified through GWAS (Erdmann et al., 2018).

1. 1. 5. Selected human genes of interest linked to CAD

As mentioned in section 1.1.3, atherosclerosis pathomechanisms lay essentially in the aspects of inflammation and lipid metabolism. Among the various genes that have been linked to CAD, *ATF3, SORT1* and *HBEGF* have been extensively studied on a molecular level regarding their disease regulatory function.

1. 1. 5. 1. Activating transcription factor 3 (ATF3)

Activating transcription factor 3 belongs to the family of activating transcription factor/cAMP responsive element binding (CREB) proteins. ATF proteins bind to the [TGACGTCA] repetitive DNA sequence on the basic region/leucine zipper (bZip) domain (Chen, 1994). Contrary to what its name may suggest, ATF3 has been shown to deactivate transcription through stabilizing inhibitory cofactors on promoter sites (Chen, 1994). In *Homo sapiens*, the gene's chromosomal locus is 1q32.3 on Chromosome 1 (Ensembl ID: ENSG00000162772). *ATF3* has been reported to be involved in various oncogenes, cytokines and cellular growth signaling pathways. Its encoded protein integrates itself into a larger Activator Protein-1 (AP-1) complex that coordinates cellular processes of morphogenesis, proliferation, differentiation, transformation and apoptosis (Wolfgang et al. 1997).

DNA-microarray study described the up-regulation of *Atf3* along with further AP-1 constituents in ischemia-reperfusion injury in kidney, intestinal and skeletal muscle tissue of rats (Chang et al. 2015). Furthermore, Nawa et al. have shown ATF3 proteins to be expressed higher in endothelial cells and macrophages within atherosclerotic plaque lesions than in unaffected vessels (Nawa et al. 2002). Additionally, the same group described *ATF3* expression in HUVEC cell death provoked by exposition towards TNF alpha and oxLDL. The latter two were reported

furthermore by Nawa et al. to be partly suppressed by *ATF3* antisense cDNA, suggesting its involvement in apoptotic mechanisms during early stages of atherogenesis (Nawa et al. 2002). In atherosclerotic plaques harvested from human cardiovascular disease victims, gene expression analysis has demonstrated a doubled expression increase of *ATF3* in affected tissue compared to visually healthy arteries (Sobolev, 2011). *In vitro* trials indicate *ATF3*-activation to be prompted by stress signals in cell death, with its scale correlating to the extent of cellular damage (Okamoto 2001). Its expression in the myocardium and kidney can be induced by ischemia and reperfusion tissue stress. Under hypoxic conditions, endothelial cells show enhanced expression when levels of nitric oxide increase (Chen 2008). In vascular smooth muscle cells, *ATF3* is induced by exposition towards H_2O_2. Its knock-down leads to cell apoptotosis, indicating its essential role in cellular survival (Lv et al. 2011). Gilchrist et al. demonstrated *ATF3*'s ability to regulate inflammation by decreasing TLR-4 surface expression in LPS stimulated macrophages as part of a negative feedback loop. ATF3 hinders the histonic deaceytlation via NF-kB and suppresses the expression of *Il6* and *Il2b* promoters (Gilchrist et al. 2006). Additionally, HDL was also shown to activate *ATF3* and lead to a decrease of Toll Like Receptors expression on macrophage cell surfaces (De Nardo 2014).

Gold et al.'s work shows further protective properties in metabolic and inflammatory aspects of atherogenesis. ATF3 appears to bind to the promotor region of *Ch25h*, suppressing cholesterol oxidation and formation of 25-hydroxycholesterol. The resulting effect indicates a diminished uptake of oxidized LDL into macrophages and a subsequent limitation of foam cell formation within atherosclerotic plaques in mice aortas (Gold et al. 2012).

1. 1. 5. 2. Sortilin 1 (SORT1)

The Sortilin 1 (*SORT1*) gene encodes for receptors of the Vacuolar Protein Selector 10 (VPS-10p) family (Petersen, 1997). Sortilin glycoproteins ensure the transfer of enzymes and protein structures within lysosomes from the endoplasmic reticulum or Golgi apparatus towards the cell's surface (Figure 1.1) (Kjolby et al. 2015). It is expressed in various tissue types, with strong levels recorded in neuronal tissues, testis and placenta and to a lesser extent in adipocytes, liver and $CD14^+$ monocytes. *SORT1* is located on chromosomal locus 1p13.3 (BioGPS Dataset, 2018; Ensembl ID: ENSG00000134243).

The Wellcome Trust Case Consortium and the German MI family GWA studies linked *SORT1* and several SNPs at its locus 1p13.3 with myocardial infarction (Samani et al. 2007; Maouche & Schunkert 2012). Furthermore, *SORT1* has been associated with abdominal aortic aneurysm as well, itself a major complication of atherosclerosis (Jones et al. 2013). The mechanisms of

sortilin's function in atherogenesis isn't fully clarified yet. In the minor allele rs599839, decreased LDL-cholesterol levels have been recorded, along with a reduction in coronary stenosis grades in comparison to patients homozygous for the more frequent alleles (Muendlein et al. 2009). In their work, Muendlein et al. presumed that rs599839 enhanced cellular LDL-uptake by increasing the expression of *SORT1*. Its over-expression in HEK293 cells demonstrated a lowering in plasmatic LDL-C levels, while they are increased by siRNA knock-down in mice (Musunuru et al. 2010; Wang et al. 2011).

Kjolby and Tveten described sortilin as a receptor directly involved in exocytosis of VLDL and endocytosis of LDL (Figure 1.1.1) Furthermore, the receptor presumably ensures its lipid regulatory role in interaction together with PCSK9 through control of LDL-receptor presence on cell surfaces by receptor-mediated endocytosis (Tveten et al. 2012; Kjolby et al. 2015). In Tveten's study on hypercholesterolemic subjects, 8 missense mutations on *SORT1* were identified. No differences in serum cholesterol levels were found between mutation carriers and non-carriers, suggesting no phenotypic consequence (Tveten et al. 2012). In vitro transfection on HeLA T-Rex cells with these *SORT1*-mutations showed the amount of bound LDL to be directly corresponding to the degree of sortilin expression on the cell surface, itself presumably altered by the transfected genetic mutation. Moreover, overexpression of *SORT1* increased the LDL cellular uptake (Tveten et al. 2012). In selective silencing though of either *LDLR* or *SORT1*, LDL-receptors appeared to play a more significant role in overall lipid level regulation though than sortilin. The study went on to indicate that a mutation on *SORT1* was unlikely to cause autonomic dominant hypercholesterolemia, a key risk factor in the development of atherosclerosis and MI (Tveten et al. 2012).

Like *ATF3*, human results of decreased LDL-cholesterol suggest *SORT1* to play a protective role in the formation of atherosclerotic plaques. In contrast though to previous findings in humans, Mortensen's sortilin-impaired mice models indicate paradoxically a decrease in LDL-cholesterol levels in blood, while additional LDLR double knock-outs lead to further decrease in APOB100 and triglycerides levels. Additionally, sortilin deficient mice show decreased LDL uptake into macrophages and subsequent foam cell formation and smaller atherosclerotic plaque size (Mortensen et al. 2014, Patel et al. 2015).

Besides lipid level regulation, sortilin's influence on atherogenesis has been also described in an inflammatory aspect. In mice models, sortilin has an inclined binding towards IL-6 and IFN-ϒ. The secretion of these pro-inflammatory cytokines is muted in sortilin-deficient macrophages and Th-1 Lymphocytes. Irradiated mice transplanted with sortilin-deficient bone

marrow demonstrated accordingly low cytokine levels, along with shrinking of its atherosclerotic plaque size (Mortensen et al. 2014).

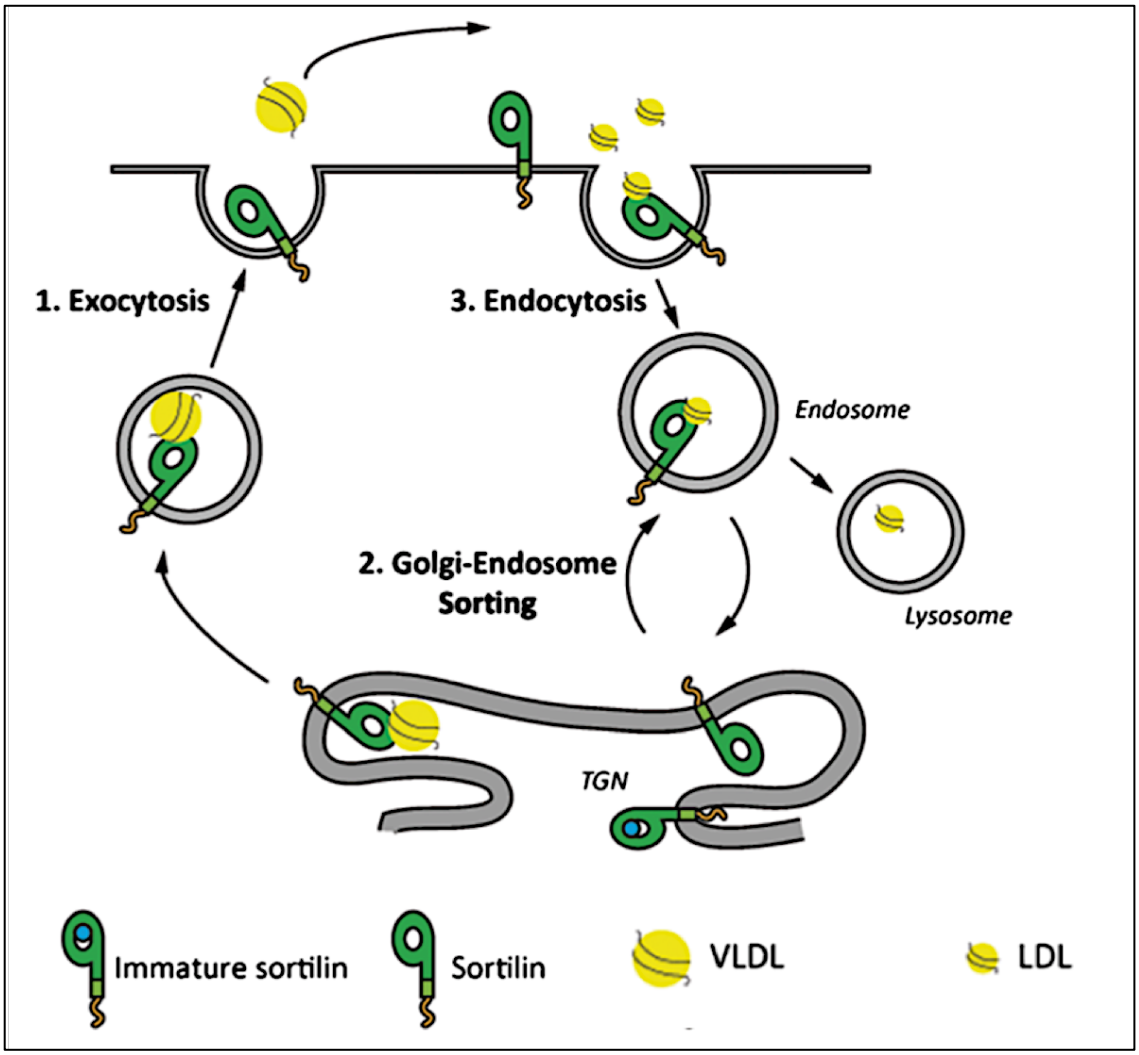

Figure 1.1.1 Sortilin 1 dependent endocytosis of LDL lipoproteins
modified from "Sortilin, encoded by the cardiovascular risk gene SORT1, and its suggested functions in cardiovascular disease" by Kolby et al., 2015

*1. 1. 5. 3. Heparin binding - epidermal growth factors (*HB-EGF)

Heparin binding - EGF (HB-EGF) is a transmembrane protein belonging to the superfamily of epidermal growth factors (EGF) and presents strong mitogenic and chemotactic properties. The chromosomal locus for its coding gene *HBEGF* is 5q31.3 (Ensembl ID: ENSG00000113070). Higashiyama et al. first described its secretion by human macrophages and smooth muscle cells. *HBEGF* is especially expressed in tissue types such as lung, heart, brain and skeletal muscle cells (Higashiyama et al. 1991).

In analyzing the three aortic wall layers, effects on cell proliferation and migration have been demonstrated on fibroblasts and aortic smooth muscle cells, while none could be identified in

endothelial cells (Higashiyama et al. 1991; Raab et al 1997) (Figure 1.1.2). Carotid balloon injury trials in rats showed increased HB-EGF expression in neointimal cells, particularly in the first two hours after the intervention (Igura et al. 1997). Infarcted myocardial tissue of rats shows high HB-EGF expression, as the interstitium undergoes fibroblastic remodeling (Tanaka et al. 2002). Within human atherosclerotic plaques, immunohistochemistry methods have specifically localized HB-EGF in intimal connective tissue (Scuderi et al., 2009).

Regarding hypercholesterolemia, patients present higher HB-EGF serum levels in ELISA analysis (Sanchez-Vizcaino et al., 2009). Additionally, remnant lipoproteins (RLP) from hypercholesterolemic patients have shown to provoke aortic smooth muscle cell proliferation in rats via HB-EGF shedding (Kawakami et al. 2003).

Monocytes collected from patients admitted for percutaneous transluminal coronary angioplasty (PTCA) after myocardial infarction show significant changes in their transcriptome, particularly in *HBEGF*'s case. After PTCA, blood samples were collected from patients 6 hours, 72 hours and 90 days after MI for MicroArray analysis. In the early hours following the ischemic event, *HBEGF* has shown to be expressed strongest. Levels lower transiently then in the subacute phase and rise again 90d after the intervention (Riedel 2012).

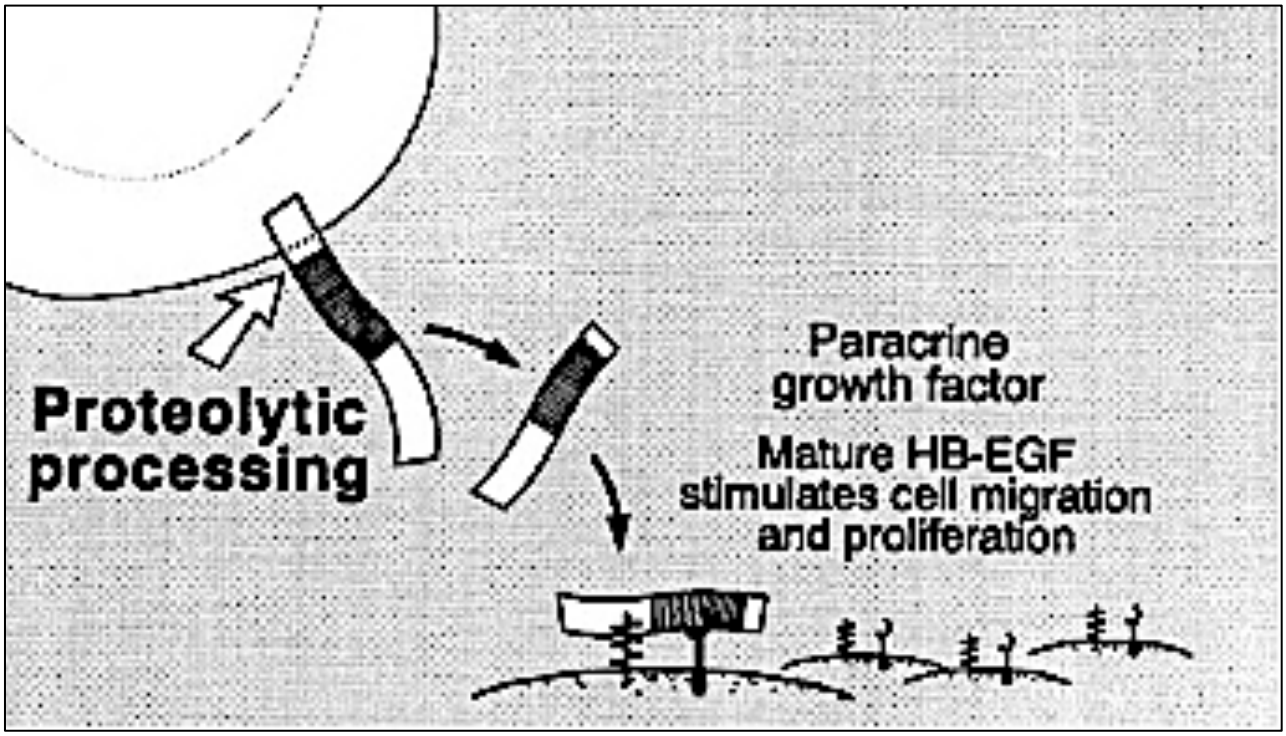

Figure 1.1.2 Paracrine mechanisms of HB-EGF in cell migration and proliferation
modified from "Heparin-binding EGF-like growth factor", Raab and Klagsbrun 1997

1. 2. The Zebrafish, a novel model organism in cardiovascular research

Different model organisms have been used to date in elucidating the pathogenesis of CAD and MI. Mammals, such as mice and rats, feature among the best established and prominent animal models in cardiogenetic studies. Within the past decade, new species have been introduced into this field. Among these recently adopted organisms, the zebrafish (*Dani rerio*) offer an attractive alternative model to mice. Thoroughly illustrated in developmental research, the zebrafish's distinctive features permit the opening of new and innovative approaches in CAD-research.

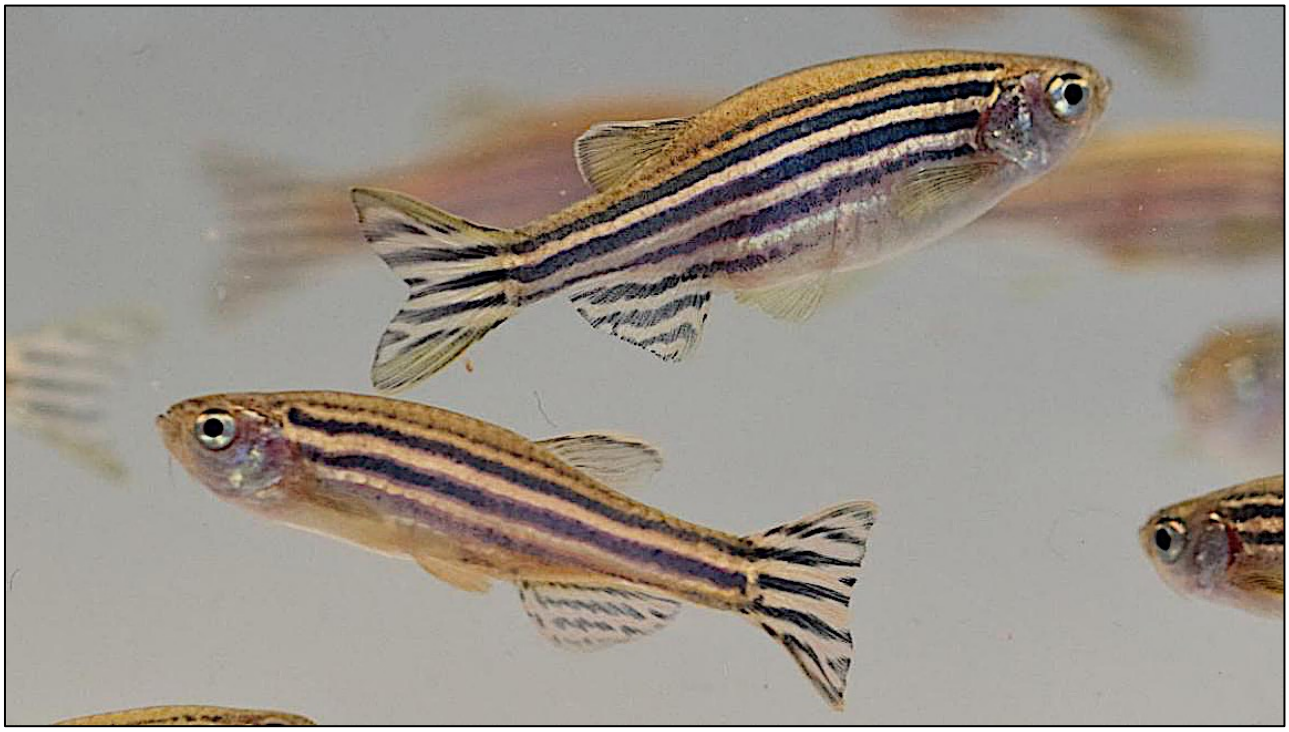

Figure 1.2 Female (top) and male (bottom) adult zebrafish (*Danio rerio*) in captivity.

1. 2. 1. General characteristics on the zebrafish

Danio rerio, also commonly known as zebrafish, is a 30 to 50mm long tropical fresh water fish indigenous to slow streams, ponds and rice fields of the Indian subcontinent (McClure et al. 2006; Spence 2008; Reed and Jennings, 2011; Parichy 2015).

The zebrafish draws its name from its characteristic horizontal stripes on the side of its body and is a popular fish among aquarium hobbyists (Hirata et al. 2003). *Danio rerio*'s taxonomy orders it to the vertebrate infraclass of *teleostei* and to the *cyprinidae* family of carp and minnow-like fish (Spence et al. 2008; Reed and Jennings, 2011). Males show a slender, torpedo-like shape, while females appear larger and distinctive by their bulky egg-carrying abdomen (Wixon, 2000) (Figure 1.2). Their circadian rhythm follows 14 hours of daylight and 10 hours

of darkness. *Danio rerio* is a poikilothermic species living in a water temperature range between 25° and 31°C. (Westerfield 2007; Spence 2008) In laboratory usage, zebrafish have been shown to have an average life span of two to five years (Gerhard et al. 2002).

1. 2. 2. Outlines in zebrafish anatomy and physiology

1. 2. 2. 1. Embryonic development

Reaching sexual maturity within 3 months confers the zebrafish a short generational time (Lawrence et al. 2012) (Figure 1.3). For optimal reproductive outcome, a state of perpetual mating season can be simulated at a constant aquarium temperature of 28,5°C under laboratory conditions (Reed and Jennings 2011). Mating generally occurs at sunrise, upon which females can spawn several hundred eggs every week for free-floating fertilization (Westerfield 2007).
Embryos develop rapidly in 0.7mm small egg shells outside of the mother's body (Kimmel 1995). Eggs and larvae bear the distinctive feature of wide-ranged optical transparency for the first 30 days of development, enabling the study the fish's development under the microscope (Kimmel 1995). Sex determination in the zebrafish is believed to be a polygenic process and is not dependent on specific gonosomal chromosome presets (Liew and Orban 2013). Environmental factors, such as temperature, can also influence sexual differentiation and can occasionally lead to the formation of gender bias within a group (Liew et al. 2012). Embryonic development of major organ systems take place within the first 72 hours after fertilization, with the cardiovascular system and blood cells already visible on the first day (Kimmel 1995). Larvae hatch on the third day, displaying a clearly visible vascular system and active blood flow under the microscope. Juveniles show then a length of 3mm and keep growing to reach adulthood after approximately 90 to 100 days of development (Kimmel 1995).

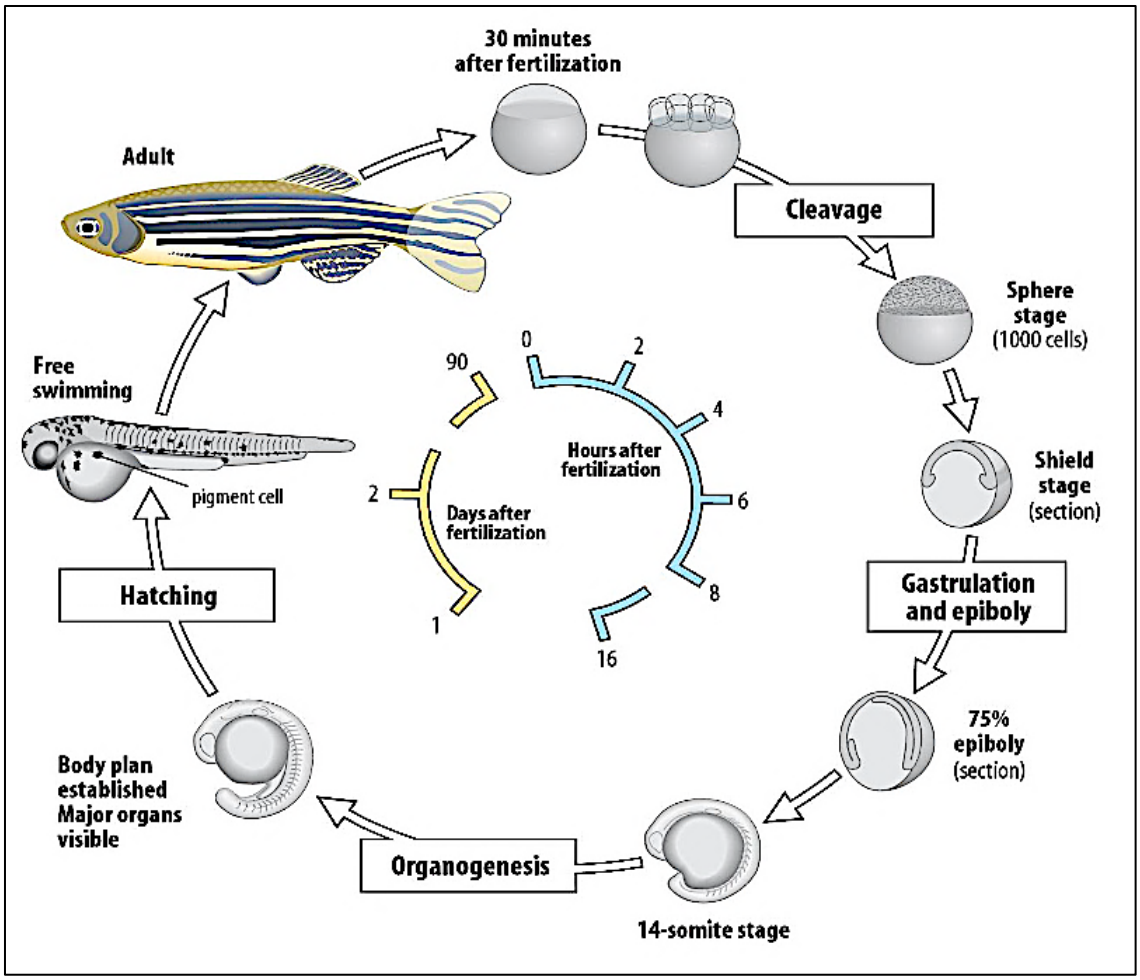

Figure 1.3 Zebrafish life cycle from fertilization to adulthood
from Wolpert's Principles of Development 2nd. Edition, Oxford University Press

1. 2. 2. 2. Cardiovascular system

Danio rerio's cardiovascular anatomy retains a basic analogy with other vertebrate species, including *Homo sapiens*. In the first hours of cardiogenesis, embryonic tissue is predominantly oxygenated through passive diffusion and does not depend *per se* on circulation provided by cardiac activity (Isogai et al. 2001; Ellertsdottir, 2010).

The embryonic heart tube structure forms as early as 18hpf, with first rhythmic heart beats and blood flow observed at 24hpf (Isogai et al. 2001; Wixon 2000). Teleost fish heart follow a simple, two-chambered sequential set-up in which blood flows in a forward order: entering from the sinus venosus into the atrium, passing the atrioventricular valve and pumped out of the ventricle into the bulbus arteriosus (Hu et al. 2001). Coronary arteries on the zebrafish heart appear very small in size, with a diameter wide enough to let a single erythrocyte fit in (Hu et al. 2001). Blood pressure measurement in adult *Danio rerio* show 0.68mmHg in the atrium, 0.42 to 2.51mmHg in the ventricle and 2.16 to 1.51mmHg from the root down to the end of the aorta at a mean resting heart rate of approximately 120 bpm (Hu et al. 2000, 2001; Tsai et al.

2011). Major arterial blood flow runs out of the bulbus into the short ventral aorta and bifurcates into pairs of right and left branchial arteries for oxygenation in the gills (Hu et al. 2000, 2001). Both pairs merge back again into the dorsal aorta (DA) that runs caudally along the main body, perfusing tissue along several parallel branched intersegmental vessels. The dorsal aorta anastomoses into the caudal vein (CV) at the end of the tail, draining venous blood back towards the trunk through the posterior cardinal vein (PCV), into the ductus Cuvier and the sinus venosus (Hu et al. 2000, 2001; Isogai et al. 2001).

Histologically, teleost fish show the same basic vascular wall layers of tunica intima, media and adventitia as in other vertebrates. The zebrafish aortic wall is particularly thin and is formed by a single endothelial cell layer, two layer of vascular smooth muscle cells and adventitious tissue comprising fibroblast and melanocytes (Miano, 2006).

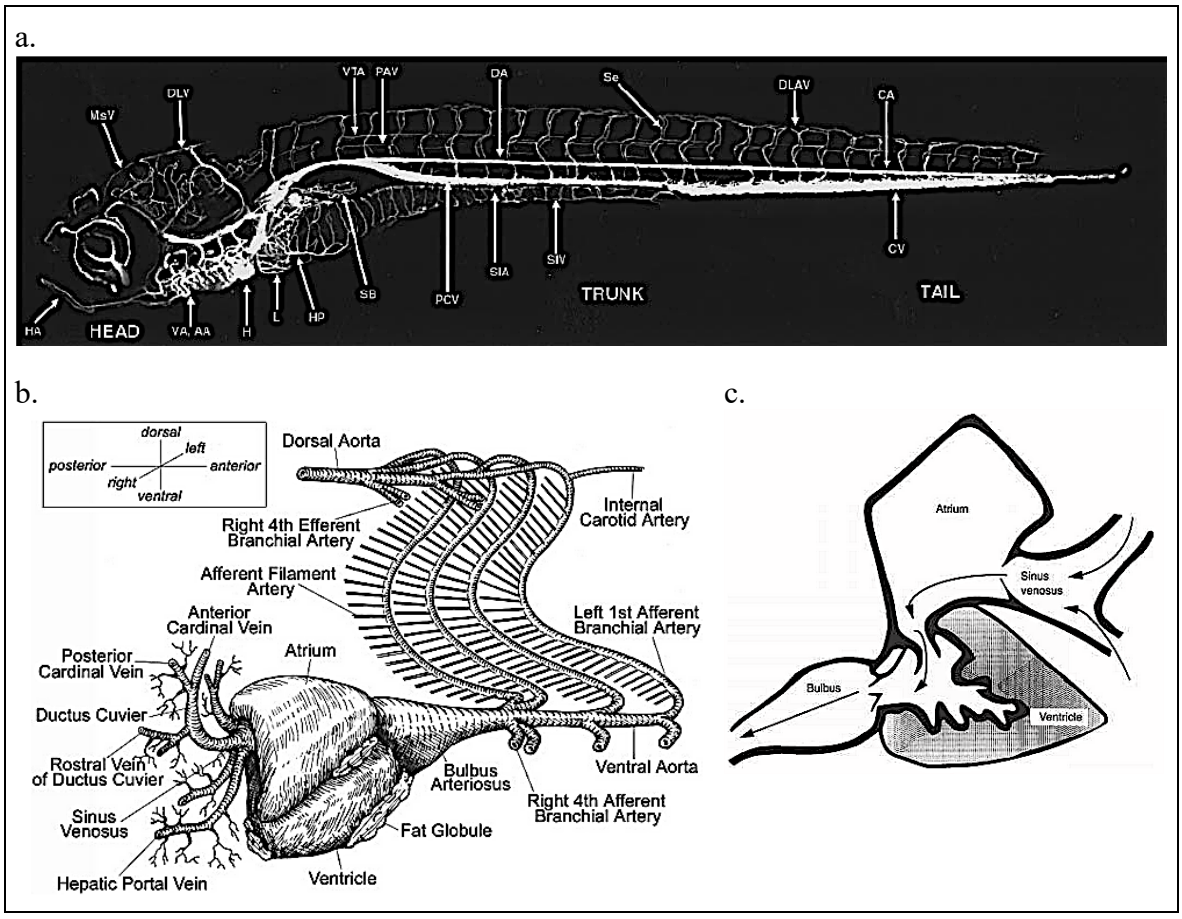

Figure 1.4 Zebrafish cardiovascular anatomy

a. Angiogramm of a 7.5dpf zebrafish larva. Modified from Isogai et al. 2001
AA: branchial archs, CA: caudal artery, CV: caudal vein, DA: dorsal artery, DlV: dorsal longitudinal vein, DLAV: dorsal longitudinal anastomotic vessel, H: heart, HA: hypobranchial artery, L: liver, MSV: medencephalic vein, PAV: parachoral artery, PCV: posterior cardinal vein, Se: intersegmental vessels, SIA: supraintestinal vein, SIV: subintestinal vein, VA: ventral aorta, VTA: vertebral artery
b. Zebrafish heart in posterior anterior view: afferent and efferent vessels, gill vasculature
Hu et al. 2001
c. Blood flow through teleost fish heart chambers https://www.rrnursingschool.biz/rainbow-trout/cardiovascular-system.html

1. 2. 2. 3. Blood

Hematopoiesis in the zebrafish occurs in the kidney's interstitial tissue and to a lesser extent in the spleen as well (Mumford et al. 2007). Both organs act additionally as prime lymphatic filter organs, as teleost fish are deprived of lymph nodes (Mumford et al. 2007).

As in birds and reptiles, oxygen in zebrafish is transported through the blood by hemoglobin in nucleated erythrocytes with aerobic cell metabolism (Menke et al., 2011). Hemostasis is ensured by thrombocytes that appear nucleated as well. Leukocyte differential count show in decreasing order 71-92% lymphocytes, 5-15% monocytes, 2-18% neutrophils, 0-2% eosinophils and 0-2% basophils. Biochemical serum values are akin to mammal species, except for elevated values for ALT, amylase and phosphorus (Murtha 2003).

1. 2. 2. 4. Diet and lipid metabolism

In the wild, the omnivorous *Danio rerio* feeds on plankton, aquatic insects and crustacean eggs (McClure et al. 2006; Spence et al 2007, 2008). In laboratories, zebrafish are usually set on paramecium diet for larvae and artemia or flake food for adults. In the first days of development, larvae usually subsist on their own egg yolk before turning to an external food source after the 5th dpf. (Westerfield 2007). Zebrafish normal diet requires high levels of cholesterol and polyunsaturated fatty acids. *Danio leopardo*, a very close relative to *Danio rerio*, has been shown to require 30cal/d (Pannevis & Earle 1994).

As a poikilothermic species, lipid intake varies upon changes in water temperature (Henderson & Tocher 1987). Lipids are stored within adipocytes of visceral, intramuscular and subcutaneous white fat tissue as triacylglycerol (Song & Cone 2007). Lipids get absorbed in fish intestines at two levels: an initial fast absorptive component delivers and solves fatty acids immediately into the plasma after feeding; a later slow component, as in mammals, delivers TAGs into chylomicrons (Sheridan 1988). Cholesterol enters enterocytes with the help of the Niemann-Pick C1-Like 1 (NPC1L1) Protein (Quinlivan & Farber 2017). Lipid transport mechanisms in fish are similar generally to mammal's, with conserved orthologues for apolipoproteins APOA-I, APOB, APOE and APOA-IV present in *Danio rerio* (Babin, 1989; Otis et al. 2015). Relative hyperlipidemia and hypercholesterolemia in comparison to other vertebrates is noticed though in teleost fish blood. In comparison to humans, LDL particles hold more TAGs elements and less cholesterol esters, whereas the latter is found more in HDL (Pedroso et al. 2012, Otis et al. 2015). Transfer of cholesteryl esters between HDL and LDL has also been observed as teleostei fish as they display a highly conserved orthologue of *cetp* (Babin, 1989). Zebrafish blood lipid levels can be influenced by diet: on additional cholesterol intake,

total cholesterol levels increase in plasma (Stoletov et al. 2009). Remarkably, six days old larvae fed a high cholesterol meal of chicken egg yolk with approx. 50% lipid composition have shown a triglyceride content increased 10-fold already 24h after feeding in comparison to a control fed group (Quinlivan & Farber 2017).

1. 2. 2. 5. Genetic properties

Danio rerio is a diploid organism presenting a set of 25 chromosomes at a genome size of approximately 1400Gb (Wixon 2000; Howe et al. 2013). Humans and teleostei fish shared a last common ancestor approximately 450 to 380 million years ago (Meyer and Schartl 1999; Postlethwait et al. 2000; Amores et al. 2011). It is believed that this forbear species underwent an extensive whole-genome duplication (WGD), specific to teleostei fish (Teleost Genome Duplication -TGD) (Amores et al. 2011). The event led to the formation of around 26.000 known protein-coding genes in Zebrafish, a number so high that hasn't been recorded in any other vertebrate species yet (Collins et al. 2012; Howe et al. 2013). A great number of these genes are distinctive to the zebrafish and are not found in human nor mice (Howe et al., 2013). The teleostei WGD essentially led to the formation of paralogue pairs, where both gene duplicates often correspond to one single mammal counterpart (Glasauer & Neuhauss 2014). Genomic material between humans and zebrafish has been shown however to be highly conserved, with a reciprocal genetic ortholgy of approximately 70%. Amid the discovered orthologues, 47% have an individual and identical link between both species (Howe et al. 2013).

1. 2. 3. Experimental usage of zebrafish in cardiovascular research

1. 2. 3. 1. Usage in cardiovascular developmental research

Zebrafish husbandry runs at a fraction of the cost necessary for mice (Goldsmith and Solari, 2003). High fecundity, optical transparency and rapid development of embryos furthermore permitted the zebrafish to become a first line model for extensive embryological studies (Kimmel et al. 1995). Furthermore, large scale mutagenesis programs on zebrafish started in the 1980s with Streisinger's works and expanded throughout the 1990s. Forward genetic approaches by applying the chemical mutagen ethylnitrosurea (ENU) induced random monogenetic variations and created a multitude of zebrafish mutant lines, permitting expanding possibilities to study organ development in young larvae and the construction of a vast embryogenesis database (Streisinger et al. 1981; Driever et al. 1996; Haffter et al. 1996; Wixon 2000). Following similar methods, more than 50 mutant lines for cardiovascular disease models

were generated, conceding insight into developmental research of congenital heart diseases (Stainier et al. 1997). Further, more modern methodic advances opened new ways for cardiogenetic studies in the zebrafish (Bournele and Beis 2016). With the ease of egg harvesting at early one-cell developmental stage, genome editing trough microinjections is readily feasible. Morpholinos, TALEN and zinc-fingers injections permit the transient silencing or over-expression of selected genes and the early subsequent examination of larvae under the microscope (Ota and Kawahara 2014). More recently, CRISPR/CAS9-based microinjections have permitted the targeted editing of a desired gene to achieve stable mutant zebrafish lines of a desired phenotype (Ota and Kawahara 2014).

1. 2. 3. 2. Zebrafish usage in atherosclerosis and hypercholesterolemia research

Atherosclerosis in fish has first been described in tuna aortas (*Thunnus thynnus*) and salmon coronary arteries (*Salmo salar*) (Vastesaeger and Delcourt 1962; Farell et al. 1986).

Relatively recently, *Danio rerio* was presented as a potent experimental model for atherosclerosis research with the first reported observations of inducible lipid accumulation in its vasculature. Using the optical transparency of zebrafish larvae, Miller et al. were able to study the progression of atherosclerotic-like lesions in living zebrafish offspring. For 10 days, wild-type larvae were placed on a 4% cholesterol-diet enriched with a lipid flurorophore dye. Increased number of oxidized lipids in fatty streaks could be observed under fluorescent microscopy along the dorsal aorta and caudal vein of the HCD-fed group.

Furthermore, inflammatory processes were suggested by findings of local macrophage accumulation with Toll-like-receptor dependent uptake of lipids. Finally, adult zebrafish on long term HCD successfully displayed an ezetimibe reversible increase in cholesterol blood levels, accompanied by punctual aortic lesions in histological cross-body sections. Surprisingly, no significant BMI increase was found between the HCD and control fed groups (Stoletov and Miller et al. 2009; Yoon et al. 2013).

By extension, Yoon et al. described 4%-HCD as able to generate interleukin-β (IL1-β) expression in the spleen and liver in a similar experimental set up. In contrast though, no TNF-α increase was recorded and the same overall inflammatory effect couldn't have been reproduced in HCD-fed larvae. Observed lesions in the adult vasculature were described as underdeveloped and closer to the early fatty streak phase, suggesting the necessity of genetic intervention to provoke more advanced stages of atherosclerosis in the zebrafish (Yoon et al. 2013).

The following year, O'hare et al. reported a successful transient *ldlr* knock-down by morpholino

microinjections in embryonic eggs and observed stronger hypercholesterolemia and increased vascular lesions with oxidized lipids in HCD-fed larvae within seven days post fertilization (O'hare et al. 2014).

1. 2. 3. 3. Current research on genes-of-interest in the zebrafish model

Results of functional studies on a*tf3* in zebrafish are scarce, with only recent publications mainly axed around its role in nerve regeneration after spinal cord and optical nerve injury (Wang et al. 2017; Solin et al. 2014). The same can be stated for *sort1* where so far, zebrafish models provided insight in its progranulin uptake role in familial frontotemporal lobar degeneration and with regards to the similar *sorl1* sortilin-related receptor 1 being a risk factor in the development of Alzheimer's disease (de Muynck et al. 2013; Lee et al. 2016). Regarding *hbegf*, knock down experiments on zebrafish larvae have described the development of pericardial edema in association with dilative cardiomyopathy, demonstrating its essential role in the process of cardiogenesis (Friedrichs et al., 2009).

1. 3. Hypothesis and aim of this work

Previous studies on *ATF3, SORT1* and *HBEGF* have indicated that these genes may play a determinant role in the pathogenesis of CAD by influencing the formation of atherosclerosis. Functional studies have been so far mainly limited to mice and cell culture models and have been poorly carried out on zebrafish. Results on hypercholesterolemia and vascular lipid accumulation by Stoletov et al. (2009) and Yoon et al. (2013) have justified the application of zebrafish as a potent atherosclerosis model, offering new insights in studies focused on the genetic basis of cardiovascular diseases such as CAD.

The aim of this study is to investigate in a time-course the gene expression of the *ATF3, SORT1* and *HBEGF* orthologues in wild-type adult zebrafish using qPCR, parallel to the progression of hypercholesterolemia and vascular lipid accumulation in response to the provided high cholesterol diet, with the prospect of cementing *Danio rerio* as a suitable model in the study of CAD and MI-related genes.

In a first stage, we will seek to prove the principle that vascular lipid deposition is inducible by a high-cholesterol dietary intake. For this, we will first undergo a comparative study on zebrafish larvae fed a 4%-cholesterol and a corresponding control diet in a short period of 5, 15 and 25 days.

In a second stage, we will extrapolate the comparative diet study onto young adult zebrafish fed on an arbitrarily set time-course of 4, 8 and 12 weeks. Blood and histology samples will be collected at each time-point for total plasma cholesterol, qRT-PCR analysis of *ATF3, SORT1* and *HBEGF Danio rerio* orthologues and cross body histological sections of zebrafish aortas.

2. Materials and Methods

2. 1. Materials

2. 1. 1. Ethical approval for animal experimentation

Experiments took place under the ethical approval code V242-7224.12-39 (77-6/14) provided on 18.12.2014 by the ministry for agriculture and environmental protection of the state of Schleswig-Holstein in Kiel, Germany (Ministerium für Energiewende, Landwirtschaft, Umwelt, Natur und Digitalisierung).

2. 1. 2. Adult and larval zebrafish wild type lines

Adult female and male zebrafish from the AB wild-type line were provided by the European Zebrafish Resource Center (EZRC) at the Karlsruhe Institute for Technology (KIT), Germany. Larvae were obtained as first-generation offspring bred from the zebrafish adults.

2. 1. 3. Zebrafish husbandry and larval nursing

Aquaculture laboratories were provided in collaboration with the Fraunhofer Research Institution for Marine Biotechnology and Cell Technology at the University of Lübeck, Germany.

2. 1. 4. Equipment and instruments

Table 2.1.1 Aquarium water storage

Equipment	Manufacturer and supplier
Fass Oval water tank; 100L	GRAF GmbH
Probau bucket; 20L	Bauhaus GmbH
Prosilent a200 air pump; 200l/h, 3.5W	JBL GmbH
Protemp S 25-300 aquarium heater; 100W	JBL GmbH

Table 2.1.2 Zebrafish husbandry facility

Equipment	Manufacturer and supplier
Zebtec Active-Blue Stand Alone Zebrafish Systemview	TECNIPLAST Deutschland GmBH

Table 2.1.3 Adult Zebrafish mating tanks

Equipment	Manufacturer and supplier
Mating Tank; 1,0l ZB10BTIE ZB10BTI ZB10BTD ZB10BTL	TECNIPLAST Deutschland GmbH
PP sieve; Ø150x280mm	Fackelmann GmbH

Table 2.1.4 Zebrafish larvae nursing

Equipment	Manufacturer and supplier
KB 115 incubator	Binder GmbH
DZ 20-AV2 digital timer	Brennenstuhl GmbH
WNB-45 water bath; 45L, 2800W	Memmert GmbH
Typ 0520609 aquarium lighting hood; 15W	Müller + Pfleger GmbH
Polystyrol transparent containers; 500ml	abcMeineVerpackung.de e.K.
Labsolute® PE Pasteur pipette ; 3ml, 150mm	Th. Geyer GmbH

Table 2.1.5 Tricaine MS-222 production

Equipment	Manufacturer and supplier
Accu-jet® pipette controller	Brand GmbH
Combimag RCH magnetic stirrer	IKA®-Werke GmbH Germany
Duran® glas beaker; 250ml	DWK Life Sciences GmbH
Scout pro SPU4001 portable balance	Ohaus Corporation
Serological sterile pipette; 10ml, 5ml	Sarstedt GmbH

Table 2.1.6 Histology

Equipment	Manufacturer and supplier
Costar Netwell™ 3x4 Insert; 74um PE mesh, Ø15mm	Corning Inc.
Cover Slips; 22x22 mm	Menzel GmbH
Cryotome Cryostar nx50	Thermo Fisher Scientific
Whatman™ folded filters; Ø240mm	GE Healthcare Life sciences GmbH

Table 2.1.7 Microscopes, optics and software

Microscope	Manufacturer and supplier
Biorevo BZ-9000 Fluorescent Microscope	KEYENCE Deutschland GmbH
IC80HD dissection microscope	Leica microsystems GmbH
Standard 20 microscope	Zeiss GmbH

Table 2.1.8 Adult zebrafish facility for cholesterol feeding experiments.

Equipment	Manufacturer and supplier
Air 550R plus air pump; 8W, 550L/h	Sera GmbH
Aquastar Aquarium with lighting hood; 54L	Eheim GmbH
Digital timer DZ 20-AV2	Brennenstuhl GmbH
Jäger Aquarium aquarium heater; 50W	Eheim GmbH

Table 2.1.9 Materials for blood collection in adult zebrafish

Equipment	Manufacturer and supplier
0,5 and 1,5 ml Eppendorf Research® Pipettes	Eppendorf GmbH
BENCH	
Biosphere® Filter Pipettes	Sarstedt GmBH
Dissection forceps	Karl Hammacher GmbH
Microlance™ 3 canules	Becon Dickinson GmbH
Petri dish	Sarstedt GmbH
PP Tube; 50ml, 15ml	Sarstedt GmbH
Safe Lock reaction tubes; 0,5ml, 1,5ml	Eppendorf GmbH
Scalpel; n. 20	FEATHER® Safety Razor Co. Ltd.

Table 2.1.10 Centrifuges, photometers and storage equipment

Equipment	Manufacturer and supplier
-20°C Ice Block	Eppendorf GmbH
5415R centrifuge	Eppendorf GmbH
Biofuge Primo R centrifuge	Heraeus Holding GmbH
BioPhotometer	Eppendorf AG
Stainless steel bead; 7mm	Qiagen GmbH
Micro Centrifuge	Carl Roth GmbH
Microplate reader Synergy HT Gen5 v1.05 software	Biotek, USA
MW17M70-Au Microwave	MDA
Profiline -80°C freezer	HERA freeze, Liebherr GmbH
Rotanta 460R centrifuge	Hettich Zentrifugen
TissueLyser LT Tissue grinder	Qiagen GmbH
Vortexer Genie 2	Scientific Industries Inc.

Table 2.1.11 Equipment for Reverse Transcription, RT-qPCR and electrophoresis

Equipment	Manufacturer and Supplier
384 well PCR plate, type 12-40-384-C	BioLabs Products
7900HT Fast Real-Time PCR-Systems	Applied Biosystems / Thermo Fisher Scientific
Electrophoresis Power Supply	Micro-Bio-Tec Brand GmbH
Gel chambers	Peqlab
Labcycler Thermocycler	Sensoquest GmbH
Scout pro 4000g scale SPU4001	Ohaus corporation
Universal Hood II UV-Chamber	BioRad Laboratories GmbH

2. 1. 5. Chemicals, reagents, diet and kits

Table 2.1.12 Aquarium water components

Chemicals	Manufacturer and supplier
Instant Ocean Sea Salt Mixture	Spectrum Brands Inc.
Methylene blue solution; 1,5%	Sigma-Aldrich GmbH
$NaCHO_3$	Carl Roth GmbH, Germany

Table 2.1.13 Zebrafish adult and larvae food

Flake food und chemicals	Manufacturer and supplier
Cholesterol; 99%	Sigma-Aldrich GmbH
Frozen artemia cysts	Sanders, USA
Sera Micron, larvae nursing	Sera GmbH
Tetramin Xl Flakes, adult fish breeding	Tetra GmbH

Table 2.1.14 Sedative production

Chemicals	Manufacturer and supplier
Puffran® Tris-HCl buffer	Carl Roth GmbH
Tricaine 3-amino benzoic acidethylesther; MS-222	Sigma-Aldrich Chemie GmbH

Table 2.1.15 Histological dies, fixers and chemicals

Chemicals	Manufacturer and supplier
2-Propanol	Roth GmbH
Aquatex embedding medium	Merck, USA
EDTA solution	Otto Fischar GmbH
Hematoxylin	Richard-Allan Scientific/ Thermofisher Scientific
Eosin	Shandon/Thermofisher Scientific
Oil Red O	Sigma Aldrich Chemie GmbH
Paraformaldehyd 4%	Morphisto GmbH
1x PBS w/o Ca^{2+} and Mg^{2+}	Lonza, Switzerland
Tissue tek freezing medium	Leica Biosystems GmbH
Type NF Immersion Oil	Nikon Inc.

Table 2.1.16 Anticoagulants employed in blood extraction procedures

Chemicals	Manufacturer and supplier
Heparin Natrium 25.000 I.E.	Ratiopharm GmbH
NaCl saline solution	Berlin-Chemie AG

Table 2.1.17 Cholesterol measurement in zebrafish plasma

Kit	Manufacturer and supplier
Cholesterol Assay Kit (Z5030055)	Biochain, USA

Table 2.1.18 mRNA extraction reagents

Kit and reagents	Manufacturer and supplier
Chloroform	Sigma Aldrich GmbH
Ethanol; 96%	J.T. Baker
Rnase Blaster Solution	Clontech Laboratories Inc.
RNase free DNase I + RDD Buffer	Qiagen
RNeasy® Plus Mini Kit	QIAGEN GmbH
TRIzol®	Thermo Scientific Fisher

Table 2.1.19 RT-qPCR reagents and kit

Reagents and kit	Manufacturer and supplier
5x first strand buffer	Invitrogen Canada
dNTPs: 100mM stock	Promega, Madison USA
DTT 0,1M	Invitrogen
Hexanucleotid Random Primer Mix	Carl Roth GmbH
M-MLV Reverse transcriptase 200U/ul	Invitrogen
PowerUp SYBR Green Master Mix	Applied Biosystems, life Technologies
Ribolock RNase Inhibitor, 40U/µl 2500U	Thermo Scientific Fisher

Table 2.1.20 Gel electrophoresis

Chemicals	Manufacturer and supplier
1x TBE; 100mM Tris Base, 83mM Boric acid, 1mM EDTA	Sigma-Aldrich GmbH Carl Roth GmbH
DNA ladder; 100bp, 21 KB, 1:10 dilution	Peqlab
LE Agarose	BioZyme GmbH
Loading buffer Loading Dye; 99% Formamid 1% Dextran Blue	Sigma-Aldrich GmbH Bio-rad
SYBR Green I; 1:200 in DMSO and 1:2 to Loading Dye	Invitrogen

Table 2.1.21 Software and databases

Software and databases	Supplier
Biorevo BZ-II Viewer	Keyence Deutschland GmbH
Ensembl; *ensembl.org*	European molecular biology laboratory - European Bioinformatics Insitute, Wellcome Genome Campus, UK
GIMP	GNOME Foundation
Matlab	Mathworks inc.
Office 2013; Word, Excel	Microsoft corp.
Primer3web; *primer3.ut.ee*	Department of Bioinformatics, University of Tartu, Estonia
Prism 7	Graphpad Software
SDS 2.2.2	Applied Biosystems / ThermofisherScientific
Zebrafish International Network; *zfin.org*	ZFIN, University of Oregon, USA

2. 1. 6. Genomic database and primer design tools

Zebrafish orthologues corresponding to the human genes of interest were identified using the *Ensembl* and *ZFIN* genomic database. Corresponding primers for RT-qPCR based on the provided exonic DNA sequences were designed with the help of *Primer3web*.

2. 1. 7. Primer sequences

Forward and reverse primers were designed to be situated over two consecutive exon boundaries to prevent amplifications of genomic DNA (gDNA). Suitable primers were chosen at a length of 18 to 27bp, a GC content of 40 to 60%, melting temperature of 55° to 64°C and a product length of approximately 100 to 250bp. The selected primer sequences were ordered from and produced by Eurofins Genomics. House-keeping primer gene sequences were obtained from Lin et al. (2008).

Table 2.1.22 Genes of interest and house-keeping gene primer sequences

Human Gene	Zebrafish orthologue		Primer Sequence 5' -> 3'	GC [%]	Tm [°C]	Length [bp]
ATF3	***atf3***	Forward	TGAACACTGAGAGACCCACC	55	59.4	218
		Reverse	TTGGTTCTTCAGCTCCTCGA	50	57.3	
HBEGF	***hbegfa***	Forward	ACTTTTGCATCCACGGAACC	50	57.3	171
		Reverse	AGAGAACCACAGCTACCACA	50	57.3	
	hbegfb	Forward	AAGGAGGAGCAGCGTTACAG	55	59.4	161
		Reverse	GTTGCCTCGAGTTTGACCTT	50	57.3	
SORT1	***sort1a***	Forward	AATCGCCGTGGTCATCATTG	50	57.3	234
		Reverse	CTCCAGTGTGTCCAGGTCAT	55	59.4	
EF1α (House-keeping)	***ef1α***	Forward	CTGGAGGCCAGCTCAAACAT	55	59,3	87
		Reverse	ATCAAGAAGAGTAGTACCGCTAGCATTAC	41,4	63,9	

2. 2. Methods

2. 2. 1. Aquaculture

2. 2. 1. 1. Zebrafish husbandry

Husbandry methods were based on protocols published in *"The zebrafish book; A guide for the laboratory use of zebrafish (Danio rerio)"* by Monte Westerfield.

Female and male adult zebrafish were kept separately in TECHNIPLAST self-cleaning aquarium racks at a density of < 7 fish/L. Aquarium water was kept at a pH=7,4 and a constant temperature of 28,5°C. Water samples were regularly subject to control for water quality and traces of pathogens. Light cycles were kept at 14 hours of daylight and 10 hours of darkness in accordance to the zebrafish circadian rhythm. Husbandry diet consisted in flake-food for morning and evening feedings and fresh brine shrimp (artemia) in the afternoons.

2. 2. 1. 2. Aquarium water production and storage

Aquarium water for larvae nursing and feeding experiments consisted in distilled water enriched with Instant Ocean Sea Salt mixture and $NaCHO_3$. To produce 100L of aquarium water, 12,5g sea salt and 18g $NaCHO_3$ was added to the according volume of distilled water. Stock water was then stored in a 100L oval tank fitted with a 100W aquarium heater and an air pump to insure a constant water temperature of 28,5°C as well as a continuous oxygenation. Egg water was prepared by adding a single drop of 1,5% methylene blue solution per liter of aquarium water. Here, methylene blue prevents fungus to grow in the water and stains unfertilized eggs in blue permitting simpler identification in the selection of viable eggs.

2. 2. 1. 3. Zebrafish breeding

Zebrafish mating habits are photoperiodic and occur in the early morning hours. For optimal breeding results, controlled mating took place in TECHNIPLAST 1L mating tanks at a ratio of one male to two females. The fish were placed the eve of the desired breeding time point in the tanks and kept separate overnight by a wall for approximately 12 hours. Within the first minutes of the morning lights, the wall was slid up to allow the zebrafish to mate and the eggs to fertilize while floating free in the water. The eggs sank to the bottom through railings into a lower compartment to be kept safe from potential parental cannibalistic behavior. The parent fish were then placed back into their aquariums and the eggs were harvested by pouring the tank water through a sieve.

2. 2. 1. 4. Larvae nursing

Embryonic eggs were kept for the first three days of development in petri dishes containing methylene blue egg water that was renewed every 12 hours. Unfertilized eggs stained in methylene blue were discarded with the help of disposable Pasteur pipettes. The egg-containing petri dishes were kept at 28,5°C within incubators under a 14h/10h light cycle. After 72hpf, hatched larvae were transferred into 500ml transparent polystyrene containers filled with aquarium water at a density of 60 larvae/L. The containers were immersed 5cm deep in a 45L water bath to be kept at a constant water temperature of 28,5°C. Lighting according to the zebrafish circadian rhythm was provided by a timer regulated aquarium lid covering the water bath. Container bottoms were cleaned every day from feces, food residues and dead larvae with the help of disposable Pasteur pipettes. A third of the container's content was replaced by fresh aquarium water every day.

2. 2. 1. 5. High cholesterol diet preparation

The preparation of the high cholesterol diet was based on methods published in "*Vascular lipid accumulation, lipoprotein oxidation, and macrophage lipid uptake in hypercholesterolemic zebrafish*." by Stoletov et al. 2009. The production of 1g 4%-HCD requires 40mg powdered cholesterol and 960mg of Tetramin flake-food for adult zebrafish or Sera micron for larvae. According to the manufacturers, these contain 11% and 7,0% raw fat content respectively. The ingredients were placed in a 250ml glass container, dissolved into diethyl ether and stirred with a spatula. The solution was then placed overnight under a fume hood to allow the diethyl ether to evaporate. The dry residual granulate was then scraped and collected with the help of a spatula into a Falcon® tube and stored in a dark and dry place.

2. 2. 1. 6. Tricaine MS-222 preparation

Tricaine (3-amino benzoic acid ethyl ester; MS-222) is a sodium-channel blocker commonly used for anesthesia and euthanasia of fish (Attili and Hughes, 2014). To produce a 125ml stock solution at concentration of 4g/L, 500mg of powdered-form tricaine was added to 123ml of distilled water in a sterilized 250ml glass beaker. The resulting acidity was gradually adjusted to pH=7,1 with approximately 2ml of Tris-HCl buffer solution (1g/L; pH=8,5) under the monitor of a pH-meter. The work solution was brought to a homogenous solution with the help of a magnetic stirrer and stored at -20°C until further usage. Before application on the zebrafish, a 100ml of 4.2% work solution was prepared by diluting 4,2ml stock solution into 95,8ml of distilled water.

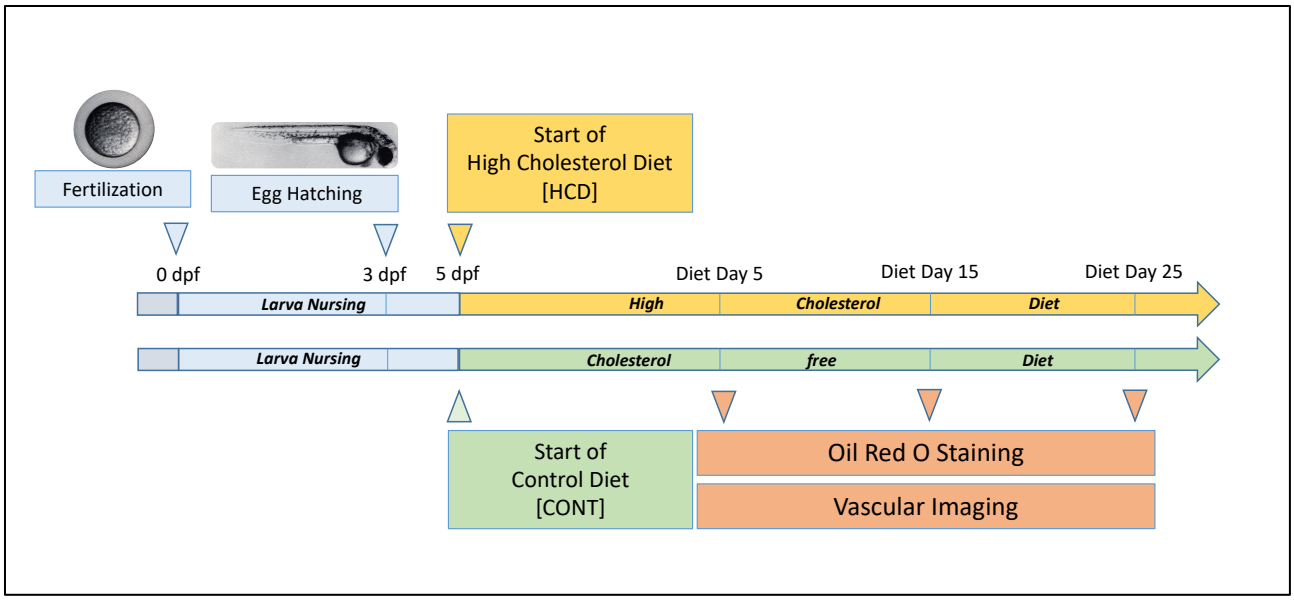

Figure 2.2.1 Experimental set-up for HCD-feeding in Larvae.
Images modified from Kimmel et al.

2. 2. 1. 7. High cholesterol diet plan in larval trials

At the age of 5dpf, three groups of 15 to 30 larvae were raised separately in containers and fed twice daily a spatula of HCD for respectively 5, 15 and 25 days. Correspondingly, three additional larvae groups were fed a control diet of Sera micron with no additional cholesterol (Figure 2.2.1).

2. 2. 1. 8. Oil Red O (ORO) lipid dye preparation

ORO stock dye was prepared by adding 0.5mg Oil Red O in powdered form to 100ml 99% 2-propanol. 60ml of ORO stock solution were added to 40ml distilled water. The solution was left to incubate for 60min at room temperature and was filtered through Whatman paper filters.

2. 2. 1. 9. Larvae ORO whole mount staining

Upon reaching the desired diet time-point, the larvae were euthanized in tricaine and placed into filter bottomed inserts on a 3x4 well plate to be fixated overnight in 4% formaldehyde at 4°C. During the staining process, the inserts containing the fixated larvae were first placed for 10min into 60% 2-propanol, then submerged for 3 hours in ORO solution. Excess ORO was then washed out of the larvae using 60% 2-propanol in two consecutive steps of 10 minutes each, followed by a rinse under running tap water. Stained larvae could then be stored in distillated water until imaging on the next day.

Table 2.2.1 Stain protocol for whole mount histology of larvae

Stain Step	Duration [min]
60% 2-Propanol (1)	10 :00 Standing
Oil Red O	180:00 Standing
60% 2-Propanol (2)	10:00 Standing
60% 2-Propanol (3)	10:00 Rinse
Distilled water	5 :00 Rinse

2. 2. 1. 10. Larval vasculature imaging

Whole-mount-stained larvae were placed under a fluorescent microscope to image the tail region in 100x magnification. The optical tissue transparency in young zebrafish larvae allow for the direct imaging of the dorsal aorta and the caudal vein. The images were cropped down to the vessels of interest using GIMP and fed into a Mathlab script. En-face calculations of fields covered by red pixels provided an estimate of the surface covered by ORO-stained lipids in the vessels of interest (Figure 7.1 in Appendix).

2. 2. 2. Histological study of vascular lipid accumulation

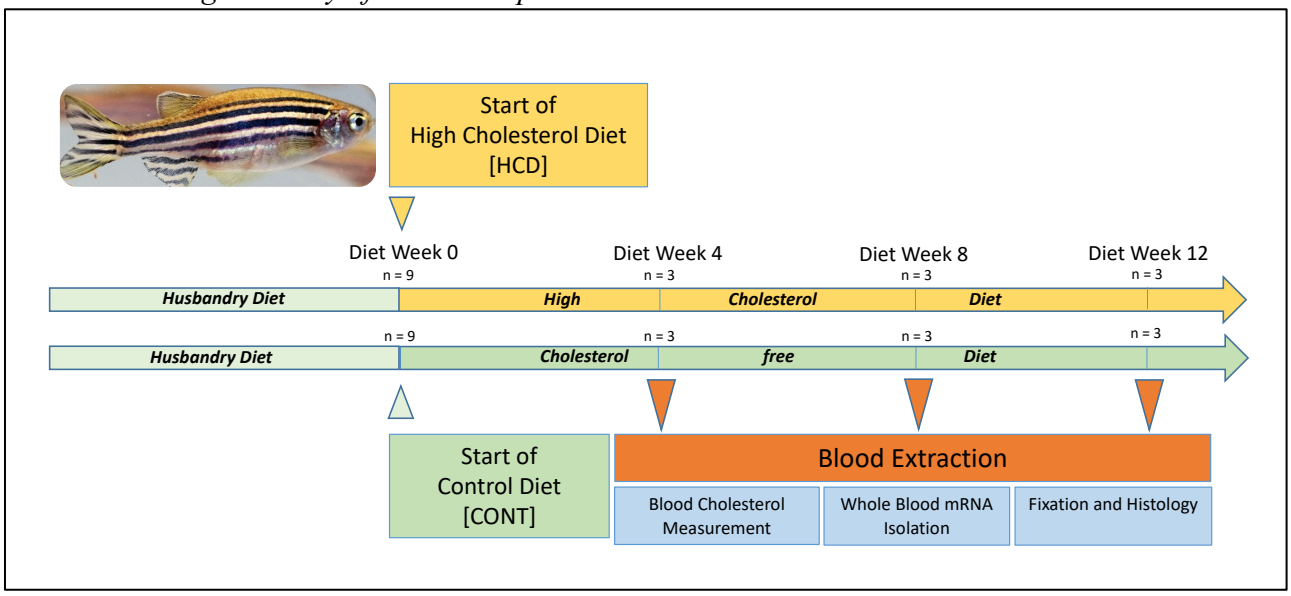

Figure 2.2.2 Experimental set-up for HCD-feeding in adult zebrafish with following blood analysis and histology.

2. 2. 2. 1. Fish tail conservation, embedding and histological sectioning

Tail amputates were conserved in 15ml Falcon tubes containing 4% PFA. In preparation of the histological cuts, the tails were embedded in EDTA for 8 days to allow tissue decalcification. The tails were then embedded in reaction tubes at room temperature with tissue freezing medium 24h before sectioning. On the following day, the samples were brought to freeze at -20°C in the cryotome. 35µm sections were obtained to maintain overall stability of the

connective tissue. With a fine brush, the frozen sections were collected and placed in NetWell™ inserts on a 3x4 plate to float free in 1xPBS solution. For tissue staining, the inserts were placed into dye- and solvent-containing wells in the following order:

Table 2.2.2 Hematoxylin & Eosin stain protocol for adult fish tails

Stain Step	Duration [min]
Hematoxylin	5 :00 Standing
Tap water	5:00 Rinse
Eosin	00:30 Standing
Tap water (1st)	00:30 Rinse
70% Ethanol	00:10 Rinse
96% Ethanol	00:10 Rinse
100% Ethanol (2nd)	00:10 Rinse
100% Ethanol (3rd)	00:10 Rinse
Xylol (1st)	3:00 Rinse
Xylol (2nd)	3:00 Rinse

Table 2.2.3 Oil red O stain protocol for adult fish tails

Stain Step	Duration [min]
60% 2-Propanol (1st)	10 :00 Standing
Oil Red O	15 :00 Standing
60% 2-Propanol (2n)	5 :00 Standing
60% 2-Propanol (3rd)	5 :00 Rinse
Distilled water (1st)	5 :00 Standing
Hematoxylin	5 :00 Standing
Tap water	1:00 Rinse

The stained sections were placed to float free in a 1xPBS-containing petri dish. The dish was placed under a dissection microscope to identify the aortic rings and separate them away from surrounding tissue. The rings were then placed on a slide, embedded in Aquatex medium and sealed under a cover slip. The slide was then imaged at 100x magnification with immersion oil microscopy.

2. 2. 3. CAD associated risk gene expression in zebrafish blood

2. 2. 3. 1. Blood extraction method from adult zebrafish

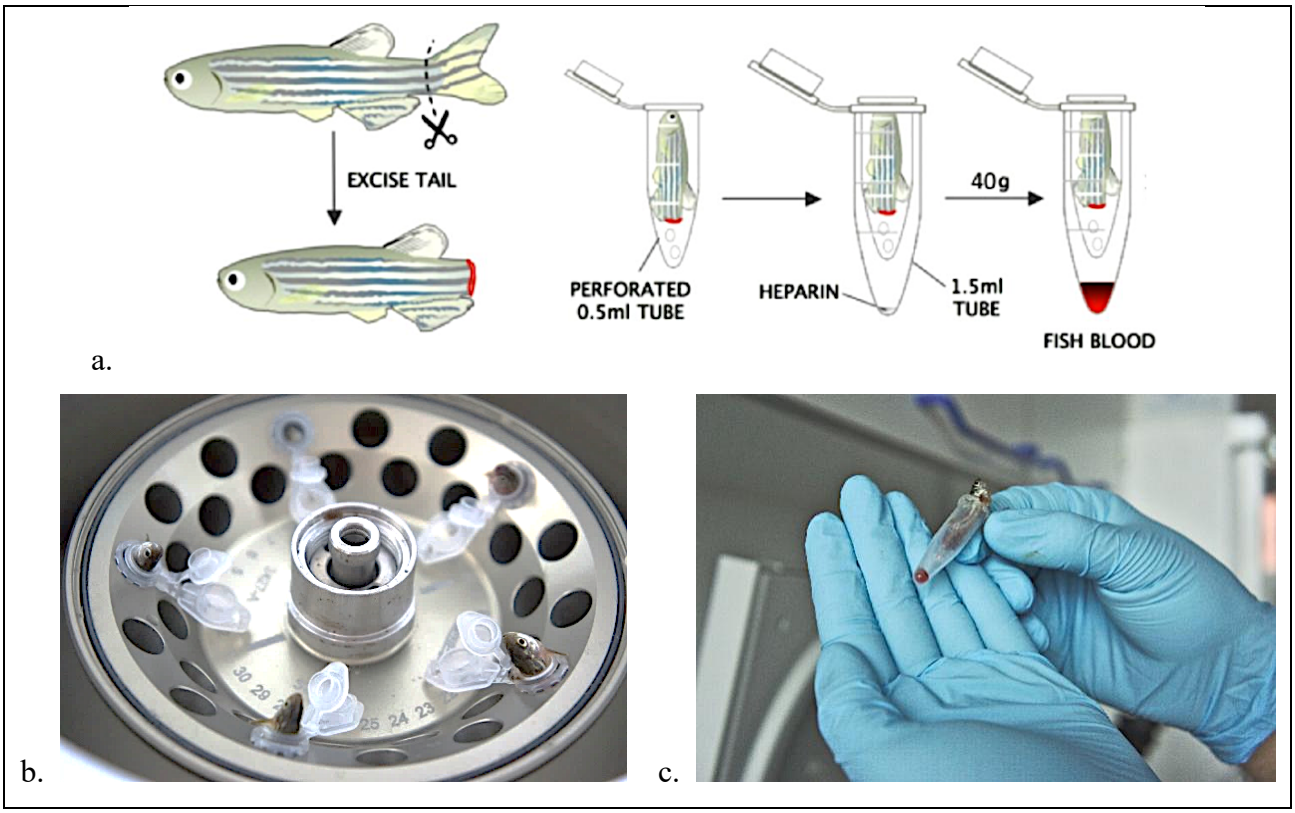

Figure 2.2.3 Blood extraction method by centrifugation in adult Zebrafish
a. Tail amputation of euthanized zebrafish prepared for centrifugation following the Babaei method; Image modified from "Novel Blood Collection Method Allows Plasma Proteome Analysis" by Babaei et al., 2012.
b. Zebrafish placed in their collecting tubes ready for extraction in the centrifuge.
c. Approximately 30µl of blood extracted form a single zebrafish in the bottom of a collecting tube after centrifugation.

Blood was extracted from adult zebrafish following methods published by Babaei et al. (2012). Blood collecting systems were prepared using 0,5ml Eppendorf Safe-Lock reaction tubes previously perforated at the bottom with cannulas. These were placed into similar but larger 1,5ml reaction tube. Both tubes were rinsed and coated beforehand with 10µl heparin to prevent the blood from clotting (Figure 2.2.2; Figure 2.2.3).

Upon reaching the desired diet length, adult zebrafish were euthanized by immersion for 15 seconds in a tricaine-filled 50ml beaker. The fish were taken out of the water with forceps and placed onto a petri dish. With a n°20 feather-scalpel, the tail was amputated at approximately 1 to 2cm from its base below the gut. The amputated fish was then placed into the upper 0,5ml tube with the head facing up and the stump looking down to the perforated bottom.

After loading the fish, all blood collecting systems were placed into the centrifuge in balanced positions. Centrifugation of the zebrafish was set to 5min at 11°C and 40g to ensure extraction

of only blood with no additional organs. By centrifugal force, blood flowed out of the stump through the perforations towards the underlying 1,5mL tube. Up to 40µl of blood can be expected. The blood containing tubes were placed afterwards on ice until the subsequent mRNA isolation. The samples can also alternatively first be stored at -80°C for later treatment. After collection, exsanguinated zebrafish were kept in 4% PFA-filled 15ml Falcon® tubes for later histological studies.

2. 2. 3. 2. Plasma cholesterol measurement

Blood samples were centrifugated at 13700g to separate the plasma. 20µl of the supernatant plasma was transferred and diluted at 1:3 in 1x-PBS. Cholesterol reading was performed on a fluorometric plate reader according to manufacturer's kit instructions

2. 2. 3. 3. Whole fish sample homogenization

A whole fish mRNA sample was used for primer validation purposes and as a positive control marker for RT-qPCR. Prior to homogenization, a single control fed AB-line adult zebrafish was euthanized by immersion into tricaine. The zebrafish was then placed on a petri dish and cut into four equal parts using a n°20 scalpel. All four parts were placed into a 2,0ml safe-lock reaction tube together with 1ml TRIzol and a steel homogenization bead. Tissue homogenization was performed by oscillation for 10min at 50 osc./sec and room temperature in a tissue grinder. The following mRNA extraction was done as described in 2.2.3.4. with adjusted volumes.

2. 2. 3. 4. mRNA isolation from blood

Methods for mRNA extraction from whole blood and whole fish tissue were based and modified from the QIAGEN RNeasy Plus Mini Kit protocols.

500µl TRIzol was added to each whole blood sample to achieve RNA stabilization and RNase inactivation. Blood pellets were mechanically disrupted by repetitive pipetting and vortexing of the content until the solution became homogeneous. Under a fume hood, 100µl of chloroform was added to each tube for protein separation. The tubes were repetitively gently inverted by hand until a milky suspension formed and were kept afterwards standing for 2-3 minutes for phase separation by decantation. A 10 min centrifugation at 16100g and 10°C then followed. This lead proteins and DNA to separate into the underlying organic phase. 300µl of the supernatant RNA-containing aqueous phase was extracted and transferred into a new tube and mixed with an equal volume of 70% ethanol prior to the washing steps. The mixture was transferred into a spin column and was centrifuged for 2min at 9300g. The flow through was discarded and 350µl of RW1 solution was applied to the columns before being centrifuged anew

for 2min at 9300g and 10°C. The flow through liquid was discarded again. Subsequently, 80µl (10µl DNase I + 70µl RDD) of DNase solution was applied to incubate for 20min onto the filter of the spin column to eliminate traces of gDNA. For the final washing, 350µl of RW1 was applied to the columns before being centrifuged for 2min at 9300g and 10°C. The flow through was discarded, 500µl of RPE was applied onto each column before being spun anew for 2min at 9300g and 10°C. The columns were kept standing for 5 minutes and the previous washing step got renewed a second time. Finally, the columns were centrifuged dry in a last step for 3min at 15700g.

To collect the isolated mRNA, each spin column was loaded with 25µl of RNase-free H_2O. The filter was let to soak for 2min before the columns were placed onto a new collecting tube and set for a last centrifugation for 3min at 9300g and 10°C.

2. 2. 3. 5. mRNA concentration reading and storage

Before transcription into cDNA, the collected mRNA samples were subject to concentration and contamination control using photometric reading. 2µl of the obtained mRNA was diluted into 98µl of RNAse-free distilled H_2O. The concentration and optical density (OD) ratio values at 260nm/280nm were measured against water as a blank in an Eppendorf Biophotometer. After the readings, the RNA samples were then stored at -80°C until reverse transcription.

2. 2. 3. 6. RNA electrophoresis and degradation check

Agarose-gel electrophoresis can be an additional method to examine the quality of obtained samples through RNA degradation check. Because the employed protocol uses SYBBR Green I, this step requires a relatively high quantity of RNA at around 1µg. Due to restricted amounts obtained from the blood samples, degradation check could only be applied on the whole fish mRNA sample. The equipment was carefully cleaned first with RNAzap to inactivate residual RNases in the surroundings. RNA samples were stained with 3µl of SYBR Green I in loading buffer and run for 60min on a 1% agarose-gel at 100V, 400mA against a 21kb DNA ladder.

2. 2. 3. 7. Reverse transcription

Table 2.2.4 Reverse Transcription master-mix

Reagents	Volume
5x First strand buffer	4µl
Ribolock 40u/µl	1µl
2mM each dNTP	1µl
Random Hexamer Primer 30,6µmol/µl	1µl
DTT 0.1M	2µl
Reverse Transcriptase 200 u/µl	1µl
Total Volume	**10µl**

Table 2.2.5 Reverse transcription steps

Stage	Temperature [°C]	Time [min]
Denaturation	68	5:00
Stabilization	4	∞
Reverse transcription	37	60:00
Enzyme deactivation	95	5:00
Storage	-20	∞

To prepare the mRNA for RT-PCR analysis, samples must be converted into more stable complementary DNA strands (cDNA). For this step, referred as reverse transcription, a master-mix solution with the necessary reagents was prepared for n+2 mRNA samples to compensate for potential pipetting errors (Tab. 2.16). mRNAs destined for reverse transcription were previously stored at -80°C. The samples were carefully thawed and diluted to an equal concentration of 30ng/µl (±10%) in RNAse-free H_2O at a total volume of 10µl. The samples were then placed into a thermocycler for a 5min denaturation step at 68°C before being cooled down on an ice block at 4°C. The samples were then centrifuged down for 5min at 1080g and room temperature. Subsequently, 10µl of RT master-mix was added to reach a total reaction volume of 20µl. The reaction tubes were vortexed and placed back into the thermocycler for reverse transcription at an incubation temperature of 37°C for 60min. In a final step, the reverse transcriptase got deactivated for 5min at 95°C. The obtained complementary DNA strands was then stored at -20°C until further usage.

2. 2. 3. 8. Primer dilution

Primers ordered at Eurofins were first resuspended with distilled H_2O according to the manufacturer's recommendation to a stock concentration of 100µmol/µl. Forward and reverse primers were kept separately, diluted again 1:10 into 100µl working solutions and stored at -20°C until further usage.

2. 2. 3. 9. Real Time Quantitative PCR

Table 2.2.6 RT-qPCR reaction master-mix

Reagents	Volume
2x Power up SYBR Green	3,75µl
H_2O	1,125µl
Forward Primer 10µmol/µl	0,5625µl
Reverse Primer 10µmol/µl	0,5625µl
cDNA or control sample	1,5µl
Total Reaction Volume	**7,5µl**

Table 2.2.7 7900HT RT-qPCR steps

Stages	Temperature [°C]	Time [min]
1 UNG-denaturation	50,0	2:00
2 Initial denaturation	95,0	10:00
3+4 Polymerase chain reaction	95,0	00:15
[40 cycles]	60,0	1:00
5 Dissociation stage	95,0	00:15
	60,0	00:15
	95,0	00:15

Real time quantitative polymerase chain reaction (RT-qPCR) allows the analysis of gene expression alteration between a treated sample and a control group. The expression level of a gene is measured by real time quantification of cDNA strands obtained by reverse transcription of the sample's mRNA. Conventionally, small amounts of DNA are amplified at an exponential rate with each adding PCR cycle. With 7900HT qPCR in particular, amplified cDNA can be quantified by the detection of SYBR Green incorporation into the produced double-strand DNA. The emitted fluorescent signal grows exponentially with each cycle and is proportional to the amount of produced cDNA copies. The measured signal is then plotted against the PCR cycle numbers on a logarithmic scale (Poitras and Houde, 2002).

Comparative quantification between both samples is obtained by setting a threshold line in the exponential growth phase of the curve to determine the corresponding cycle number (Ct). On a

logarithmic plot, this growth phase appears linear. To avoid measuring false signals, the threshold line must be set sufficiently above the initial background signal, yet low enough under the plateau phase of the PCR. The higher the starting quantity of a specific transcript mRNA strand in the sample, the lower the obtained Ct-value will be in qPCR. In turn, low Ct-values can be interpreted as an increased production of the corresponding protein in response to the applied treatment. Additionally, the expression level of housekeeping genes is measured for each sample in a separate well on the same qPCR plate. House-keeping genes, for instance here *ef1α*, are essential to cellular function and are expressed at a constant level in all types of tissue. The obtained results permit then to normalize the Ct-values of the genes of interest (*Real-PCR handbook*, Life Science Technologies 2012; Eisenberg and Levanon, 2013)

For each gene of interest, a master mix solution containing a gene specific primer pair and necessary reagents for the qPCR-polymerase was prepared for a triplicate run of HCD- and control-fed samples as well as a positive and a negative control reaction (Tab. 2.24). To counter pipetting error, the master mix volume was prepared for n=8+2 reaction. 6µl of master mix was loaded into its respective position on a 384-well plate. cDNA samples of HCD and control fed fish were diluted at 1:5 and distributed in volumes of 1,5µl into each respective technical triplicate well. 1,5µl whole fish cDNA in 1:15 dilution and H_2O were added into single wells with the according master-mix for their respective positive and negative control reaction. The fully loaded plate was then sealed with foil, centrifuged down for 5min at 1080g and 20°C and stored for maximum 72 hours at 4°C until analysis in the 7900HT (Tab. 2.25).

2. 2. 3. 10. Primer validation

Ordered primers were evaluated applying the 7900HT RT-qPCR program (Tab. 2.25) on whole fish cDNA samples in four steps of a 1:5 serial dilution, starting with 1:1 at 100 ng/µl down to 1:625 with n=3 triplicate runs per dilution step. H_2O was used as a negative control to rule out contamination. Serial dilution allows to assess the amplification of the desired PCR products at different template concentrations. Additionally, evaluation of the dissociation curve and the gel-electrophoresis of the resulting PCR permit to check the specificity of the amplified PCR product. Specific products are represented as a single peak in the melting curve and a single band at the expected product length on the gel-electrophoresis.

2. 2. 3. 11. Agarose gel-electrophoresis and UV-visualization

Following RT-qPCR, gel-electrophoresis permits the visualization of the amplified genetic products under UV-light. Here, the appearing products are checked if they materialize as single bands at the expected bp-length. The gel was prepared at a 1,5% agarose concentration in 1x

TBE. The mixture was brought into an Erlenmeyer flask and boiled in a microwave for 7min. The clear liquid was then slightly cooled for 5min, with the flask placed in a water-bath at room temperature under a magnetic stirrer. The liquid was then poured into the chamber mold to solidify into a gel. Once hardened, the gel was placed in the electrophoresis chamber and immersed in 1x TBE. On the qPCR plates, samples were mixed with 3µl SYBR Green I-containing loading buffer per well, vortexed and centrifuged down for 5min at 1080g. The dyed samples were then individually loaded into their respective gel pouch. The PCR products were run against a 100bp ladder as electrophoresis was set at 400mA, 150W, 120V for 80min. Following the run, the gel was finally placed in an UV-chamber for imaging.

2. 2. 3. 12. Relative gene expression analysis

Relative expression analysis was performed using the ΔΔCt-method (Livak and Schmittgen, 2001). Ct values of sample triplicates were averaged and normalized against the averaged housekeeping equivalent to calculate ΔCt. The HCD-ΔCt is subtracted by ΔCt of the control group to obtain ΔΔCt. For relative comparison between both groups, $2^{-\Delta\Delta Ct}$ can be calculated for each gene of interest in corresponding sample pairs.

2. 2. 4. Statistical data analysis

Statistical analysis of the obtained data was performed using GraphPad Prism.

2. 2. 4. 1. Analysis of larval vasculature imaging data

An averaged lipid coverage value with standard deviation was calculated in each vessel of interest for each respective diet time-point. Normal distribution was verified employing D'Agostino-Pearson test. Statistical significance was evaluated by applying Mann-Whitney U test and Kruskal-Wallis one-way ANOVA with $p<0.05$.

2. 2. 4. 2. Analysis of relative gene expression data.

An averaged $2^{-\Delta\Delta Ct}$-value with standard deviation was determined for all three biological replicates. Values in HCD-fed groups were normalized against their control-fed equivalents. Normal distribution analysis was verified employing D'Agostino-Pearson test. Statistical significance was evaluated by applying unpaired Student's t-test with $p<0.05$.

3. Results

3.1. Vascular lipid accumulation in larvae under HCD

Based on Stoletov et al.'s protocol, a 4% high cholesterol diet was prepared with the aim to test the induction of lipid deposition in the zebrafish's vasculature. The diet was tested on larvae within the time frame provided by their optical transparency. Upon reaching the desired length at 5, 15 and 25 days of diet, the larvae were stained in ORO and hematoxylin. The dorsal aorta and caudal vein were imaged under the microscope and lipid covered surfaces were quantified.

3.1.1. Descriptive study of ORO whole-mount stained larvae

In figure 3.1.1, representative images are displayed of ORO whole-mount stained larvae of both diet groups after 5, 15 and 25 days of feeding. At all three time-points, all control-fed fish show no red stained lipid deposits in the dorsal aorta nor in the caudal vein. In the HCD-fed larvae, distinctive lipid streaks occur in the vasculature. These materialize first as limited and punctual drops at 5 days of diet. The streaks grow and develop into more sizeable streaks in the 15-day group. The deposits appear thicker in the caudal vein than in the dorsal aorta. Additionally, ORO stains accumulate in the intersegmental arteries and the liver. At the end of the trial, the complete vasculature appears extensively covered with lipids. As the larva reaches the age of 30 days, optical transparency decreases as pigmentation starts to develop and overshadow the vasculature, particularly above the caudal vein. Microscopic images of whole-mount stained larvae reflect the results found in the time-course plots (Fig. 3.1.5).

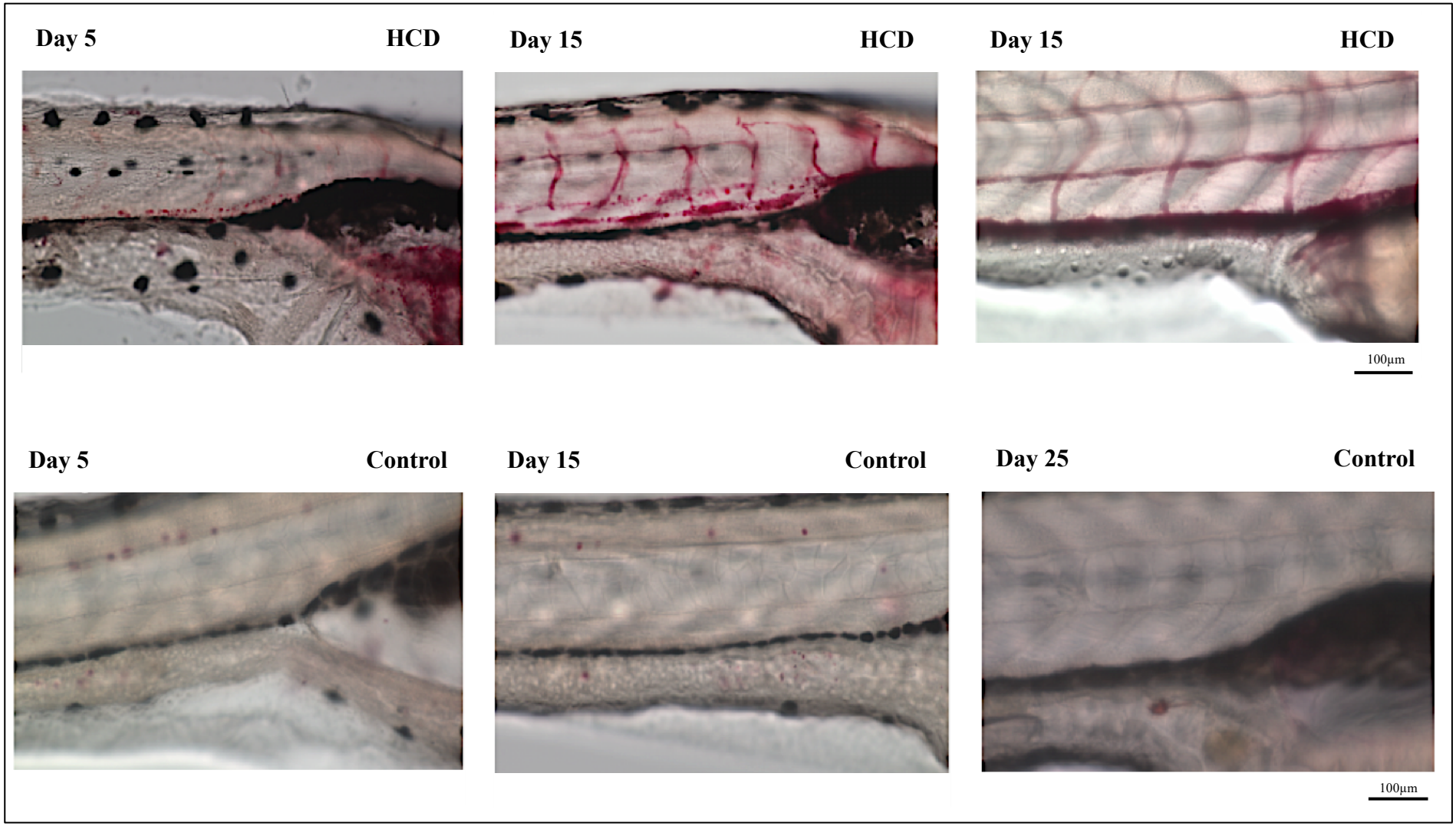

Figure 3.1.1 Microscopy images of Oil red O whole-mount stained larvae of HCD- and control-groups at 5, 15 and 25 days of diet (100x).

3. 1. 2. Lipid covered surface quantification in major tail vessels

After imaging of the whole-mount stained larvae, surfaces covered by Oil Red O-stained lipids in the dorsal aorta and the caudal vein were quantified in the tail section of both groups (Figure 7.1).

3. 1. 2. 1. Results at 5 days of diet

At 5 days of feeding, average surface measurements of ORO-stained lipids in the caudal vein was found to be significantly higher in the HCD-fed group. In comparison, the control group showed close to no vascular deposits (CV: HCD 3.16% ±0.70; CONT 0.39% ±0.15; U=43 p=0.007) (Fig. 3.1.2).

In the dorsal aorta, average coverage is moderate yet still significantly higher in the cholesterol-fed group as well (DA: HCD 1.30% ±0.48; CONT 0.13% ±0.05; U=62 p=0.0485).

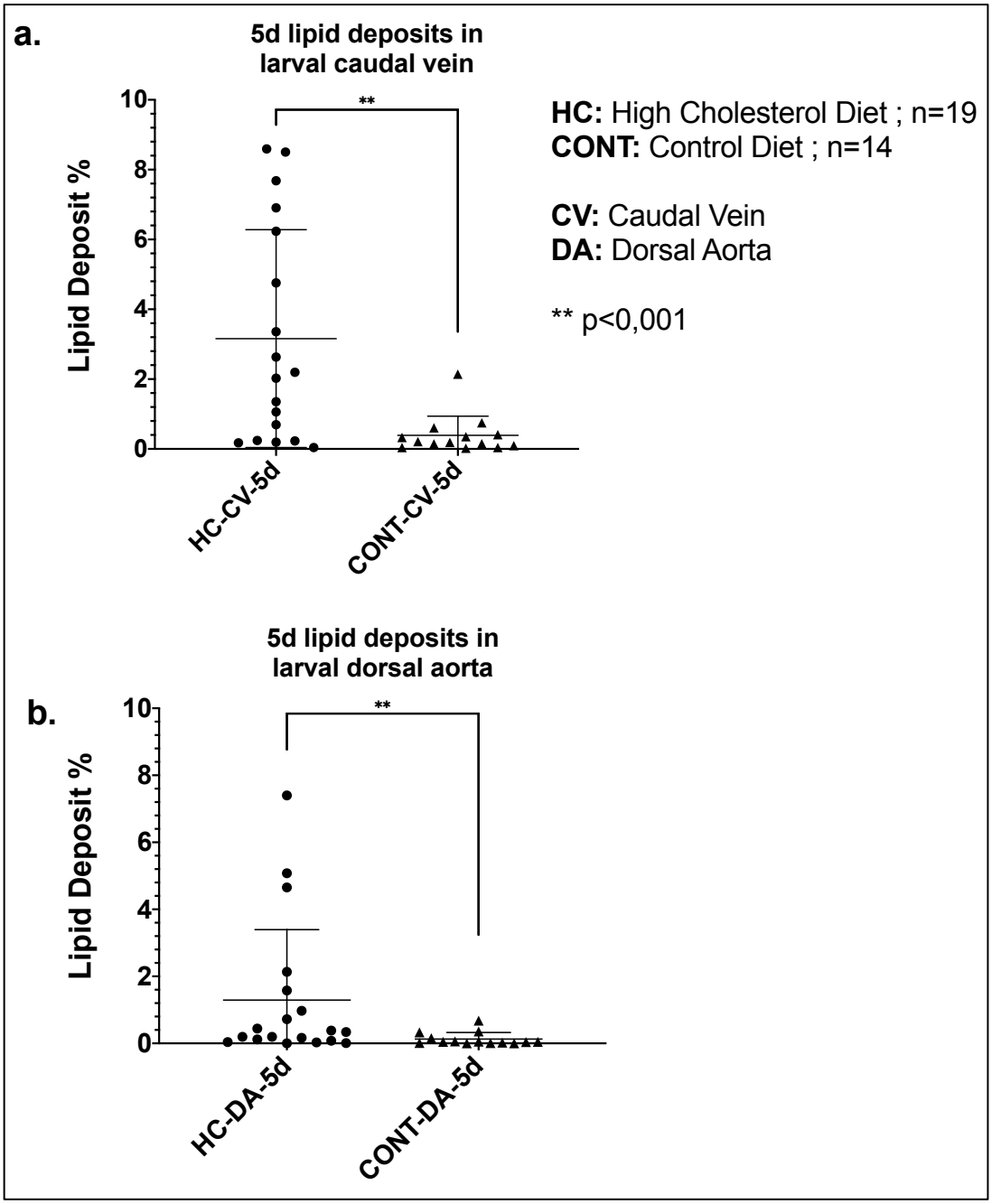

Figure 3.1.2 Lipid deposit coverage in major tail vasculature of zebrafish larvae at 5 days HC and control diet

3. 1. 2. 2. Results at 15 days of diet

After 15 days of feeding, the coverage of lipid deposits in the caudal vein remains significantly larger in the high cholesterol group than in control (CV: HCD 12.34% ±1.12; CONT 0.14% ±0.06; U=0, $p<0.0001$) (Fig. 3.1.3).

A similar clear difference is observed in the dorsal aorta, in which the lipid covered surface in the HCD-group reaches an average of approximately 20% while remaining inexistent in the control group (DA: HCD 22.04 ±1.75; CONT 0.09% ±0.05; U=0, $p<0.0001$).

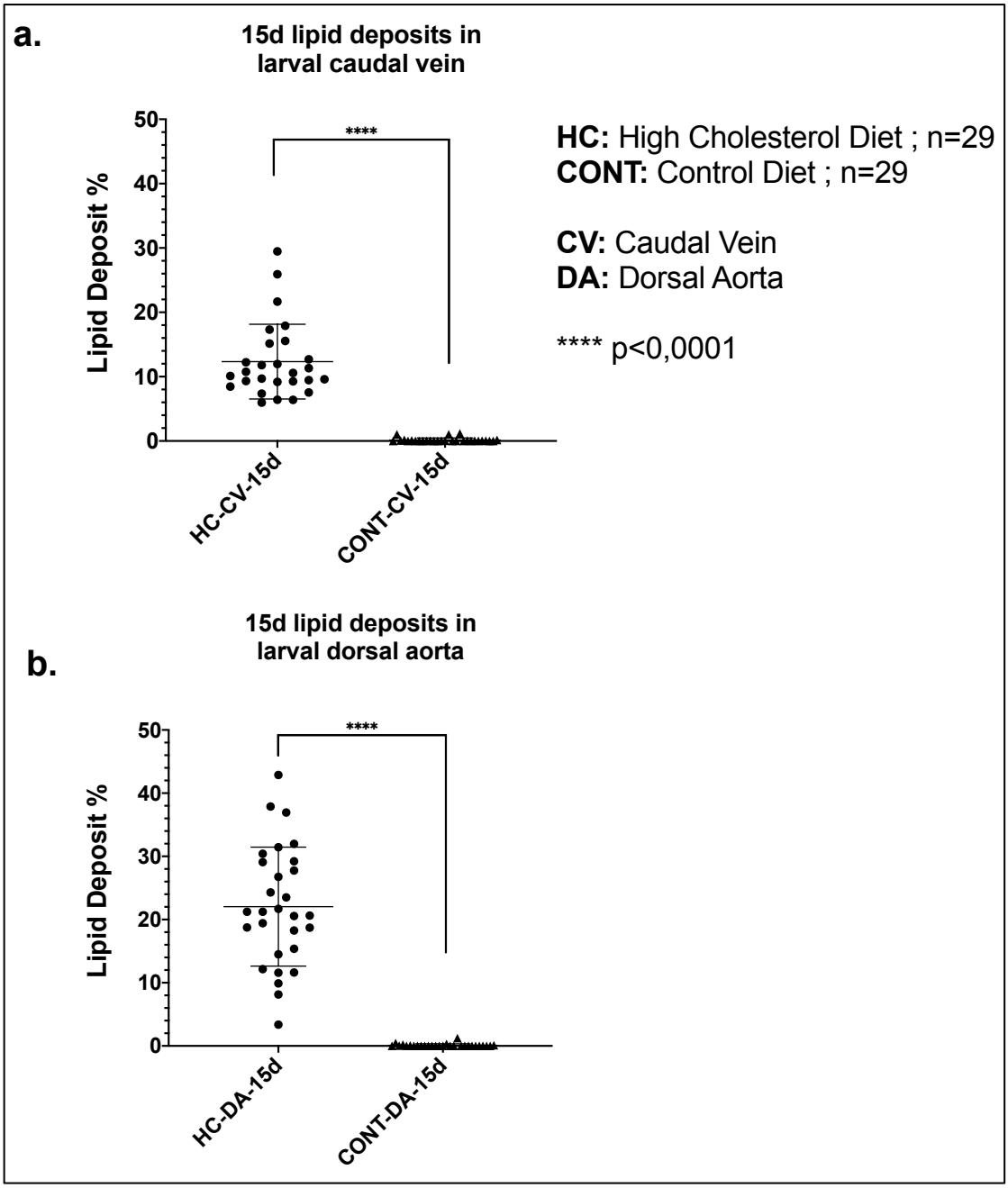

Figure 3.1.3 Lipid deposit coverage in major tail vasculature of zebrafish larvae at 15 days HC and control diet

3. 1. 2. 3. Results at 25 days of diet

In the last measured time-point, the vascular lipid coverage remains significantly greater in both vessels for the cholesterol-fed group. In the caudal vein, the control-fed larvae show close to no deposits (CV: HCD 13.79% ±1.27; CONT 0.26% ±0.08; U=0, p<0,0001) (Fig. 3.1.4).

An identical result is observed in the dorsal aorta (DA: HCD 14.06% ±2.10; CONT 0.18% ±0.09; U=0, p<0,0001).

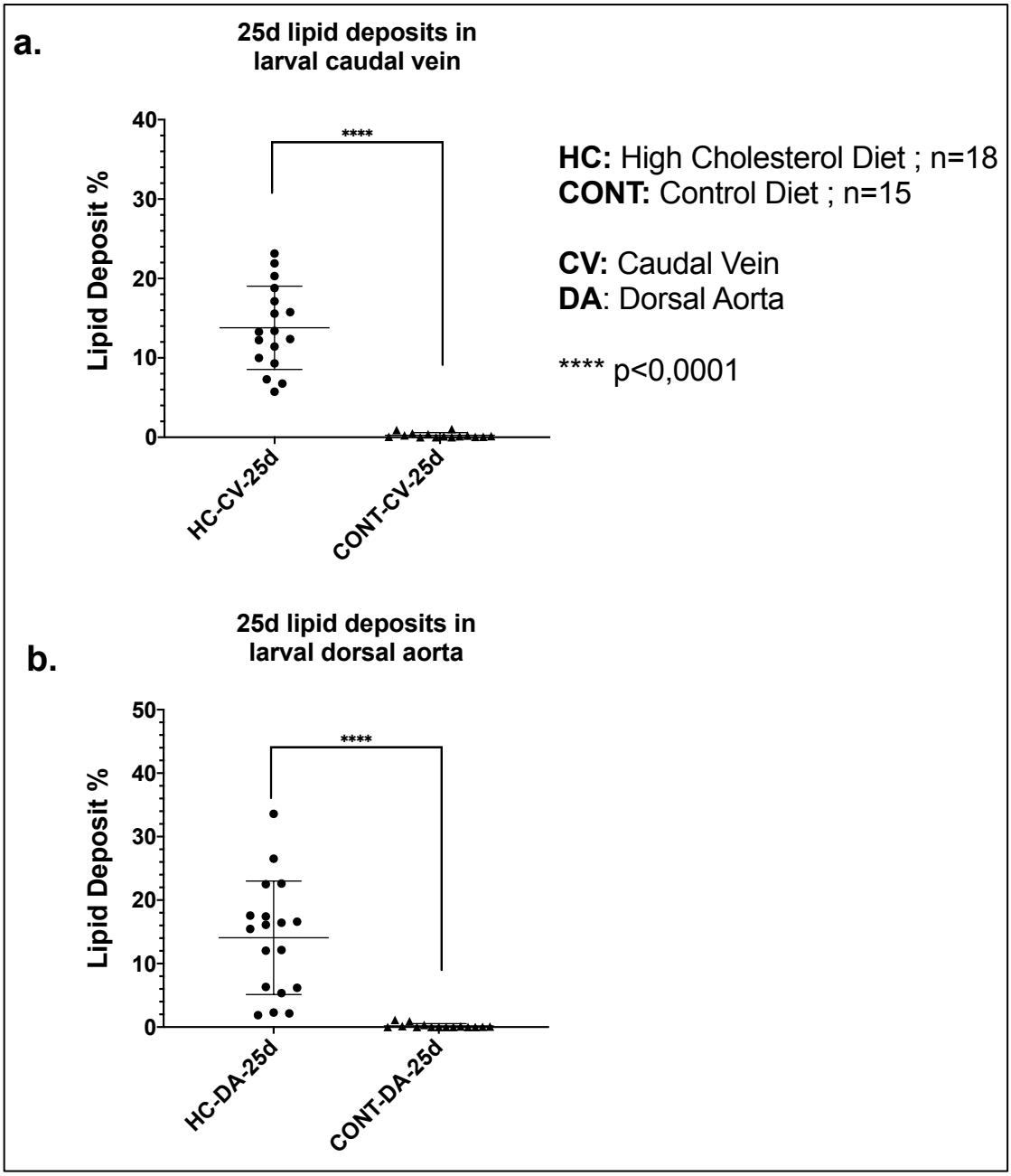

Figure 3.1.4 Lipid deposit coverage in major tail vasculature of zebrafish larvae at 25 days HC and control diet

3. 1. 2. 4. Evolution of vascular lipid deposits under HCD

On a time-course plot, the evolution of ORO stained lipids covering the vasculature can be studied throughout the three chosen time-points (Fig. 3.1.5).

At 5 days of high cholesterol diet, both vessels show a low initial lipid coverage, with average levels minimally higher in the caudal vein than in the dorsal aorta (CV: 3.16% ±0.70; DA: 1.30% ±0.48).

At the 15-day time-point, the amount of deposits increases sharply, with the highest levels being recorded in the dorsal aorta (DA: 22.04 ±1.75). Average coverage in the

caudal vein increase in a similar manner, remaining though in contrast to earlier stages below values found in the DA (CV: 12.34% ±1.12).

At 25 days of diet, the extent of lipid coverage come to equal levels in both vessels. The ORO-covered surface in the caudal vein shows a limited increase but remains overall stagnant (CV: 13.79% ±1.27). In the DA, the covered levels decrease and close in to merge with values measured in the CV (14.06% ±2.10).

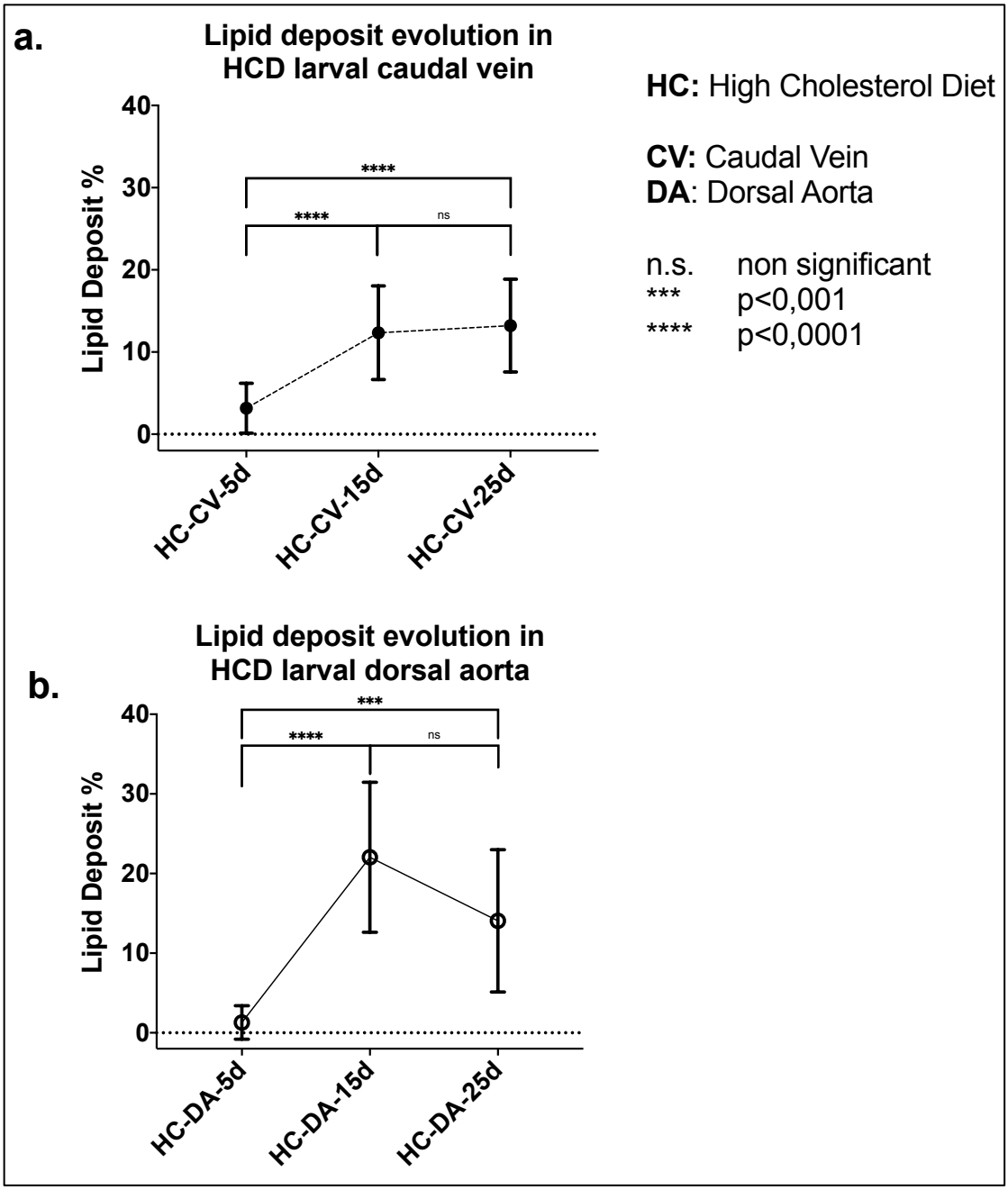

Figure 3.1.5 Vascular lipid deposit evolution in larvae fed 5, 15 and 25 days HCD.

3. 2. Cholesterolemic, vascular and genetic response to HCD in adult zebrafish

3. 2. 1. High Cholesterol Diet effects on blood lipid levels in zebrafish adult vasculature

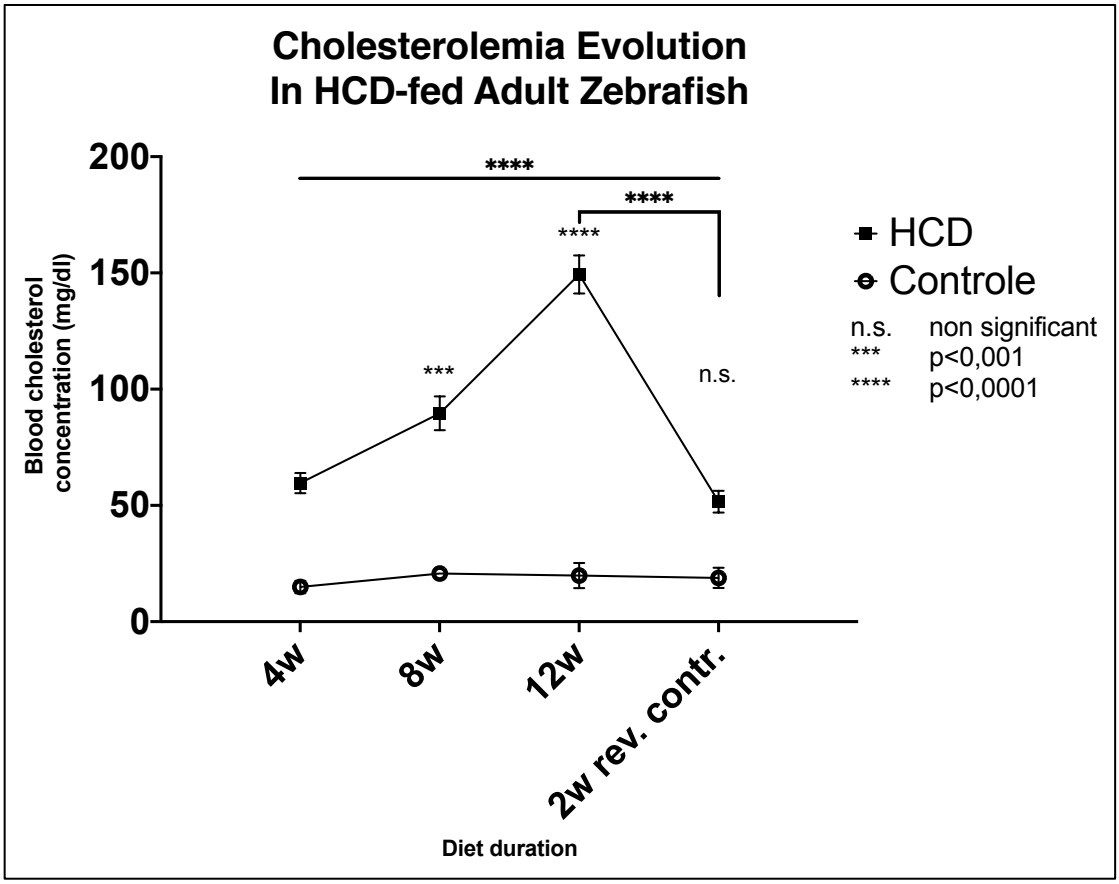

Figure 3.2.1 Total cholesterol concentrations measured in adult zebrafish blood fed up to 12 weeks HCD and control diet with subsequent 2-week reversal.

Next, the high cholesterol diet was tested for its ability to develop hypercholesterolemia in adult zebrafish. In a time-course of 12 weeks, blood was collected by centrifugation every four weeks from respectively n=3 HCD- and control-fed fish (Fig. 3.2.1). Total cholesterol concentrations in plasma were evaluated by fluorometric methods. Effect reversal was verified by setting the remaining fish back on a cholesterol-free diet in the last three weeks of the trial. Throughout the diet, plasmatic cholesterol concentrations remain higher in HCD than in control fed fish (Fig. 3.1.6). At 4 weeks, treated fish present an initial 4-fold concentration increase than in control (HCD 59.60mg/dl ±3.57; CONT 14.92mg/dl ±2.16). Cholesterol concentrations grow exponentially throughout the 8-week mark in the HCD group while remaining stagnant in control (HCD 89.62mg/dl ±5.92; CONT 20.68mg/dl ±1.95; 4w vs. 8w p=0.001). After 12 weeks, the

ratio between both groups increases and reaches a 7.5-fold higher cholesterol concentration (HCD 149.33mg/dl ±6.67; CONT 19.82mg/dl ±4;40). From the 4th to the 12th week of feeding, levels increase 2.5-fold (4w vs. 12w p<0.0001). Finally, blood cholesterol concentrations are seen to drop after a 2-week reversal on control diet (HCD 51.58mg/dl ±3.81; CONT 18.84mg/dl ±3.54; 4w vs. 2w rev. contr. p=0,0905 [n.s].; 12w vs. 2w rev. contr. p<0.0001).

3. 2. 2. Vascular histology of adult zebrafish tail sections

3. 2. 2. 1. Anatomical overview of the vasculature in the zebrafish tail

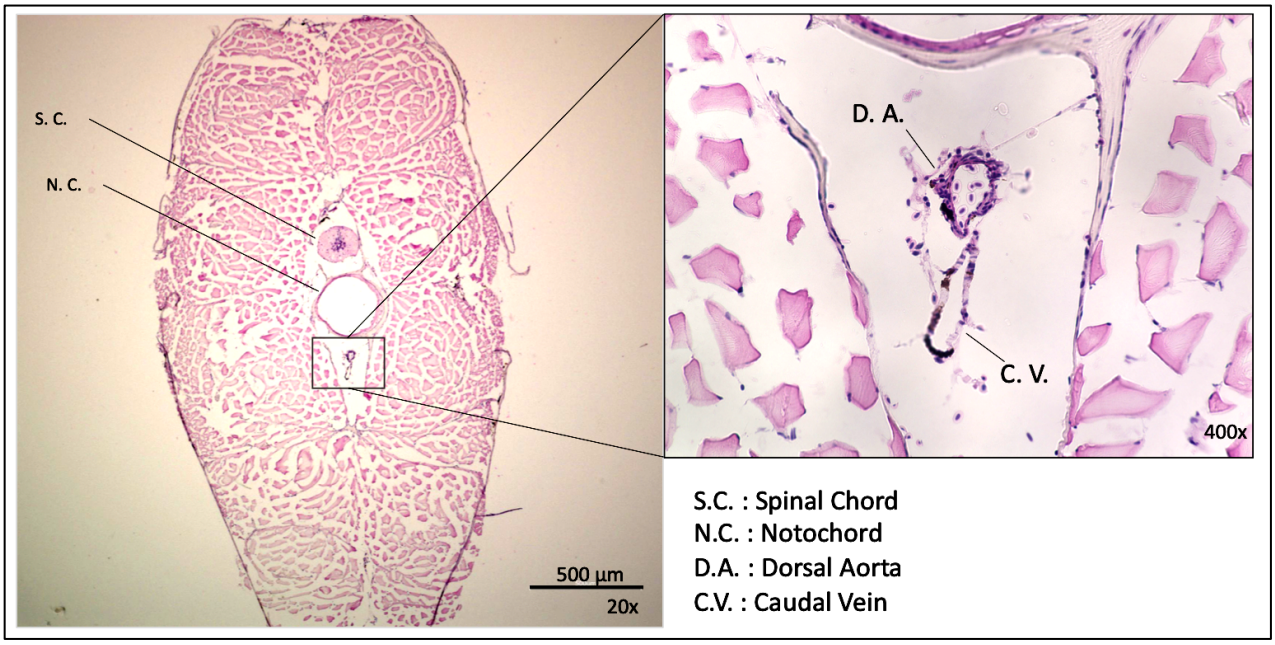

Figure 3.2.2 Tail vasculature in a hematoxylin and eosin stained of adult zebrafish (20x and 400x)

Hematoxylin and Eosin stained transverse sections of a single zebrafish tail were used to provide a referential anatomical overview of the regional vasculature. The used fish originates from husbandry-diet fed batches. H&E staining was done using the method described in Table 2.2.2. and slides were imaged at 20x and 400x magnification. Figure 3.2.2. shows the central position of the dorsal aorta surrounded by the caudal musculature. The aorta's diameter ranges from approximately 10 to 100µm along the caudal region, depending on its position along the tail. Key recognizable landmarks for its identification are the dorsal positioned notochord ring and the ventral situated caudal vein.

3. 2. 2. 2. Descriptive study of ORO-stained dorsal aortas in adult zebrafish

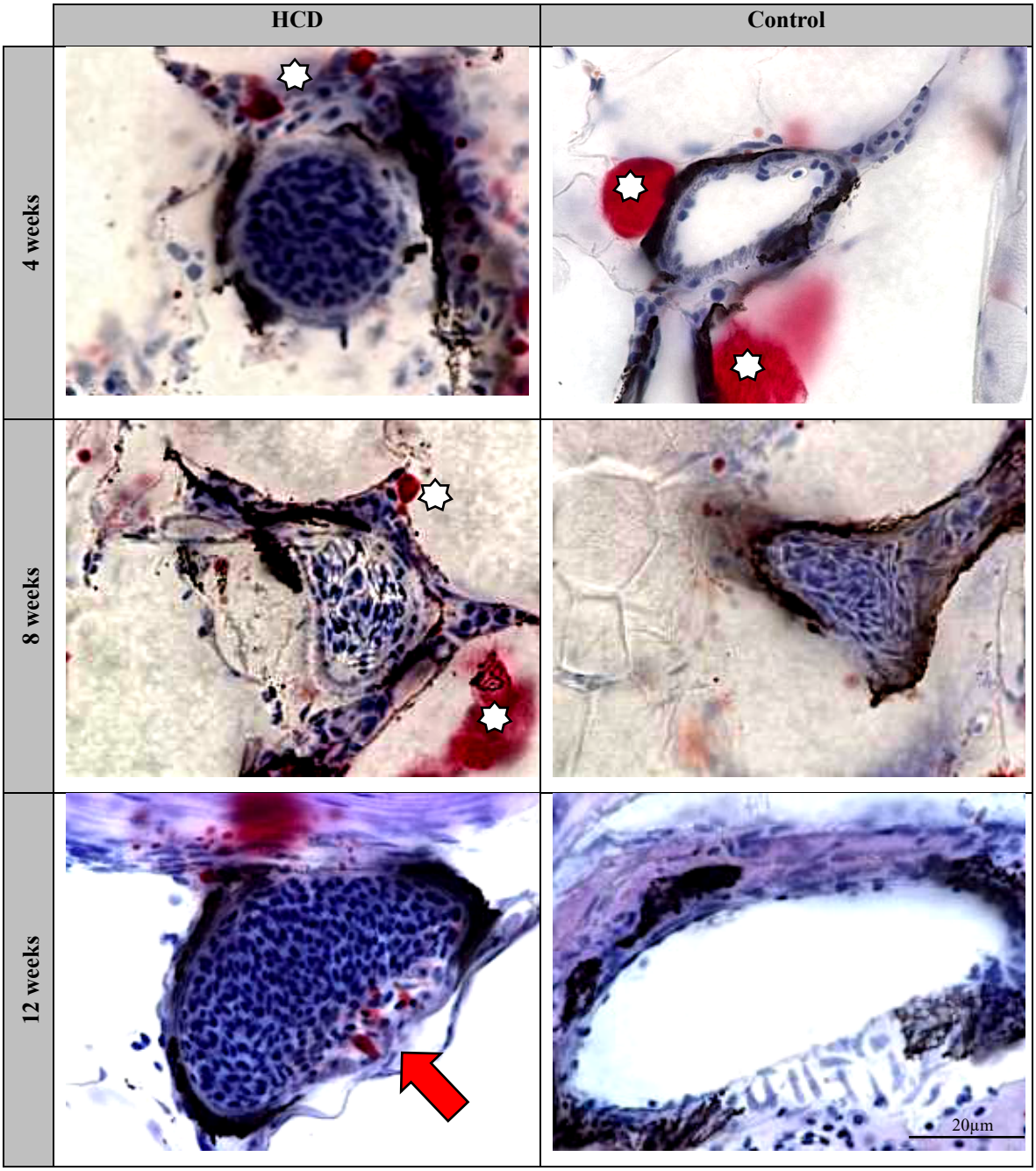

Figure 3.2.3 Visualizations of ORO and hematoxylin stained dorsal aortas of adult zebrafish after 4, 8 and 12 weeks of HCD and control diet (1000x).
Lipid accumulation in the aortic wall is represented by an arrow, ORO artefacts are marked by stars.

After gaining blood from the zebrafish, an additional 1cm of the tail was sectioned for histological study of the region's main vessels. The sections were stained in Oil Red O and hematoxylin following methods in Table 2.2.3. The slides were then imaged under the microscope at 1000x magnification using oil immersion (Figure 3.2.3.). Overall, considerable melanocytic tissue can be seen coming from the adventitious tissue around

the aortic rings. ORO-grain artifacts appear as well (represented by stars). The aortic lumens appear either filled with erythrocytes or empty. Aortic walls of 4-weeks-fed fish on both diet show no recognizable thickening nor lipid deposit. At 8 and 12 weeks, control-fed adults show no deposits either. In HCD groups, the formation of lipid deposits in the aortic wall appears still limited. At the 12-weeks stage, two out of three fish show localized thickening of the aortic wall with enclosed ORO stained tissue.

3. 3. Expression analysis of *atf3*, *sort1* and *hbegf* in HCD-fed zebrafish blood

3. 3. 1. RNA degradation check in whole fish sample

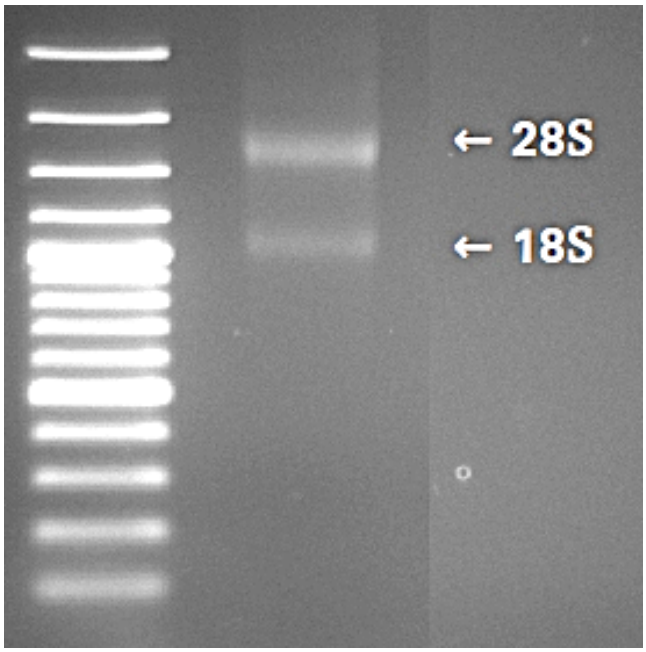

Figure 3.3.1 UV-imaged agarose-gel of whole adult zebrafish extracted mRNA

RNA can be tested for its integrity using electrophoresis on an agarose gel. On the UV-image seen in Figure 3.2.1, two distinctive bands appear in the foreground. These represent the large and small ribosomal rRNA subunits, respectively 28S and 18S in eukaryote organisms. In the background, messenger RNA presents itself as a long smear with no distinctive bands to be expected. mRNA collected and isolated from whole fish sample can thus be evaluated as not degraded and is suitable to cDNA conversion.

3. 3. 2. Validation of primers for genes

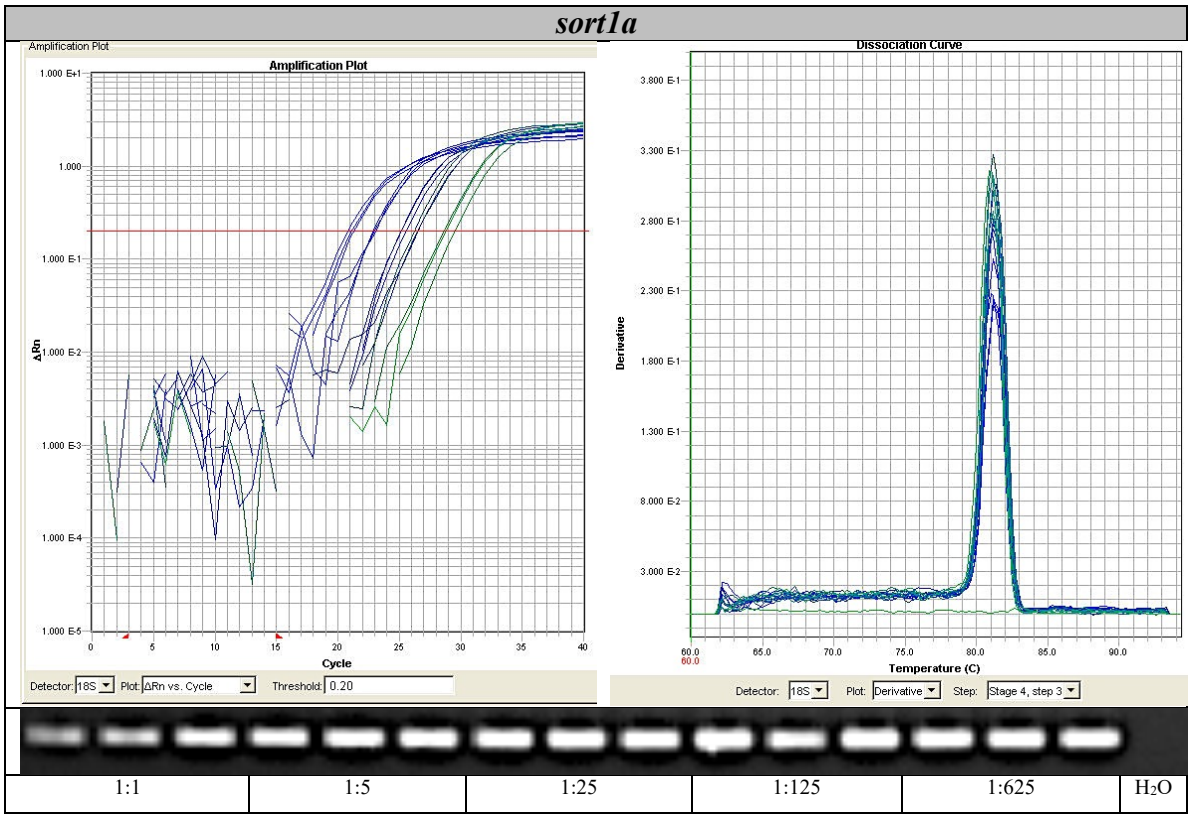

Figure 3.3.2 Results of primer validation for *sort1a.*
Further primer Validations results are found in the Appendix Section

The exploration of the *Ensembl* database provided the exonic sequences of the corresponding zebrafish orthologues. For *ATF3*, a single orthologue could be determined. In the case of *SORT1* and *HBEGF*, two paralogues could be identified for each: *hbegfa / hbegfb* and *sort1a / sort1b*. No exonic sequences could be provided yet by the database for *sort1b* at the time of the study. According to the database, the *atf3*, *sort1a* and *hbegfa/hbegfb* orthologues appear to be conserved to a degree of 72,68%, 61.25% and 44,23%/41.83% respectively in *Danio rerio*.

The validation of primers designed for the zebrafish orthologue is a necessary step before PCR application onto experimental samples. Here, the primers were tested on a whole fish mRNA as the genes are expected to be expressed throughout the complete organism. For validation, the replication of a single, specific product at lowering concentration must be ensured. 7900HT qPCR steps shown in Table 2.2.7 have been applied for this purpose. Figure 3.5.3 to 3.5.6 show the specific product expression in technical triplicates on a serial cDNA sample dilution of up to 1:625. The corresponding electrophoresis gels show uniform bands at their expected product length. Negative control result is obtained where water substitutes cDNA.

3. 3. 3. qPCR analysis of hypercholesterolemic zebrafish blood

Concentrations of mRNA extracted out of zebrafish blood ranged from approximately 30 to 120ng/µl. All samples were diluted to fit a uniform concentration of 30ng/µl ±10% before reverse transcription into cDNA.

Inclusion criteria defining positive results was delimited to specific expression in at least two out of three biological replicates. In each zebrafish sample, at least two out of three positive technical triplicates must be specifically expressed with maximum Ct-values of 38 cycles. When genes are expressed in both HCD- and control-fed groups, relative expression was calculated using the Livak method.

3. 3. 3. 1. atf3

Table 3.3.1 UV-visualization of agarose-gel electrophoresis for qPCR amplification of *atf3* in adult zebrafish blood at 4, 8 and 12 weeks of feeding.

Diet length	Fish	Gene	Gel
			HC HC HC Ctrl Ctrl Ctrl WF H_2O
4 Weeks	Fish pair 1	*atf3*	 *
		ef1α	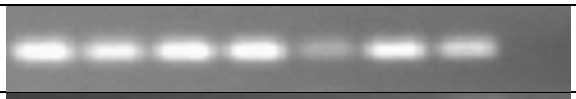
	Fish pair 2	*atf3*	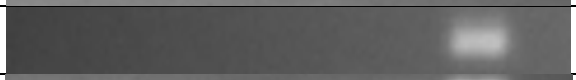
		ef1α	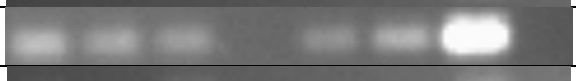
	Fish pair 3	*atf3*	
		ef1α	
8 Weeks	Fish pair 4	*atf3*	
		ef1α	
	Fish pair 5	*atf3*	
		ef1α	
	Fish pair 6	*atf3*	
		ef1α	
12 Weeks	Fish pair 7	*atf3*	
		ef1α	
	Fish pair 8	*atf3*	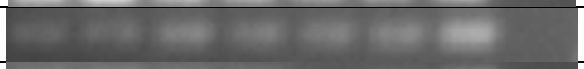
		ef1α	
	Fish pair 9	*atf3*	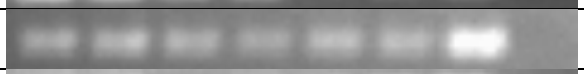
		ef1α	

**The sequence of the imaged UV-bands has been here corrected to fit the presentation order of the results. The band order on the original agarose-gel is found in an inverted pattern.*

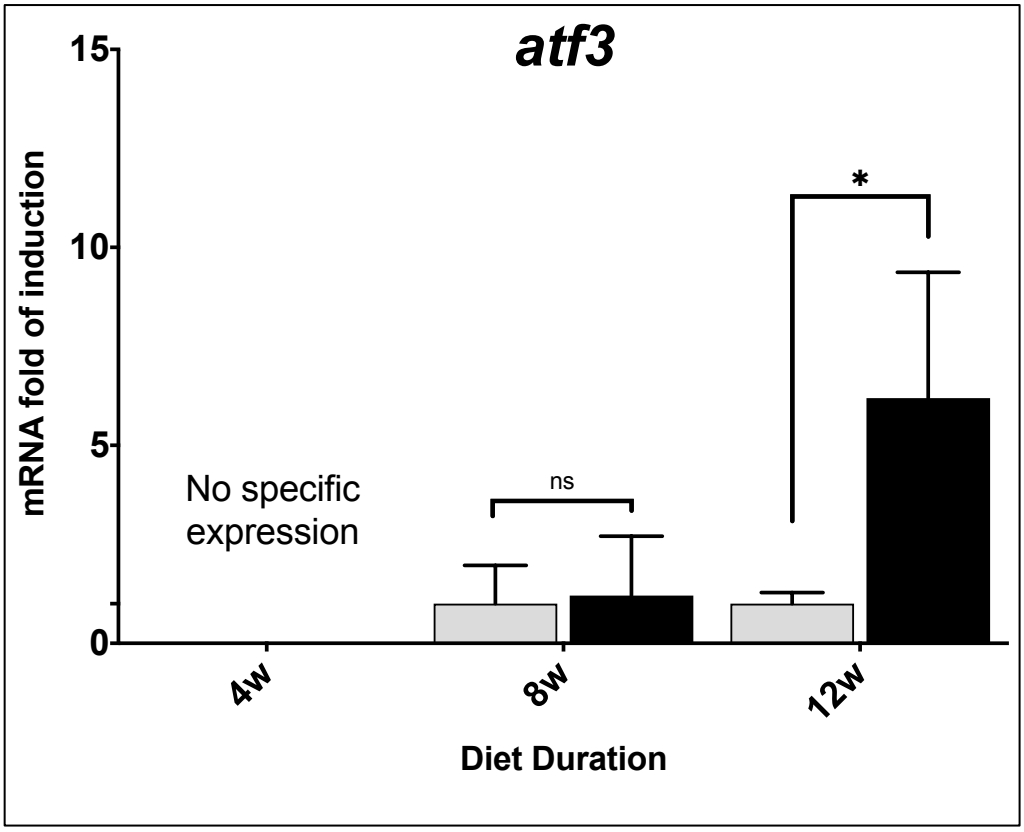

Figure 3.3.3 Relative expression of *atf3* in blood extracted from 4-, 8- and 12 weeks-fed adult zebrafish

At 4 weeks of feeding, the obtained electrophoresis bands show the gene expression of *atf3* in HCD- and control-fed fish pair 1 (Table 3.2.1). In pairs 2 and 3, none to very weak expression can be respectively observed at this time-point. UV-bands corresponding to the housekeeping gene amplification appear as expected for all three studied pairs in blood-extract samples. In the internal controls, the whole fish sample shows a positive reaction while the water sample remains negative, indicating no contamination. As predefined standards in section 3.3.3. are not reached, the results suggest that 4 weeks of high cholesterol feeding do not lead to a specific differential expression of *atf3* yet in zebrafish blood.

Expression criteria are met though in studied fish of both diet groups at 8 weeks of feeding, as qPCR and electrophoresis results indicate positive amplification of specific products (Figure 3.2.6). Relative expression calculation reveals an initial, yet non-significant 1.2-fold up-regulation of *atf3* in the HCD fed zebrafish (*atf3* 8w: 1.2-fold ±1.49; p=0,851).

The increase in relative expression between both groups accentuates after 12 weeks of diet. All three zebrafish blood samples in both HCD and control indicate expression bands at appropriate PCR cycles as predefined in section 3.3.3. At 12 weeks of diet,

mRNA transcription reaches a significant 6.2-fold of induction in the HCD-fed group in relation to cholesterol-free fed fish (*atf3* 12w: 6.2-fold ±3.18; p=0.048).

3. 3. 3. 2. hbegfa and hbegfb

Table 3.3.2 UV-visualization of agarose-gel electrophoresis for qPCR amplification of *hbegfa* in adult zebrafish blood at 4, 8 and 12 weeks of feeding.

Diet length	Fish	Gene	Gel HC HC HC Ctrl Ctrl Ctrl WF H_2O
4 Weeks	Fish pair 1	*hbegfa*	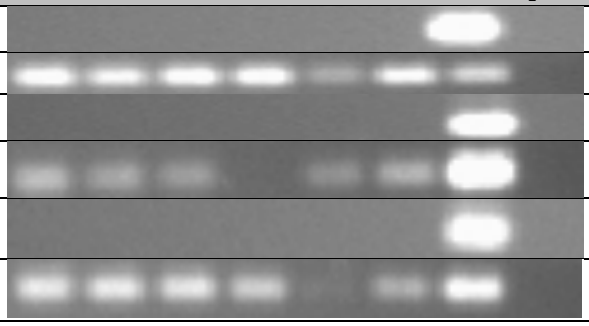
		ef1α	
		hbegfa	
	Fish pair 2	*ef1α*	
		hbegfa	
	Fish pair 3	*ef1α*	
8 Weeks	Fish pair 4	*hbegfa*	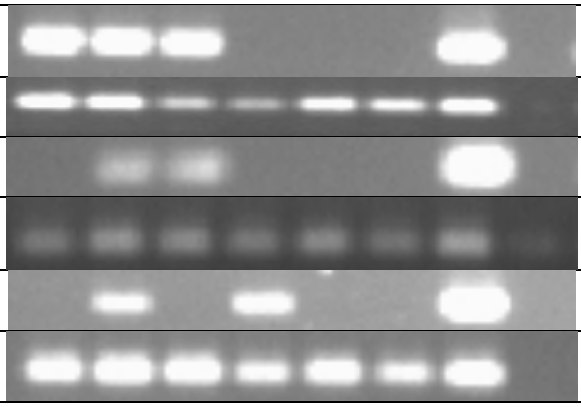
		ef1α	
	Fish pair 5	*hbegfa*	
		ef1α	
	Fish pair 6	*hbegfa*	
		ef1α	
12 Weeks	Fish pair 7	*hbegfa*	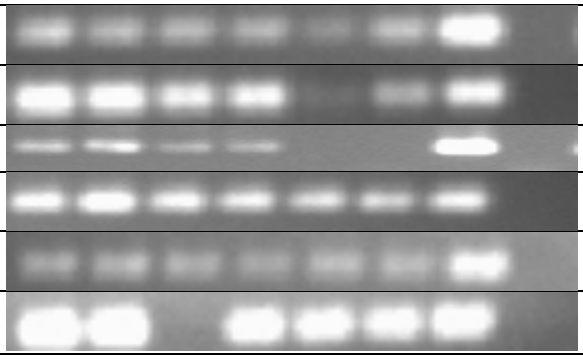
		ef1α	
	Fish pair 8	*hbegfa*	
		ef1α	
	Fish pair 9	*hbegfa*	
		ef1α	

Table 3.3.3 UV-visualization of agarose-gel electrophoresis for qPCR amplification of *hbegfb* in adult zebrafish blood at 4, 8 and 12 weeks of feeding.

Diet Length	Fish	Gene	Gel
			HC HC HC Ctrl Ctrl Ctrl WF H_2O
4 Weeks	Fish pair 1	*hbegfb*	
		ef1α	
	Fish pair 2	*hbegfb*	
		ef1α	
	Fish pair 3	*hbegfb*	
		ef1α	
8 Weeks	Fish pair 4	*hbegfb*	
		ef1α	
	Fish pair 5	*hbegfb*	
		ef1α	
	Fish pair 6	*hbegfb*	
		ef1α	
12 Weeks	Fish pair 7	*hbegfb*	
		ef1α	
	Fish pair 8	*hbegfb*	
		ef1α	
	Fish pair 9	*hbegfb*	
		ef1α	

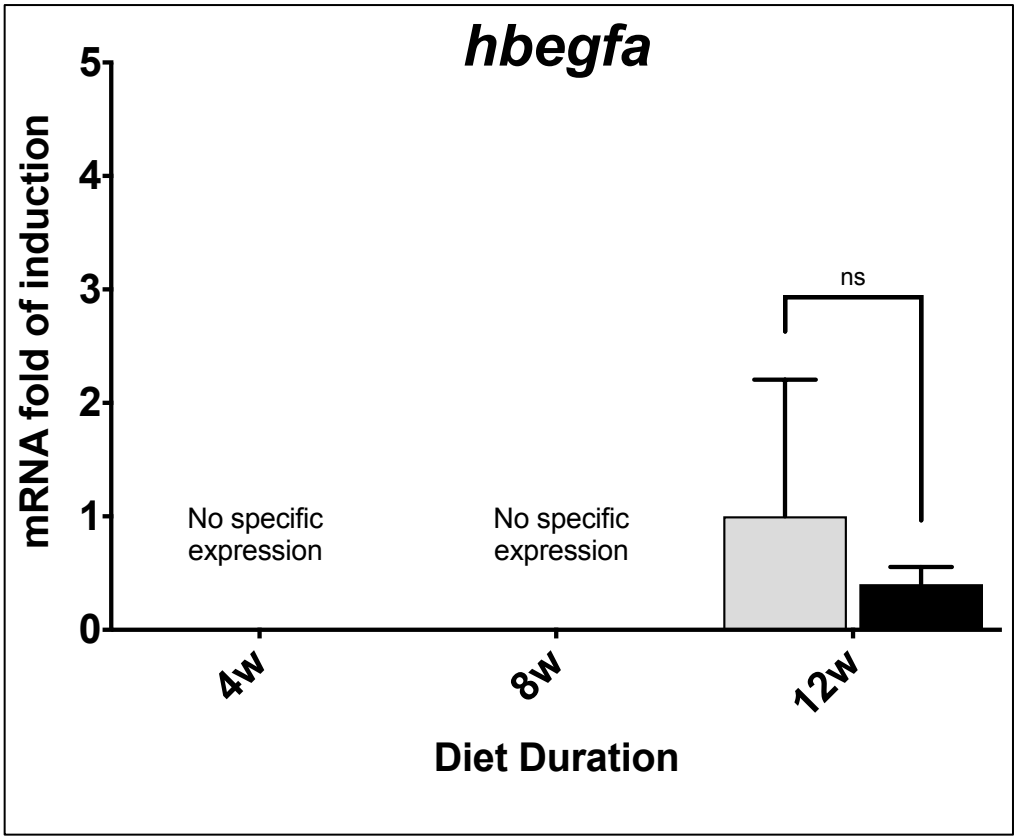

Figure 3.3.4 Relative expression of the *hbegfa* paralogue in blood extracted from 4-, 8- and 12 weeks-fed adult zebrafish

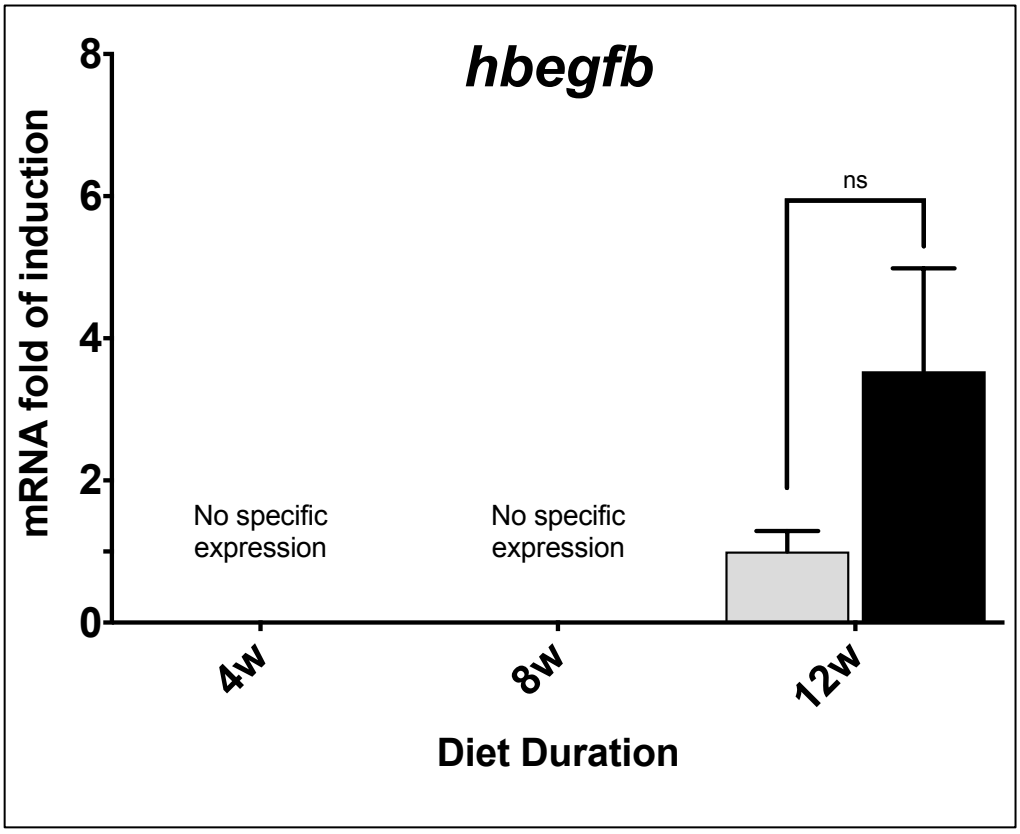

Figure 3.3.5 Relative expression of the *hbegfb* paralogue in blood extracted from 4-, 8- and 12 weeks-fed adult zebrafish

Amplification results of positive and negative controls as well as the *ef1a* housekeeping gene indicate that the PCR-reaction proceeded as intended (Table 3.2.2 and 3.2.3).
At 4 weeks, no expression of *hbegfa* nor *hbegfb* is recorded in blood samples of both diet groups.

At 8 weeks, agarose gel images indicate a transient, yet inconsistent expression pattern throughout the six zebrafish. In *hbegfa,* product bands develop first in the HCD-fed group. Only HCD-fed fish 4 presents a positive and specific expression in its technical triplicates. In *hbegfb*, specific PCR products are found in HCD-fed fish 4 and 5 as well as control-fed fish 4. None is seen in the remaining control-fed samples. Consequently, the Livak method cannot be applied to calculate the relative expression of *hbegfb* between both diet-groups at 8 weeks of diet.
Persistent bands appear in PCR samples of 12 weeks-fed fish, permitting in this case to calculate the relative expression between both groups. Here, the Livak method reveals a non-significant 0.4-fold downregulation of the *hbegfa* paralogue in the HCD-fed fish (Figure 3.2.7; *hbegfa* 12w: 0.40-fold ±0.15; p=0.442). In *hbegfb*, the opposite tendency can be observed. At 12 weeks, *hbegfb* is expressed in average 3.5-fold higher in HCD-fed fish. The difference in expression levels remains though non-significant. (Figure 3.2.8; 12w *hbegfb*: 3.53-fold ±1.45; p=0.102).

3. 3. 3. 3. sort1a

Table 3.3.4 UV-visualization of agarose-gel electrophoresis for qPCR amplification of *sort1a* in adult zebrafish blood at 4, 8 and 12 weeks of feeding.

Diet Lenght	Fish	Gene	Gel							
			HC	HC	HC	Ctrl	Ctrl	Ctrl	WF	H_2O
4 Weeks	Fish 1	*sort1a*								
		ef1α								
	Fish 2	*sort1a*								
		ef1α								
	Fish 3	*sort1a*								
		ef1α								
8 Weeks	Fish 4	*sort1a*								
		ef1α								
	Fish 5	*sort1a*								
		ef1α								
	Fish 6	*sort1a*								
		ef1α								
12 Weeks	Fish 7	*sort1a*								
		ef1α								
	Fish 8	*sort1a*								
		ef1α								
	Fish 9	*sort1a*								
		ef1α								

At the first diet mark, gel electrophoresis shows no bands in HCD- nor control-fed fish (Table 3.2.4). Results in internal and external controls indicate though that an amplification reaction took place in the presence of cDNA sample. Consequently, the result leads to conclude that no *sort1a* mRNA transcript is to be found in zebrafish blood tissue samples at 4 weeks of either HCD nor control diet.

Sortilin expression appears similarly limited at 8 weeks of feeding. Solely HCD fish 4

shows a positive gene expression in all technical triplicates. Its paired control-fed fish presents two out three positive amplifications.

At 12 weeks of feeding, *sortilin* shows a uniform expression affecting only High cholesterol-fed fish, with fish 8 and 9 showing all and fish 7 two out of three triplicates with positive and specific amplification at appropriate cycle numbers. All matching control runs show no expression of the gene, rendering non-determinable Ct-values. Even though the obtained qPCR parameters do not permit the calculation of relative quantification at this time-point, results here suggest that the *sort1a* orthologue expression in blood tissue can be triggered by a long term HCD-diet.

4. Discussion

In this study, we examined the usage of *Danio rerio* as a model to explore the expression of certain human genes related to coronary artery disease and myocardial infarction. To create an atherogenic context, a high cholesterol diet (HCD) was produced and evaluated first on zebrafish larvae. In a second stage, the expressions in blood tissue of the selected *ATF3, SORT1* and *HBEGF* orthologues were studied over a time-course of 12 weeks in adult zebrafish. Additionally, the progression of blood cholesterol concentrations and lipid accumulation in response to HCD was evaluated.

4. 1. 4%-HCD leads to lipid accumulation in larval vascular structures

The effect of HC-diet on zebrafish vasculature could be studied thanks to the tissue's transparency during the first 30 days of larval development. On a time-course of up to 25 days, three larval groups were studied in an interval of 10 days starting at 5dpf. At each time point, histological analysis of both the dorsal aorta and the caudal vein in the tail region was studied after whole-mount Oil Red O staining of the larvae. Following imaging, lipid-covered fields stained in red were measured in relation to the vessel's surface. The effect was studied in comparison to control-fed larvae under the same conditions.

The obtained results indicate a successful accumulation of lipids in the vasculature at all three time-points in HCD-fed larvae. At each time-point, surface coverage ratios remained significantly higher in HCD-fed groups than in controls (Figures 3.1.2-4). Additionally, the results show that lipid deposition by HCD is a dynamic process that increases with time. With the employed quantification method, the effect's maximum was measured at 15 days in the dorsal aorta and 25 days in the caudal vein, with approximately 22% and 14 % surface coverage respectively (Figure 3.1.5).

Echoing results were found by Stoletov et al. after administrating a 4%-HCD to wild-type AB larvae, starting at 5dpf for 10 days. In their study, a fluorescent BODIPY lipid was added to the diet. Dispersed fluorescence in the caudal vein was observed, with

intensity levels approximately 5 times higher in HCD-fed fish than in control (Stoletov et al. 2009). In contrast to the results in Figure 3.1.5, the group reports however that most fluorescent deposits were found in the caudal vein, while only some were observed in the dorsal aorta. Yoon et al. describe in their results that most deposits were found in the same main vessel as well. Positive fluorescence in the aorta has been observed nevertheless, particularly in vascular bifurcation regions (Yoon et al. 2013). Stoletov et al. suggested that the effect in their result may be explained by arteriovenous shunts in the early vascular system of the zebrafish together with a similar histological constituency of the vascular wall in both vessels at this early stage of development (Stoletov et al., 2009). Miano et al.'s histologic description confirms this, stating that the 10µm diameter dorsal aorta is surrounded each by a single layer of endothelial and vascular smooth muscle cells in 7dpf old larvae. Peripheral growth in the thickness of mural layers appeared to develop only in elder 30dpf larvae (Miano et al., 2006).

At the 25th diet-day mark, the studied larvae were 30 days old and reached the end of their optical transparency. At this age, melanocytic tissue began to form and hindered the lipid surface measurements. Obtained images indicate though towards a persisting and potentially even stronger accumulation in both the DA and CV (Figure 3.1.1). In this case, the ratio decreases and is limited to approximately 14% and 13% of lipid coverage respectively. The discrepancy between the histologic indications and quantification results could be explained by methodic limitations due to the nature of the employed analysis script. In fact, the script has been designed to simply recognize red pixels on a two-dimensional surface. The obtained measurements vary according to the predefined threshold identifying red pixels in the Matlab script. Furthermore, if the ORO-covered surface is overlaid by melanocytic tissue represented as darker pixels, the underlying lipid covered surface in the vessel can't be recognized and be accounted for. The matter could eventually be circumvented by employing melanin-free zebrafish mutant lines instead, such as *casper*, in which the larvae remains transparent even over the 30dpf mark (White et al 2008). The hindering melanocytic tissue would thus not be expressed, and lipid coverage estimates could be measured in even more advanced juvenile states.

Furthermore, it must be considered that the experiments took place under conditions of a constant aquarium temperature set at 28,5°C, while the fish's viable thermic range encountered in its natural habitat can differ widely. In a review article, Fang and Miller

remind us that zebrafish are a poikilothermic species and since their body temperature does not remain constant, it is highly dependent on thermal exchanges with the surrounding water. Accordingly, variation towards colder temperatures can lead to alteration in glycolytic activity of the zebrafish. The resulting oxidative stress could thus favor lipid oxidation and atherosclerotic development in the fish's vasculature (Shaklee et al., 1977; Fang and Miller, 2012).

To claim that an atherogenic process is indeed taking place under the high cholesterol diet, it is essential to able to show that an oxidative and inflammatory process is underway. By employing Oil Red O, one must also bear in mind that the dye used in this study only stains neutral lipids. Stoletov et al. were able though to demonstrate that by adding the BODIPY fluorescent dye into the 4%-HC-diet given to the larvae at comparable time points, lipids accumulating in the larval DA and CV walls correspond precisely to oxidized lipids (Stoletov et al. 2009). Additionally, Fang et al.'s mass spectrometry result in 2 weeks HCD-fed larvae present a significant increase in oxidized cholesteryl esters (Fang et al. 2010). Additional results suggest that an inflammatory process takes place, as Stoletov et al. described the accumulation of macrophages and granulocytes in caudal vein walls of HCD-fed lyz:DsRed2 larvae (Stoletov et al. 2009). Surprisingly, qPCR results by Yoon et al. of pooled whole larvae fed up to 20 days 4% HCD could not indicate an inflammatory development on a cytokinic level, as IL-1β TNF-α and IL-6, known to be involved in atherogenesis, showed no expression variation. Furthermore, no significant difference in leukocyte accumulation within the vasculature could be observed in their experiments (Yoon et al 2013).

In summary, findings published by Stoletov, Yoon and Fang support the results observed in the first part of this study. Indeed, a 4%-HCD is seen to be provoking an atherogenic process in the larval vascular system, albeit corresponding more likely to earlier stages found as fatty streaks in mammalian and human models (Stoletov et al. 2009, Fang et al. 2010, Yoon et al. 2013).

4. 2. 4%-HCD leads to a hypercholesterolemic response in adult zebrafish

After demonstrating the ability for HCD to provoke lipid depositions comparable to fatty streaks in the vasculature of zebrafish larvae, an equivalent diet was administrated to adult fish to study its aptitude to provoke hypercholesterolemia. The fish were studied again during three time points in pairs of treated and control groups. The measurement interval was set to 4 weeks, at which blood was gained by centrifugation. After plasma separation, total blood cholesterol concentrations were measured by photometric reading.

Over the course of 12 weeks, total cholesterol levels in zebrafish adults are shown to rise steadily and become significantly higher in HCD than in control-fed fish at identical diet timepoints (Figure 3.2.1). At 8 weeks of HCD, total cholesterol levels reach an approximately 4.5-fold induction. After 12 weeks, the ratio increases to approximately 7.5-fold. The process is reversible after setting the fish back on a normal diet for a further period of two weeks, indicating that the additional cholesterol provided in the food intake to most likely cause the hypercholesterolemic state.

The outcome reflects again results published by Stoletov et al. in which hypercholesterolemia was induced in adult wild-type zebrafish under a similar cholesterol diet. Here, a 4-fold increase in fish fed 8 to 12 weeks HCD was recorded. Absolute recorded levels were much higher though, with an average concentration reaching 800mg/dL total cholesterol, as opposed to 150mg/dL in the present experiment (Figure 3.2.1). Results in Figure 3.2.1 draw parallels as well to Yoon et al.'s publication, where prolonged HCD of up to 19 weeks led to a 1,5-fold increase of total plasma cholesterol at approximately 450 mg/dl. No increase in BMI could be observed either (Yoon et al., 2013). Stoletov et al. reported that these total cholesterol levels are comparable to results found in Hartvigsen's LDLR -/- mouse model on 1% Cholesterol diet. Indeed, hypercholesterolemia was achieved in this mouse model along with atherosclerotic lesions, but without signs of obesity or hypertriglyceridemia (Hartvigsen et al., 2007).

Even though the here obtained results of cholesterol levels indicate essentially similar trends seen in Stoletov and Yoon's publications, absolute values differ considerably.

One must consider also the likely deviating initial lipid content in the adult food flake provided by different manufacturers serving as basis for the prepared HCD mixtures. For instance, the Tetramin flake food employed here displays a raw fat content of 11% (Table 2.1.13), while the Stoletov and Yoon groups based their mixture on artificial artemia provided by another manufacturer. According to their product catalogue, the artificial artemia diet contained 65% protein and highly unsaturated fatty acid (*Azoo product catalogue 2010*). With the HCD produced in this study, Figure 3.2.1 shows lower baseline values in control-fed fish with plasmatic cholesterol concentrations ranging from approximately 15 to 20 mg/dL, while the equivalent values in the previously mentioned publications lay between approximately 200 and 300mg/dL. This in turn would explains the larger cholesterol level increments seen in the here obtained results.

In essence, the results of the HCD trials indicate the possibility to provoke hypercholesterolemia in wild-type zebrafish adults. To achieve similar results in mice, genetic intervention into key lipid regulation pathways is required, such as the disruption of the LDL receptor (Stylianou et al. 2012). Fang et al. state that atherogenesis in wild-type zebrafish is likely due to the presence of CETP, which in contrast is not expressed in wild-type mice (Fang et al. 2014). As mentioned in 1.2.1, teleostei fish display a highly conserved orthologue of *CETP* that ensures the transfer of cholesteryl esters from HDL towards LDL (Babin, 1989). *cetp*-inhibitors from natural extracts have shown to avoid dyslipidemia in zebrafish despite being placed under a HCD (Schlegel et al. 2016). Thus, increased LDL-cholesterol levels would be accentuated by *cetp* expression under hypercholesterolemic conditions, emphasizing the effect of risk factors leading towards atherogenesis (Fang et al, 2014).

4. 3. 12 weeks of 4%-HCD points towards fatty streaks forming in adult zebrafish aortas

After gaining blood at the predefined diet timepoints, tail portions of the zebrafish used for the experiment were kept for cryosections. After ORO and hematoxylin staining, the dorsal aorta was imaged under oil immersion and a descriptive study of the aortic rings was undertaken.

A previously in hematoxylin and eosin stained section of the tail provided an overview of the regional vessels and its surrounding structures (Figure 3.2.2). In the ORO-stained tissue, pronounced melanocytic overlay from the adventitia was found in over a majority of the obtained aortic rings (Figure 3.2.3). Dark tissue superimpositions hindered mostly a precise histological study of the already delicately thin vessel walls. Furthermore, sporadic artifacts of ORO-grains appeared mostly around the vessels, occasionally protruding onto the field of view. To maintain the cryosectioned tissue stable and its water-rich tissue interconnected, relatively thick sections of the tail had to be made at 35 µm. This led nevertheless in certain slides during the process of embedding under cover slips to the overlay of surrounding tissues onto the aortic region, rendering them unsuitable for analysis.

In the slides kept for study, the aortic walls at 4 weeks of diet appeared widely clear of lipid depositions in both diet groups. The same result was seen at 8 weeks. After 12 weeks of HCD, two out of three fish showed sporadic local thickening of the aortic wall with enclosed ORO stained lipids (Figure 3.2.3). The aortic walls of corresponding control-fed fish were clear of comparable deposits.

In the published literature, most vascular histology results of HCD experiments in zebrafish are based on the larval model. Again, Stoletov and Yoon et al.'s work serves as only references for results in adult fish. Based on their results, Yoon et al. remark that adult wild type zebrafish may be resistant towards the formation of lipid deposits in the vasculature and suggest the necessity of genetic manipulation to achieve deposit formation (Yoon et al., 2013). Additionally, results are limited so far to wild type zebrafish of the AB line. The susceptibility of other commonly used zebrafish strains in laboratories, such as *tübingen*, remains yet unknown.

Considering the limitations encountered in the employed methods of sectioning and staining, certain changes in the experimental design could provide better results. As discussed in 4.2, the total cholesterol levels measured in the zebrafish plasma remains lower than results provided in comparable published studies. Even though a 4% cholesterol diet appears to be an adopted standard in this type of experiment, an increase in content and a longer diet length may translate into more pronounced lipid deposits in the aortic wall of adult zebrafish. Additionally, more precise histologic quantification analysis might be possible by employing melanin-free *casper* lines to possibly render the aortic walls clear of any melanocytic overlay (White et al., 2008). Surface analysis, as performed in optically transparent larvae, could provide a more tangible and quantifiable answer to the formation of fatty streaks. At last, one might consider as well studying the complete vascular anatomy of the zebrafish. In this work, and presumably as well as in publications so far, the tail region was chosen for the simplicity of its anatomical structure. This leaves more rostral laying structures, especially in the proximity of the heart, further uncharted.

In conclusion, it is yet unclear under the obtained results if the produced 4%-HCD can realistically and consistently lead to the formation of fatty streaks in the dorsal aorta of wild-type adult zebrafish after only 12 weeks of feeding. Melanocytic tissue in the adventitia hinders clear and quantifiable analysis of the aortic wall. Longer high cholesterol diets in pigment-free zebrafish or genetical disruption in lipid pathway may provide a more satisfiable answer. Additionally, the size of the atheroma is far from hindering the blood flow to stenosis grades severely enough to provoke ischemia. Nevertheless, the observed results give indications that fatty streak lesions do begin to form at this stage. Observing a potentially more pronounced atheromatous growth under an extended cholesterol diet would then be of interest.

4. 4. CAD-related gene orthologues indicate regulation changes in zebrafish blood tissue in response to 4%-HCD

Upon obtaining the blood samples through centrifugation of the zebrafish, RNA was extracted and transcribed into cDNA. Following the validation of the designed primer sequences, expression levels of the orthologue genes in the target tissue were evaluated and compared between both diet groups using qPCR methods and analysis after Livak and Schmittgen. The resulting fold-of-induction calculations reflect changes in genetic regulation in response to dietary cholesterol exposure. The analysis of the cycle-values was backed by UV-visualization of the agarose electrophoresis-gels from the corresponding qPCR products.

4. 4. 1. 12 weeks of 4%-HCD upregulates atf3 expression in zebrafish blood

qPCR analysis of atf3 after 12 weeks of 4%-HC diet resulted in a 6.2-fold expression increase in comparison to control-fed fish (Figure 3.3.6). No expression alteration could be observed with certitude at earlier time points.

In the literature, the expression of the activating transcription factor 3 gene in human, mice and rat models has been largely described as reflecting conditions of tissue damage and inflammation (section 1.5.1). More precisely, its presence has been linked with mechanisms limiting the expression of cytokines during an already ongoing inflammatory process (Gilchrist et al. 2006). Additionally, its upregulation has been reported in ischemic tissue and atherosclerotic plaques (Nawa et al. 2002; Chang et al. 2015). Under the aspect of cholesterol metabolism, *ATF3's* expression was shown to be prompted by the presence of oxidized LDL (Nawa et al. 2002). By forming part of the AP-1 proteinic structures that bind onto promotor sites, ATF3 can indirectly limit cholesterol oxidation into 25-hydroxycholesterol and the subsequent formation of foam-cells by downregulating *Ch25h* (Chen et al. 1994; Gold et al. 2012). Furthermore, HDL has been described to activate *ATF3* with the consequence of decreasing the presence of Toll-Like receptors on macrophage cell-surfaces (De Nardo 2014). With regards to findings in zebrafish models, cardiovascular studies on *atf3* have been so far very scarce. A related transcription factor gene, *atf4*, has been described however in zebrafish models to lead to hyperlipidemia and hepatic steatosis following its

overexpression (Yeh et al. 2017).

The significant expression increase obtained here in the wild-type zebrafish coincides with hints of fatty streaks beginning to form in the dorsal aorta at 12 weeks of HCD along with elevated plasmatic total cholesterol levels induced by the diet. The conjunction of the obtained results give reason to believe that *ATF3*, a CAD-related gene in human, is seen to undergo similar expression alterations in its wild-type zebrafish orthologue under hypercholesterolemic conditions. In the presumed presence of limited fatty streaks and records of elevated plasmatic cholesterol levels, *atf3*'s upregulation can be assumed to form part of mechanisms refraining atheromatous inflammation in the vasculature. It remains unclear though if its expression in this zebrafish model is primarily prompted by hypercholesterolemia or by atheromatous changes in the vascular wall.

Greater certitude in *ATF3*'s protective role towards the development of atherosclerosis could potentially be achieved by applying similar diet experiments on zebrafish holding for instance a loss-of-function mutation. Such conditions would permit the investigation of potential increase in atheromatous plaque size due to the potential accentuation of inflammatory pathways.

4. 4. 2. 12 weeks of 4%-HCD leads to opposite responses of both hbegf paralogues

In the last studied diet time-point, an expression throughout all three triplicates of both paralogues was observed and expression levels could thus be evaluated. Remarkably, the regulation of both *a* and *b* paralogues appeared to head in opposite directions. While *hbegfa* shows a downregulation, *hbegfb*'s expression increases 3.5-fold. The measured increase hasn't however revealed itself to be statistically significant in the studied sample size. As in *atf3*, no specific response towards HCD was observed in samples taken at 4 and 8 weeks of feeding.

In the literature, *HBEGF* has been outlined as one of several genes to be expressed in blood monocytes during the acute and subacute phase following a myocardial infarction (Riedel 2012). Its expression has been observed as well in the infarcted tissue itself following an ischemic injury (Igura et al. 1997; Tanaka et al. 2002). Immunohistochemical traces of the HB-EGF protein has also been illustrated within atheromatous plaques (Scuderi et al. 2009). Furthermore, it has been shown that hypercholesterolemia is also susceptible to increase the levels of HB-EGF in the serum (Sanchez-Vizcaino et al. 2009).

Here, the qPCR results in the zebrafish illustrate that despite the presence of metabolic risk factors favoring atherogenesis, a rather low and delayed, however probably onsetting expression of the *hbegfb* paralogue can be observed. In fact, a moderate induction could at first likely be sustained at latent levels by the hypercholesterolemic state. According to the literature, an increased expression would then most likely only be observed after tissue ischemia. Indeed, the HB-EGF protein plays into the enhancement of tissue remodeling and chemotaxis towards the ischemic tissue (Higashiyama et al. 1991; Raab et al 1997; Tanaka et al. 2002). In a stricter sense, *HBEGF* and its zebrafish orthologue would then play a more intricate role in the process of tissue repair following infarction than in atherogenesis itself. Tissue infarction in the here fed zebrafish isn't likely, as the hinted fatty streak formation after 12 weeks of HCD do not appear sufficiently severe enough to provide the necessary grades of vascular stenosis. Additionally, the obtained result may indicate that in the zebrafish in particular, *hbegfb*'s expression would impose itself further over its *a* paralogue.

A higher confidence in the here obtained result could certainly be achieved by increasing the population size of biological replicates as well as prolonging the cholesterol feeding trials. Additional qPCR analysis of blood after ischemic damage, created by a stenotic plaque or deliberate interruption of blood flow, could add certainty into the *hbegf* paralogues regulation profile in the zebrafish.

4. 4. 3. sort1a is expressed in blood of 12 weeks 4%-HCD-fed zebrafish, not in control

UV-visualization of agarose-gels obtained after qPCR revealed a consistent *sort1a* expression in the 12-week HCD-fed group. In the corresponding control-fed fish, no gene expression could be observed in the blood. No consistent expression at earlier time points could be observed either (Table 3.3.4).

GWA studies have linked SORT1 to myocardial infarction in humans (Samani et al. 2007; Maouche and Schunkert 2012). Its encoded protein, sortilin, plays an intricate role in lysosomal transport between organelles and the cell-surface (Kjolby et al. 2015). As a cell-surface receptor, sortilin is able to bind serum LDL and slightly lower cholesterol levels through endocytosis (Tveten et al. 2012). Finally, sortilin appears to be key in the secretion of IL-6 and IFN-ϒ cytokines from macrophages and lymphocytes, suggesting that its influence on atherogenesis lies rather in an inflammatory aspect (Mortensen et al. 2014; Kjolby et al. 2015).

Here, sortilin's apparent upregulation in the zebrafish blood comes along significantly increased cholesterol serum levels after 12 weeks of 4%-HCD (Table 3.2.1). The results found in Tveten's study give reason to believe that sortilin's expression in HCD-fed fish may be triggered by hypercholesterolemia resulting from the administrated diet. However, Tveten states that sortilin does not appear to crucially lower cholesterol levels on its own, as the LDL-receptor seems to play here a more essential role in this regard (Tveten et al. 2012).

From an inflammatory point of view and with regards to Mortensen's and Kjolby's findings, sortilin's increased expression in the blood appears on the one hand to likely arise from leukocytic cytokine secretions in response to atherogenesis. On the other hand, its expression in the blood could also originate from thrombocytes in reaction to hypercholesterolemia. Indeed, Ogawa et al. have described the release of soluble sortilin (sSortlin) into the serum by activated platelets in the blood of patients with CAD risk-factors such as hypertension, dyslipidemia, or diabetes (Ogawa et al. 2016). Contrary to Mundlein's results showing the expression of the frequent minor sortilin allele rs599839 as a protective factor, Ogawa et al. argue that the presence of the sortilin protein – for the least in soluble form - is rather itself a risk factor for the build-up of CAD (Muendlein et al. 2014; Ogawa et al. 2016).

Contemplating the results obtained in the histological descriptive study of the zebrafish aortas, an effective sortilin expression might in part be responsible for the rather limited formation of fatty streaks in the zebrafish (Table 3.1.1). As Yoon et al. stated that wild-type zebrafish appear to be resistive towards plaque formation despite cholesterol feeding, *sort1a* emerges as a prime candidate for genetic disruption to induce atherosclerotic lesions in the zebrafish model (Yoon et al 2013).

4. 4. 4. General limitations on employed methods

Naturally, the methods employed in this study do not come without certain limitations.

First, not every expression profile of each gene paralogue could be studied. Particularly in sortilin's case, only *sort1a* was considered, while no primer sequences for the *b* paralogue was ready for design when the PCR-experiment took place. Now that the sort1b sequence is publicized on the ZFIN databank and looking back at the distinct results obtained in *hbegfa* and *hbegfb*, an analysis of the second sortilin paralogue could clarify any differential expression in the gene pair in reaction to a high cholesterol diet.

Second, collecting blood by centrifugation has proven itself as relatively effective, but the limited amounts of approximately 30µl to 40µl translated however into a restricted RNA-harvest (Figure 2.2.3). The initially low RNA-concentration of 30 to 120ng/µl extracted from the blood lead to low concentrations of transcribed cDNA. In turn, this translates into relatively high Ct-values when applying qPCR and hampered precision in the analysis of the results. Furthermore, RNA degradation in the blood samples couldn't be inspected since the available material amount was not sufficient. Additionally, it was decided to work with blood tissue in its entire cellular constituency, since the limited volume extracted from each individual adult fish blood didn't allow for further differential centrifugation unless all samples are pooled. Previously, Stoletov and Yoon have indicated having extracted not more than 2µl of blood per adult fish for plasma cholesterol measurements by puncturing directly into the zebrafish's heart (Stoletov et al. 2009; Yoon et al. 2013). Considering this, Babaei's centrifugation method appears in comparison to be nevertheless the only published method to date assuring a rapid, relatively high-yielding and pure blood extraction (Babaei et al. 2012).

Next, one needs to consider the relatively low adult zebrafish population size employed in this genetic profiling study. Unlike in larvae - which were readily available owing to the high fecundity of the zebrafish - the number of available adult zebrafish was sufficient to meet the requirement of using biological triplicates. The timepoint of the experiments coincided with the early establishing of the zebrafish platform at our institute and the very limited number of available fishes. More statistically exact results could certainly be obtained with higher numbers of fish samples if experiments based on these methods are to be reproduced. Furthermore, the limited number of zebrafish available for this experiment did not permit uniformly gendered cohorts.

In addition, one must critically evaluate by which extent these results can be transposed onto humans or other organisms despite the high orthologal conservancy found for the studied genes. Vice-versa, one must also be reminded that the genes studied here in the zebrafish were initially discovered in humans mainly after the event of myocardial infarction, in other words with advanced CAD due to high grade atherosclerotic changes in the vasculature. As the results of the histological study and the expression profile of the *hbegf* paralogue may have indicated, this study was performed at early stages of fatty streaks in the fish organism. Generally, 12 weeks of 4%-HCD appeared to be just about the stage at which the expression of the studied genes of interest

appeared to set in. The obtained results should spark the interest in prolonging the HC diet for longer periods, possibly even applied onto genetically edited zebrafish, in order to investigate further advanced stages of atherosclerosis as found in humans or other mammal organisms.

5. Conclusion and outlook

Danio rerio appears for certain to be a potent experimental model that opens the doors to new possibilities in the cardiogenetic research field.

In this study, it has been demonstrated that a 4% high cholesterol diet is capable of provoking lipid depositions in young larvae as well as hypercholesterolemia in the adult zebrafish, reproducing results published by Stoletov and Yoon. More specifically, regulatory changes of CAD-linked orthologal genes in the blood of adult zebrafish could be observed following their exposure to 4%-HCD, partially reflecting genetic alterations found in patients after MI. However, the histological study of the zebrafish aortas has not been able to show with absolute certainty if fatty streaks could indeed be observed after only 12 weeks of feeding. The encountered limitation could certainly be circumvented by employing mutant lines with prolonged optical transparency instead.

Since this study has been performed in wild-type fish of the AB line, interest should be sparked into investigating its reproducibility in zebrafish of other common experimental strain such as *tübingen.* Potentially, a wild-type strain even more susceptible for atherosclerosis could thus be identified. Furthermore, the obtained results and recommendations in the literature encourage to carry out a prolongation of the high cholesterol diet -potentially at different concentrations- in genetically modified fish with disrupted or enhanced pathways essential in the formation of atherosclerosis.

A standardized and systematic screening of a variety of CAD-linked genes is conceivable in the zebrafish atherosclerosis model. Such an undertaking is feasible by using a variety of genome editing techniques that can be employed at early cellular stages easily accessible in the young zebrafish. Several genes come into consideration, such as the here studied *atf3* and *sort1a* or other orthologues from an ever-expanding catalogue of CAD-linked genes in humans. Mutant zebrafish carrying a loss- or gain-of-function for a gene, as seen in MI victims, could thus be created. Recently, O'hare et al. have inaugurated this approach with the description of a successful larval model carrying a transient loss-of-function of the LDL-receptor achieved by morpholino injection. The obtained fish were exposed to up to seven days of 4%-HCD and manifested increased accumulation and oxidation of lipid plaques in the vasculature together with transcription alterations of genes linked to cholesterol metabolism

(O'Hare et al. 2014). In 2018, Liu et al. achieved similar results in 5-day HCD-fed larvae by creating a stable *ldlr* knock-out line with the help of CRISPR-CAS9 (Liu et al. 2018)

With the additional discovery of genes not directly linked to inflammatory or lipid metabolic pathways, the attention could be furthermore shifted towards other possible conditions leading towards CVDs, such as hypertension or diabetes. Additionally, other tissues involved in the pathological process besides blood, such as the arterial wall or infarcted organs, can be studied in the zebrafish based on adaptations of the methods employed here.

Today, the zebrafish adds itself to the ranks of several established experimental models in cardiovascular disease research. Thanks to its distinctive features, new approaches are possible in the elucidation of pathomechanisms leading towards atherosclerosis. Understanding key genetic alterations in the blood will improve diagnostic possibilities for patients at onsetting and potentially even reversible stages of atherogenesis. The improved understanding of its genetic background will thus certainly permit identifying patients at higher risk for developing cardiovascular diseases. Optimized drug design and an earlier as well as more personalized treatment and prevention using gene therapy will hence be possible in the future for the nowadays still common cause of death of myocardial infarction.

6. Abstract (Deutsch)

Einleitung

Laut WHO zählen kardiovaskuläre Erkrankungen, insbesondere die koronare Herzkrankheit (KHK), zu den führenden Todesursachen weltweit (WHO 2017; 2018). Zur verursachenden Grunderkrankung der Atherosklerose wurde eine Vielzahl umweltabhängiger sowie intrinsischer Faktoren identifiziert (Torpy et al. 2009). In den letzten Jahrzehnten konnte die molekulargenetische Forschung erhebliche Fortschritte in der Erkennung genetischer Aspekte der Erkrankung erreichen (Erdmann et al., 2018). Somit konnten eine immer weiterwachsende Anzahl an Genen mit der KHK und dem daraus resultierenden Myokardinfarkt in Verbindung gebracht werden. Unter anderem gehören *ATF3* (Nawa et al. 2002; Sobolev, 2011; Gold et al. 2012), *SORT1* (Samani et al. 2007; Maouche & Schunkert 2012) und *HBEGF* (Tanaka et al. 2002; Scuderi et al. 2009; Riedel 2012) zu den meistuntersuchten Loci, die mit der Bildung von Atherosklerose in Zusammenhang gestellt wurden und eine Expressionsänderung im Rahmen einer KHK mit atherosklerotischen Gefäßveränderung oder nach dem Ereignis eines Myokardinfarktes vorzeigen.

Bisher wurden in der molekulargenetischen Forschung in überwiegender Mehrheit Mäuse sowie Zellkulturen als *in vivo* Modelle eingesetzt. Der Zebrafisch (*Danio rerio*) wurde in der letzten Dekade dank der kurzen Generationszeit, der optisch transparenten Larven und dem relativ einfachen Zugang zur Geneditierung als ein neuer und stetig bevorzugter Modellorganismus in der kardiovaskulären Forschung eingesetzt (Stoletov et al. 2009; Yoon et al. 2013; O'Hare et al. 2014). Somit beschrieben die Stoletov sowie Yoon Arbeitsgruppen erstmalig die Bildung von atherosklerotischen Plaques in den Gefäßen von Wildtyp-Zebrafishlarven, die einer hypercholesterinämischen Fütterung unterzogen wurden.

Basierend auf diesen Vorkenntnissen ist das Ziel dieser Arbeit die Expressionsanalyse von Orthologen der KHK-assoziierten *ATF3*-, *SORT1*- und *HBEGF* Gene in Wildtyp Zebrafischen, die einer hypercholesterinämischen Fütterung unterzogen wurden.

Materialien und Methoden

In einer ersten Phase wurde eine 4%-cholesterinhaltige Fütterung auf Basis einer handelsüblichen Fischzuchtfütterung hergestellt. Dessen Auswirkung wurde auf die Aorta optisch transparenter Wildtyp-Larven der AB-Reihe in einem Zeitraum von 5, 15 und 25 Tagen nach Zeugung unter dem Mikroskop beobachtet. In der zweiten Phase wurde das Diätmodell auf ausgewachsene AB-Zebrafische in einem Zeitraum von 4, 8 und 12 Wochen extrapoliert. Blutproben wurden zur Bestimmung der Cholesterinämie entnommen sowie zur Expressionsanalyse der *ATF3*-, *SORT1*- und *HBEGF*-Orthologen mittels RT-qPCR im Vergleich zu kontrollgefütterten Fischen. Zusätzlich

wurden histologische Untersuchungen an Hauptgefäßen des Schwanzes in ORO-Färbung gefertigt.

Ergebnisse und Diskussion

Unter einer 4%-HC Diät wurden Lipidablagerungen in den Gefäßwänden von Larven sowie ausgewachsenen Wildtyp-Zebrafischen beobachtet. Zusätzlich zeigte sich erstmalig, dass eine mehrwöchige 4%-HC Diät zu einer Änderung der Genregulation der berücksichtigten orthologen Gene im Zebrafischblut führt. Diese korrelieren zum Teil mit bereits beobachteten Änderungen der Genregulationen im menschlichen Blut nach dem Ereignis eines Myokardinfarktes. Die histologischen Untersuchungen der korrespondierenden adulten Fische konnten jedoch aufgrund der überliegenden aortalen Melanozyten nicht mit Sicherheit beweisen, ob sich Lipidablagerungen in der Aortenwand bereits nach 12 Wochen 4%-HC Diät bildeten. Der Einsatz gewebetransparenter Fische der *casper* Linie und die Verlängerung der HC-Diät könnten womöglich eindeutigere Ergebnisse darüber verschaffen.

Schlussfolgerung und Ausblick

Der Zebrafisch erscheint als aussichtsreicher Modellorganismus für die Erforschung des genetischen Hintergrundes der Atherosklerose und der damit verbundenen kardiovaskulären Erkrankungen. Basierend auf ähnlichen HC-Diäten konnte die O'Hare und Liu Arbeitsgruppen bereits die Bildung von Lipidablagerungen in den Gefäßen von *ldlr*-knock out Zebrafischen beschreiben (O'Hare et al. 2014; Liu et al. 2018). Mit den jetzigen Möglichkeiten der gezielten Genom-Editierung mittels CRISPR-CAS9 könnten weitere experimentelle Zebrafischlinien mit Knock-Outs beliebiger KHK-assoziierten Gene erschaffen werden und damit eine Charakterisierung in hohem Durchfluss dieser Gene auf ihre atherogenen oder arterioproktektiven Eigenschaften ermöglichen. Ein genaues Verständnis der genetischen Pathomechanismen hinter der Atherosklerose könnte somit in Zukunft eine gezielte und personalisierte Diagnostik und womöglich sogar Gentherapien zur Prävention kardiovaskulärer Erkrankungen bei Hochrisiko Patienten ermöglichen.

7. Appendix

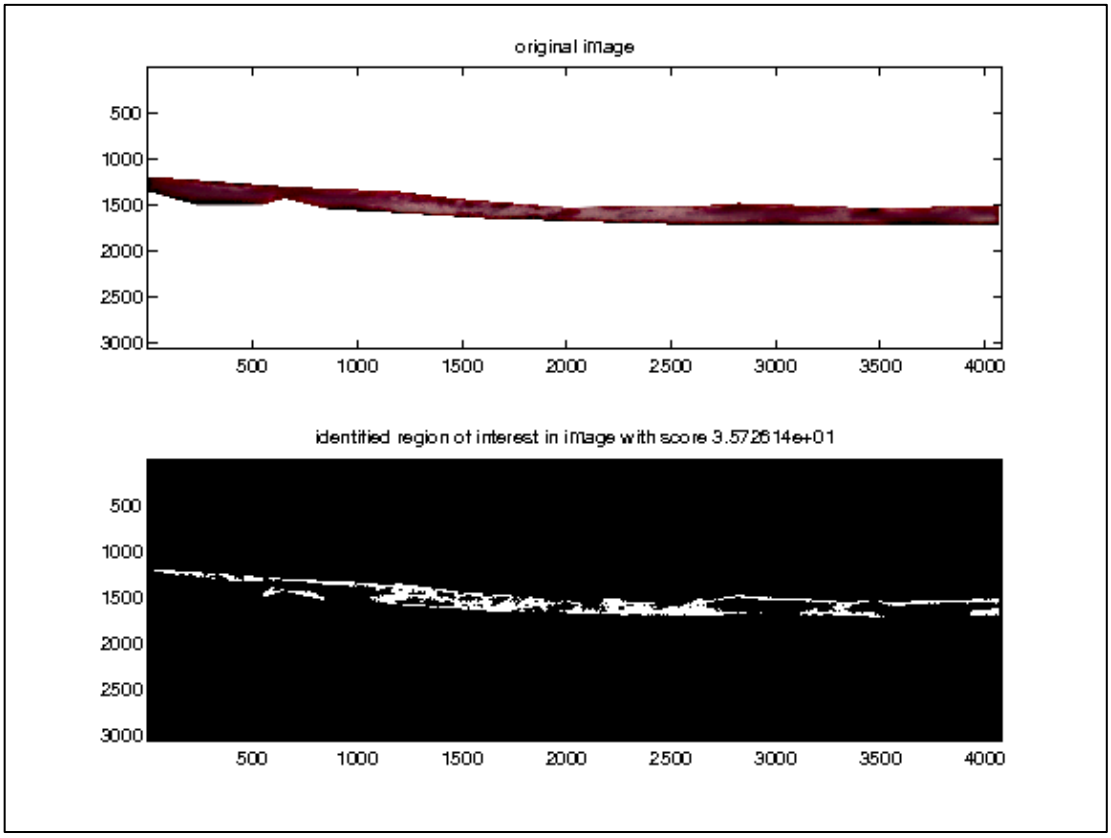

Figure 7.1 Analysis example of ORO-stained lipids covering the surface of a dorsal aorta in a 15 days HCD-fed larva.

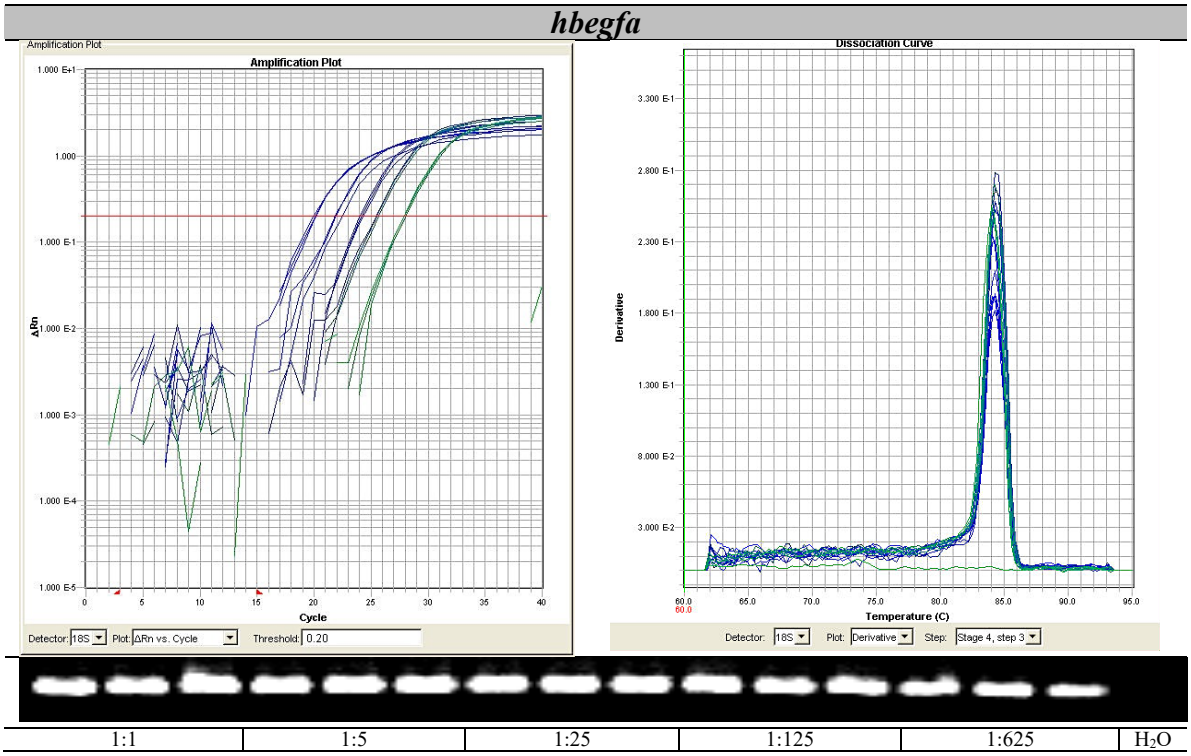

Figure 7.2 Primer validation for *hbegfa*

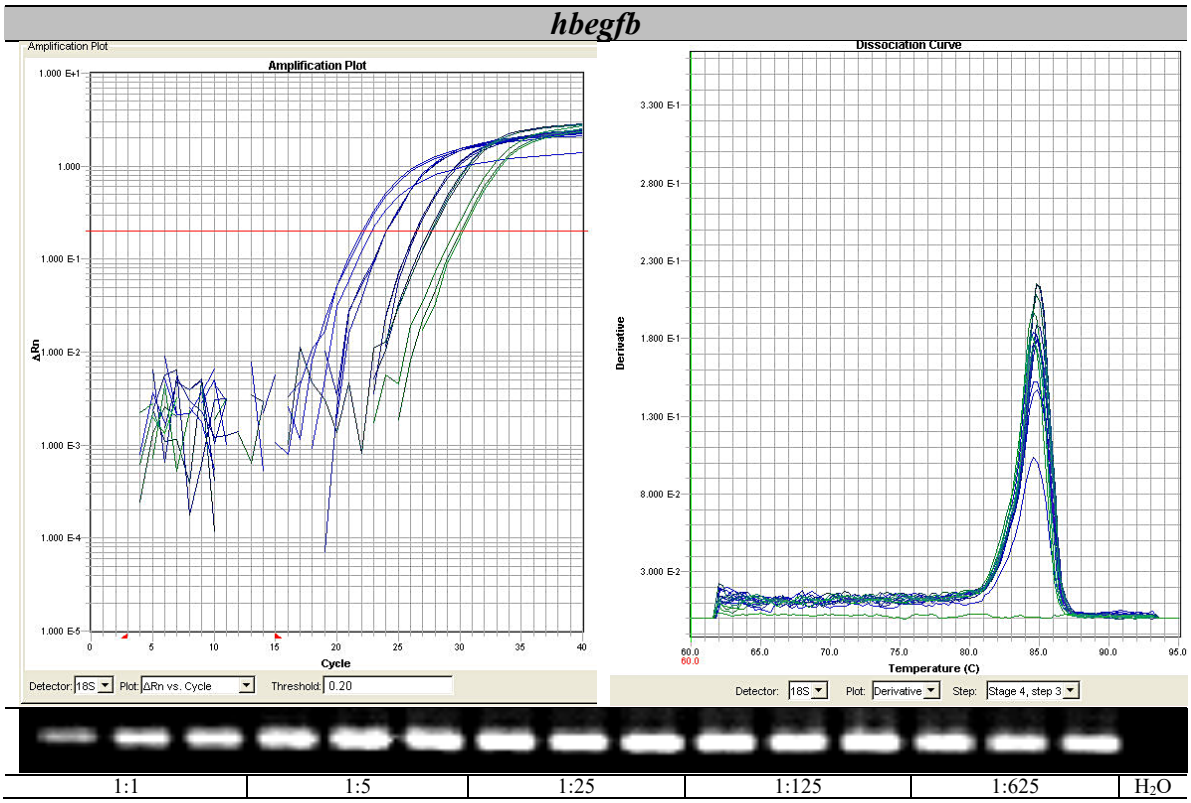

Figure 7.3 Primer validation for *hbegfb*

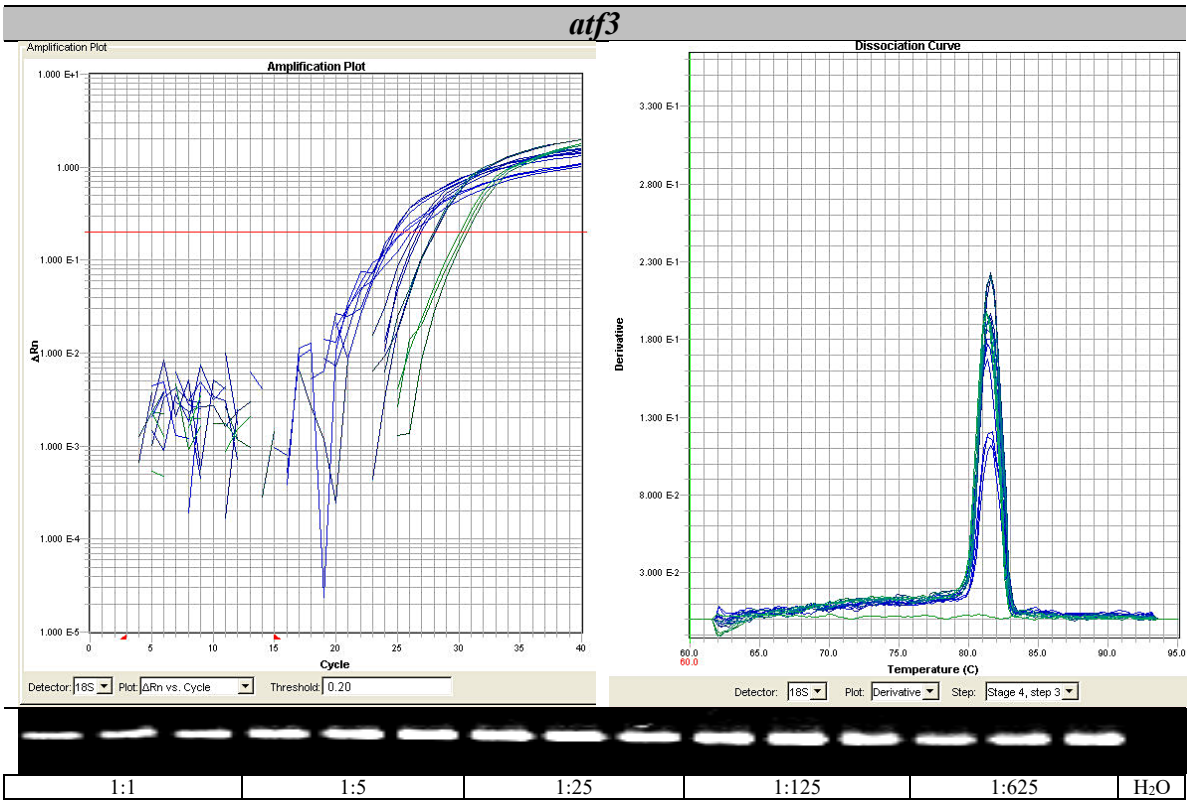

Figure 7.4 Primer validation for *atf3*

8. References

Amores, Angel, Julian Catchen, Allyse Ferrara, Quenton Fontenot, et John H. Postlethwait. 'Genome Evolution and Meiotic Maps by Massively Parallel DNA Sequencing: Spotted Gar, an Outgroup for the Teleost Genome Duplication'. *Genetics* 188, nº 4 (August 2011): 799-808. https://doi.org/10.1534/genetics.111.127324.

Attili, Seetharamaiah, et Simon M. Hughes. 'Anaesthetic Tricaine Acts Preferentially on Neural Voltage-Gated Sodium Channels and Fails to Block Directly Evoked Muscle Contraction'. *PLoS ONE* 9, nº 8 (August 2014). https://doi.org/10.1371/journal.pone.0103751.

Azoo 'P2-9 AZOO 9 in 1 SPECIFIC FOODS', *Azoo product catalogue 2010*

Babin, P. J., and J. M. Vernier. 'Plasma Lipoproteins in Fish.' *Journal of Lipid Research* 30, no. 4 (January 1989): 467–89.

Bournele, Despina, and Dimitris Beis. 'Zebrafish Models of Cardiovascular Disease'. *Heart Failure Reviews* 21, no. 6 (November 2016): 803–13. https://doi.org/10.1007/s10741-016-9579-y.

CARDIoGRAM, Jeanette Erdmann, Klaus Stark, Ulrike B. Esslinger, Philipp Moritz Rumpf, Doris Koesling, Cor de Wit, et al. 'Dysfunctional Nitric Oxide Signalling Increases Risk of Myocardial Infarction'. *Nature* 504, no. 7480 (December 2013): 432–36. https://doi.org/10.1038/nature12722.

Chang, Nai-Jen, Wen-Hui Weng, Kuo-Hsuan Chang, Eric Kar-Wai Liu, Cheng-Keng Chuang, Chih-Cheng Luo, Cheng-Hung Lin, Fu- Chan Wei, and See-Tong Pang. 'Genome-Wide Gene Expression Profiling of Ischemia-Reperfusion Injury in Rat Kidney, Intestine and Skeletal Muscle Implicate a Common Involvement of MAPK Signaling Pathway'. *Molecular Medicine Reports* 11, no. 5 (May 2015): 3786–93. https://doi.org/10.3892/mmr.2015.3235.

Chen, B. P., G. Liang, J. Whelan, and T. Hai. 'ATF3 and ATF3 Delta Zip. Transcriptional Repression versus Activation by Alternatively Spliced Isoforms'. *The Journal of Biological Chemistry* 269, no. 22 (June 1994): 15819–26.

Chen, Shih-Chung, Yu-Chi Liu, Kou-Gi Shyu, and Danny Ling Wang. 'Acute Hypoxia to Endothelial Cells Induces Activating Transcription Factor 3 (ATF3) Expression That Is Mediated via Nitric Oxide'. *Atherosclerosis* 201, no. 2 (December 2008): 281–88. https://doi.org/10.1016/j.atherosclerosis.2008.02.014.

Collins, John E., Simon White, Stephen M.J. Searle, et Derek L. Stemple. 'Incorporating RNA-seq data into the zebrafish Ensembl genebuild'. *Genome Research* 22, nº 10 (October 2012): 2067-78. https://doi.org/10.1101/gr.137901.112.

Davis, Norma E. 'Atherosclerosis - An Inflammatory Process', n.d., 4.

De Muynck, Louis, Sarah Herdewyn, Sander Beel, Wendy Scheveneels, Ludo Van Den Bosch, Wim Robberecht, et Philip Van Damme. 'The Neurotrophic Properties of Progranulin Depend on the Granulin E Domain but Do Not Require Sortilin Binding'. *Neurobiology of Aging* 34, nº 11 (November 2013): 2541-47. https://doi.org/10.1016/j.neurobiolaging.2013.04.022.

De Nardo, Dominic, Larisa I. Labzin, Hajime Kono, Reiko Seki, Susanne V. Schmidt, Marc Beyer, Dakang Xu, et al. 'High Density Lipoprotein Mediates Anti-Inflammatory Transcriptional Reprogramming of Macrophages via the Transcriptional Repressor ATF3'. *Nature Immunology* 15, no. 2 (February 2014): 152–60. https://doi.org/10.1038/ni.2784.

Driever, W, L Solnica-Krezel, A F Schier, S C F Neuhauss, J Malicki, D L Stemple, D Y R Stainier, et al. 'A Genetic Screen for Mutations Affecting Embryogenesis in Zebrafish' (October 1996).

Eisenberg, Eli, et Erez Y. Levanon. 'Human Housekeeping Genes, Revisited'. *Trends in Genetics: TIG* 29, nº 10 (October 2013): 569-74. https://doi.org/10.1016/j.tig.2013.05.010.

Ellertsdóttir, Elín, Anna Lenard, Yannick Blum, Alice Krudewig, Lukas Herwig, Markus Affolter, and Heinz-Georg Belting. 'Vascular Morphogenesis in the Zebrafish Embryo'. *Developmental Biology* 341, no. 1 (May 2010): 56–65. https://doi.org/10.1016/j.ydbio.2009.10.035.

Erdmann, J., C. Willenborg, J. Nahrstaedt, M. Preuss, I. R. Konig, J. Baumert, P. Linsel-Nitschke, et al. 'Genome-Wide Association Study Identifies a New Locus for Coronary Artery Disease on Chromosome 10p11.23'. *European Heart Journal* 32, no. 2 (January 2011): 158–68. https://doi.org/10.1093/eurheartj/ehq405.

Erdmann, Jeanette, Anika Großhennig, Peter S Braund, Inke R König, Christian Hengstenberg, Alistair S Hall, Patrick Linsel-Nitschke, et al. 'New Susceptibility Locus for Coronary Artery Disease on Chromosome 3q22.3'. *Nature Genetics* 41, no. 3 (March 2009): 280–82. https://doi.org/10.1038/ng.307.

Erdmann, Jeanette, Patrick Linsel-Nitschke, and Heribert Schunkert. 'Genetic Causes of Myocardial Infarction: New Insights from Genome-Wide Association Studies'. *Deutsches Ärzteblatt International* 107, no. 40 (2010): 694.

Erdmann, Jeanette, Thorsten Kessler, Loreto Munoz Venegas, et Heribert Schunkert. 'A Decade of Genome-Wide Association Studies for Coronary Artery Disease: The Challenges Ahead'. *Cardiovascular Research* (March 2018). https://doi.org/10.1093/cvr/cvy084.

Fang, Longhou, and Yury I. Miller. 'Emerging Applications for Zebrafish as a Model Organism to Study Oxidative Mechanisms and Their Roles in Inflammation and Vascular Accumulation of Oxidized Lipids'. *Free Radical Biology & Medicine* 53, no. 7 (October 2012): 1411–20. https://doi.org/10.1016/j.freeradbiomed.2012.08.004.

Fang, Longhou, Chao Liu, and Yury I. Miller. 'Zebrafish Models of Dyslipidemia: Relevance to Atherosclerosis and Angiogenesis'. *Translational Research* 163, no. 2 (February 2014): 99–108. https://doi.org/10.1016/j.trsl.2013.09.004.

Fang, Longhou, Chao Liu, Yury I. Miller. 'Zebrafish Models of Dyslipidemia: Relevance to Atherosclerosis and Angiogenesis'. *Translational Research* 163, nº 2 (February 2014): 99-108. https://doi.org/10.1016/j.trsl.2013.09.004.

Fang, Longhou, Yury I. Miller. 'Emerging Applications for Zebrafish as a Model Organism to Study Oxidative Mechanisms and Their Roles in Inflammation and Vascular Accumulation of Oxidized Lipids'. *Free Radical Biology & Medicine* 53, nº 7 (October 2012): 1411-20. https://doi.org/10.1016/j.freeradbiomed.2012.08.004.

Fang, Longhou, Richard Harkewicz, Karsten Hartvigsen, Philipp Wiesner, Soo-Ho Choi, Felicidad Almazan, Jennifer Pattison, et al. 'Oxidized Cholesteryl Esters and Phospholipids in Zebrafish Larvae Fed a High Cholesterol Diet: MACROPHAGE BINDING AND ACTIVATION'. *Journal of Biological Chemistry* 285, no. 42 (October 2010): 32343–51. https://doi.org/10.1074/jbc.M110.137257.

Fang, Longhou, Simone R. Green, Ji Sun Baek, Sang-Hak Lee, Felix Ellett, Elena Deer, Graham J. Lieschke, Joseph L. Witztum, Sotirios Tsimikas, and Yury I. Miller. 'In Vivo Visualization and Attenuation of Oxidized Lipid Accumulation in Hypercholesterolemic Zebrafish'. *Journal of Clinical Investigation* 121, nº 12 (December 2011): 4861-69. https://doi.org/10.1172/JCI57755.

Farrell, A. P., R. L. Saunders, H. C. Freeman, and T. P. Mommsen. 'Arteriosclerosis in Atlantic Salmon. Effects of Dietary Cholesterol and Maturation.' *Arteriosclerosis,*

Thrombosis, and Vascular Biology 6, no. 4 (July 1986): 453–61. https://doi.org/10.1161/01.ATV.6.4.453.

Finegold, Judith A., Perviz Asaria, and Darrel P. Francis. 'Mortality from Ischaemic Heart Disease by Country, Region, and Age: Statistics from World Health Organisation and United Nations'. *International Journal of Cardiology* 168, no. 2 (September 2013): 934–45. https://doi.org/10.1016/j.ijcard.2012.10.046.

Finn, A. V., M. Nakano, J. Narula, F. D. Kolodgie, and R. Virmani. 'Concept of Vulnerable/Unstable Plaque'. *Arteriosclerosis, Thrombosis, and Vascular Biology* 30, no. 7 (July 2010): 1282–92. https://doi.org/10.1161/ATVBAHA.108.179739.

Friedrichs, Frauke, Christian Zugck, Gerd-Jörg Rauch, Boris Ivandic, Dieter Weichenhan, Margit Müller-Bardorff, Benjamin Meder, et al. 'HBEGF, SRA1, and IK: Three Cosegregating Genes as Determinants of Cardiomyopathy'. *Genome Research* 19, nº 3 (March 2009): 395-403. https://doi.org/10.1101/gr.076653.108.

Gerhard, Glenn S., Elizabeth J. Kauffman, Xujun Wang, Richard Stewart, Jessica L. Moore, Claudia J. Kasales, Eugene Demidenko, et Keith C. Cheng. 'Life Spans and Senescent Phenotypes in Two Strains of Zebrafish (Danio Rerio)'. *Experimental Gerontology* 37, nº 8-9 (September 2002): 1055-68.

Gilchrist, Mark, Vesteinn Thorsson, Bin Li, Alistair G. Rust, Martin Korb, Kathleen Kennedy, Tsonwin Hai, Hamid Bolouri, and Alan Aderem. 'Systems Biology Approaches Identify ATF3 as a Negative Regulator of Toll-like Receptor 4'. *Nature* 441, no. 7090 (May 2006): 173–78. https://doi.org/10.1038/nature04768.

Glasauer, Stella M. K., and Stephan C. F. Neuhauss. 'Whole-Genome Duplication in Teleost Fishes and Its Evolutionary Consequences'. *Molecular Genetics and Genomics* 289, no. 6 (December 2014): 1045–60. https://doi.org/10.1007/s00438-014-0889-2.

Gold, Elizabeth S., Stephen A. Ramsey, Mark J. Sartain, Jyrki Selinummi, Irina Podolsky, David J. Rodriguez, Robert L. Moritz, and Alan Aderem. 'ATF3 Protects against Atherosclerosis by Suppressing 25-Hydroxycholesterol–induced Lipid Body Formation'. *The Journal of Experimental Medicine* 209, no. 4 (9 April 2012): 807–17. https://doi.org/10.1084/jem.20111202.

Goldsmith P., Solari R. (2003). The role of zebrafish in drug discovery. *Drug Discovery World* Spring, 74–78

Haffter, P., M. Granato, M. Brand, M. C. Mullins, M. Hammerschmidt, D. A. Kane, J. Odenthal, et al. 'The Identification of Genes with Unique and Essential Functions in

the Development of the Zebrafish, Danio Rerio'. *Development (Cambridge, England)* 123 (December 1996): 1–36.

Hartvigsen, Karsten, Christoph J. Binder, Lotte F. Hansen, Apaïs Rafia, Joseph Juliano, Sohvi Hörkkö, Daniel Steinberg, Wulf Palinski, Joseph L. Witztum, et Andrew C. Li. 'A Diet-Induced Hypercholesterolemic Murine Model to Study Atherogenesis without Obesity and Metabolic Syndrome'. *Arteriosclerosis, Thrombosis, and Vascular Biology* 27, nº 4 (April 2007): 878-85. https://doi.org/10.1161/01.ATV.0000258790.35810.02.

Herold, Gerd, ed. Innere Medizin 2018: eine vorlesungsorientierte Darstellung: unter Berücksichtigung des Gegenstandskataloges für die Ärztliche Prüfung: mit ICD 10-Schlüssel im Text und Stichwortverzeichnis. Köln: Gerd Herold, (2018).

Higashiyama, S., J. A. Abraham, J. Miller, J. C. Fiddes, et M. Klagsbrun. 'A Heparin-Binding Growth Factor Secreted by Macrophage-like Cells That Is Related to EGF'. *Science (New York, N.Y.)* 251, nº 4996 (February 1991): 936-39.

Hirata, Masashi, Kei-ichiro Nakamura, Takaaki Kanemaru, Yosaburo Shibata, et Shigeru Kondo. 'Pigment Cell Organization in the Hypodermis of Zebrafish'. *Developmental Dynamics* 227, nº 4 (August 2003): 497-503. https://doi.org/10.1002/dvdy.10334.

Howe, Kerstin, Matthew D. Clark, Carlos F. Torroja, James Torrance, Camille Berthelot, Matthieu Muffato, John E. Collins, et al. 'The Zebrafish Reference Genome Sequence and Its Relationship to the Human Genome'. *Nature* 496, no. 7446 (April 2013): 498–503. https://doi.org/10.1038/nature12111.

Howe, Kerstin, Matthew D. Clark, Carlos F. Torroja, James Torrance, Camille Berthelot, Matthieu Muffato, John E. Collins, et al. 'The Zebrafish Reference Genome Sequence and Its Relationship to the Human Genome'. *Nature* 496, nº 7446 (April 2013): 498-503. https://doi.org/10.1038/nature12111.

Howe, Kerstin, Matthew D. Clark, Carlos F. Torroja, James Torrance, Camille Berthelot, Matthieu Muffato, John E. Collins, et al. 'The Zebrafish Reference Genome Sequence and Its Relationship to the Human Genome'. *Nature* 496, nº 7446 (April 2013): 498-503. https://doi.org/10.1038/nature12111.

Hu, Norman, David Sedmera, H. Joseph Yost, and Edward B. Clark. 'Structure and Function of the Developing Zebrafish Heart'. *The Anatomical Record* 260, no. 2 (October 2000): 148–57. https://doi.org/10.1002/1097-0185(20001001)260:2<148::AID-AR50>3.0.CO;2-X.

Hu, Norman, H Yost, and Edward B. Clark. 'Cardiac Morphology and Blood Pressure in the Adult Zebrafish'. *The Anatomical Record* 264 (September 2001): 1–12. https://doi.org/10.1002/ar.1111.

Igura, T, Sumio Kawata, J.-i Miyagawa, Y Inui, S Tamura, Kazunori Fukuda, K Isozaki, et al. 'Expression of Heparin-Binding Epidermal Growth Factor Like Growth Factor in Neointimal Cells Induced by Balloon Injury in Rat Carotid Arteries'. *Arteriosclerosis, thrombosis, and vascular biology* 16 (January 1997): 1524-31. https://doi.org/10.1161/01.ATV.16.12.1524.

Isogai, Sumio, Masaharu Horiguchi, and Brant M. Weinstein. 'The Vascular Anatomy of the Developing Zebrafish: An Atlas of Embryonic and Early Larval Development'. *Developmental Biology* 230, no. 2 (February 2001): 278–301. https://doi.org/10.1006/dbio.2000.9995.

James Henderson, R., and Douglas R. Tocher. 'The Lipid Composition and Biochemistry of Freshwater Fish'. *Progress in Lipid Research* 26, no. 4 (January 1987): 281–347. https://doi.org/10.1016/0163-7827(87)90002-6.

Jones, Gregory T., Matthew J. Bown, Solveig Gretarsdottir, Simon P. R. Romaine, Anna Helgadottir, Grace Yu, Gerard Tromp, et al. 'A Sequence Variant Associated with Sortilin-1 (SORT1) on 1p13.3 Is Independently Associated with Abdominal Aortic Aneurysm'. *Human Molecular Genetics* 22, no. 14 (July 2013): 2941. https://doi.org/10.1093/hmg/ddt141.

Kawakami, Akio, Akira Tanaka, Tsuyoshi Chiba, Katsuyuki Nakajima, Kentaro Shimokado, et Masayuki Yoshida. 'Remnant Lipoprotein-Induced Smooth Muscle Cell Proliferation Involves Epidermal Growth Factor Receptor Transactivation'. *Circulation* 108, nº 21 (November 2003): 2679-88. https://doi.org/10.1161/01.CIR.0000093278.75565.87.

Kimmel, Charles B., William W. Ballard, Seth R. Kimmel, Bonnie Ullmann, et Thomas F. Schilling. 'Stages of Embryonic Development of the Zebrafish'. *Developmental Dynamics* 203, nº 3 (July 1995): 253-310. https://doi.org/10.1002/aja.1002030302.

Kjolby, Mads, Morten Schallburg Nielsen, and Claus Munck Petersen. 'Sortilin, Encoded by the Cardiovascular Risk Gene SORT1, and Its Suggested Functions in Cardiovascular Disease'. *Current Atherosclerosis Reports* 17, no. 4 (April 2015). https://doi.org/10.1007/s11883-015-0496-7.

Lawrence, Christian, Isaac Adatto, Jason Best, Althea James, et Kara Maloney. 'Generation Time of Zebrafish (*Danio Rerio*) and Medakas (*Oryzias Latipes*) Housed in the Same

Aquaculture Facility ‘. Special Features. *Lab Animal*, (June 2012). https://doi.org/10.1038/laban0612-158.

Lee, Jinyoung, Samuel M. Peterson, and Jennifer L. Freeman. ‘Sex-Specific Characterization and Evaluation of the Alzheimer’s Disease Genetic Risk Factor *Sorl1* in Zebrafish during Aging and in the Adult Brain Following a 100 Ppb Embryonic Lead Exposure: Characterization of Zebrafish *Sorl1*’. *Journal of Applied Toxicology* 37, no. 4 (April 2017): 400–407. https://doi.org/10.1002/jat.3372.

Lee, Jinyoung, Samuel M. Peterson, et Jennifer L. Freeman. ‘Sex-Specific Characterization and Evaluation of the Alzheimer’s Disease Genetic Risk Factor *Sorl1* in Zebrafish during Aging and in the Adult Brain Following a 100 Ppb Embryonic Lead Exposure: Characterization of Zebrafish *Sorl1*’. *Journal of Applied Toxicology* 37, nº 4 (April 2017): 400-407. https://doi.org/10.1002/jat.3372.

Liew, Woei Chang, and László Orbán. ‘Zebrafish Sex: A Complicated Affair’. *Briefings in Functional Genomics* 13, no. 2 (March 2014): 172–87. https://doi.org/10.1093/bfgp/elt041.

Liew, Woei Chang, Richard Bartfai, Zijie Lim, Rajini Sreenivasan, Kellee R. Siegfried, and Laszlo Orban. ‘Polygenic Sex Determination System in Zebrafish’. Edited by Berta Alsina. *PLoS ONE* 7, no. 4 (April 2012): e34397. https://doi.org/10.1371/journal.pone.0034397.

Lin, C., E. Spikings, T. Zhang, et D. Rawson. ‘Housekeeping Genes for Cryopreservation Studies on Zebrafish Embryos and Blastomeres’. *Theriogenology* 71, nº 7 (April 2009): 1147-55. https://doi.org/10.1016/j.theriogenology.2008.12.013.

Livak, Kenneth J., et Thomas D. Schmittgen. ‘Analysis of Relative Gene Expression Data Using Real-Time Quantitative PCR and the 2−ΔΔCT Method’. *Methods* 25, nº 4 (December 2001): 402-8. https://doi.org/10.1006/meth.2001.1262.

Liu et al., ‘Modeling hypercholesterolemia and vascular lipid accumulation in LDL receptor mutant zebrafish’, *Journal of Lipid Research* 59, nº 2 (February 2018): 391-99, https://doi.org/10.1194/jlr.D081521.

Lloyd-Jones, Donald M., Byung-Ho Nam, Ralph B. D’Agostino, Sr, Daniel Levy, Joanne M. Murabito, Thomas J. Wang, Peter W. F. Wilson, and Christopher J. O’Donnell. ‘Parental Cardiovascular Disease as a Risk Factor for Cardiovascular Disease in Middle-Aged Adults: A Prospective Study of Parents and Offspring’. *JAMA* 291, no. 18 (May 2004): 2204. https://doi.org/10.1001/jama.291.18.2204.

Lv, Dandan, Dan Meng, Fang-Fang Zou, Li Fan, Ping Zhang, Ying Yu, and Jing Fang. 'Activating Transcription Factor 3 Regulates Survivability and Migration of Vascular Smooth Muscle Cells'. *IUBMB Life* 63, no. 1 (January 2011): 62–69. https://doi.org/10.1002/iub.416.

Lv, Dandan, Dan Meng, Fang-Fang Zou, Li Fan, Ping Zhang, Ying Yu, et Jing Fang. 'Activating Transcription Factor 3 Regulates Survivability and Migration of Vascular Smooth Muscle Cells'. *IUBMB Life* 63, nº 1 (January 2011): 62-69. https://doi.org/10.1002/iub.416.

Mahmood, Syed S., Daniel Levy, Ramachandran S. Vasan, et Thomas J. Wang. 'The Framingham Heart Study and the Epidemiology of Cardiovascular Disease: A Historical Perspective'. *The Lancet* 383, nº 9921 (March 2014): 999-1008. https://doi.org/10.1016/S0140-6736(13)61752-3.

Maouche, S., et H. Schunkert. 'Strategies Beyond Genome-Wide Association Studies for Atherosclerosis'. *Arteriosclerosis, Thrombosis, and Vascular Biology* 32, nº 2 (February 2012): 170-81. https://doi.org/10.1161/ATVBAHA.111.232652.

Marenberg, M. E., N. Risch, L. F. Berkman, B. Floderus, and U. de Faire. 'Genetic Susceptibility to Death from Coronary Heart Disease in a Study of Twins'. *The New England Journal of Medicine* 330, no. 15 (April 1994): 1041–46. https://doi.org/10.1056/NEJM199404143301503.

Maxfield, Frederick R., et Ira Tabas. ' Role of cholesterol and lipid organization in disease'. *Nature* 438 (November 2005): 612.

Mayer, Björn, Jeanette Erdmann, and Heribert Schunkert. 'Genetics and Heritability of Coronary Artery Disease and Myocardial Infarction'. *Clinical Research in Cardiology: Official Journal of the German Cardiac Society* 96, no. 1 (January 2007): 1–7. https://doi.org/10.1007/s00392-006-0447-y.

McClure, M. M., P. B. McIntyre, and A. R. McCune. 'Notes on the Natural Diet and Habitat of Eight Danionin Fishes, Including the Zebrafish Danio Rerio'. *Journal of Fish Biology* 69, no. 2 (August 2006): 553–70. https://doi.org/10.1111/j.1095-8649.2006.01125.x.

Mendis, Shanthi, Weltgesundheitsorganisation, and World Heart Federation, eds. *Global Atlas on Cardiovascular Disease Prevention and Control*. Geneva: World Health Organization, (2011).

Menke, Aswin L., Jan M. Spitsbergen, Andre P. M. Wolterbeek, and Ruud A. Woutersen. 'Normal Anatomy and Histology of the Adult Zebrafish'. *Toxicologic Pathology* 39, no. 5 (August 2011): 759–75. https://doi.org/10.1177/0192623311409597.

Menotti, A., and P. E. Puddu. 'How the Seven Countries Study Contributed to the Definition and Development of the Mediterranean Diet Concept: A 50-Year Journey'. *Nutrition, Metabolism, and Cardiovascular Diseases: NMCD* 25, no. 3 (March 2015): 245–52. https://doi.org/10.1016/j.numecd.2014.12.001.

Meyer, Axel, and Manfred Schartl. 'Gene and Genome Duplications in Vertebrates: The One-to-Four (-to-Eight in Fish) Rule and the Evolution of Novel Gene Functions'. *Current Opinion in Cell Biology* 11, no. 6 (December 1999): 699–704. https://doi.org/10.1016/S0955-0674(99)00039-3.

Miano, Joseph M., Mary A. Georger, Adam Rich, et Karen L. De Mesy Bentley. « Ultrastructure of Zebrafish Dorsal Aortic Cells ». *Zebrafish* 3, nº 4 (2006): 455-63. https://doi.org/10.1089/zeb.2006.3.455.

Mortensen, Martin B., Mads Kjolby, Stine Gunnersen, Jakob V. Larsen, Johan Palmfeldt, Erling Falk, Anders Nykjaer, and Jacob F. Bentzon. 'Targeting Sortilin in Immune Cells Reduces Proinflammatory Cytokines and Atherosclerosis'. *The Journal of Clinical Investigation* 124, no. 12 (2014): 5317–5322.

Muendlein, Axel, Simone Geller-Rhomberg, Christoph H. Saely, Thomas Winder, Gudrun Sonderegger, Philipp Rein, Stefan Beer, Alexander Vonbank, and Heinz Drexel. 'Significant Impact of Chromosomal Locus 1p13.3 on Serum LDL Cholesterol and on Angiographically Characterized Coronary Atherosclerosis'. *Atherosclerosis* 206, no. 2 (October 2009): 494–99. https://doi.org/10.1016/j.atherosclerosis.2009.02.040.

Mumford, Sonia, Jerry Heidel, Charlie Smith, John Morrison, Beth MacConnell, and Vicki Blazer. 'Fish Histology and Histopathology', (2007), 357.

Murtha, Jill M., Weici Qi, and Evan T. Keller. 'Hematologic and Serum Biochemical Values for Zebrafish (Danio Rerio)'. *Comparative Medicine* 53, no. 1 (February 2003): 37–41.

Musunuru, Kiran, Alanna Strong, Maria Frank-Kamenetsky, Noemi E. Lee, Tim Ahfeldt, Katherine V. Sachs, Xiaoyu Li, et al. 'From Noncoding Variant to Phenotype via SORT1 at the 1p13 Cholesterol Locus'. *Nature* 466, no. 7307 (August 2010): 714–19. https://doi.org/10.1038/nature09266.

Nawa, Tigre, Makiko T Nawa, Mimi T Adachi, Isao Uchimura, Reiko Shimokawa, Kazuhiko Fujisawa, Akira Tanaka, Fujio Numano, and Shigetaka Kitajima.

‘Expression of Transcriptional Repressor ATF3/LRF1 in Human Atherosclerosis: Colocalization and Possible Involvement in Cell Death of Vascular Endothelial Cells’. *Atherosclerosis* 161, no. 2 (April 2002): 281–91. https://doi.org/10.1016/S0021-9150(01)00639-6.

O’Hare, Elizabeth A., Xiaochun Wang, May E. Montasser, Yen-Pei C. Chang, Braxton D. Mitchell, and Norann A. Zaghloul. ‘Disruption of *Ldlr* Causes Increased LDL-c and Vascular Lipid Accumulation in a Zebrafish Model of Hypercholesterolemia’. *Journal of Lipid Research* 55, no. 11 (November 2014): 2242–53. https://doi.org/10.1194/jlr.M046540.

Ogawa, Kazuyuki, Takahiro Ueno, Tadao Iwasaki, Takeshi Kujiraoka, Mitsuaki Ishihara, Satoshi Kunimoto, Tadateru Takayama, Takashi Kanai, Atsushi Hirayama, et Hiroaki Hattori. « Soluble Sortilin Is Released by Activated Platelets and Its Circulating Levels Are Associated with Cardiovascular Risk Factors ». *Atherosclerosis* 249 (2016): 110-15. https://doi.org/10.1016/j.atherosclerosis.2016.03.041.

Okamoto, Yoshichika, Alysia Chaves, Jingchun Chen, Robert Kelley, Keith Jones, Harrison G. Weed, Kevin L. Gardner, et al. ‘Transgenic Mice with Cardiac-Specific Expression of Activating Transcription Factor 3, a Stress-Inducible Gene, Have Conduction Abnormalities and Contractile Dysfunction’. *The American Journal of Pathology* 159, no. 2 (August 2001): 639–50.

Ota, Satoshi, and Atsuo Kawahara. ‘Zebrafish: A Model Vertebrate Suitable for the Analysis of Human Genetic Disorders: Zebrafish Suitable for Genetic Analysis’. *Congenital Anomalies* 54, no. 1 (February 2014): 8–11. https://doi.org/10.1111/cga.12040.

Otis, J. P., E. M. Zeituni, J. H. Thierer, J. L. Anderson, A. C. Brown, E. D. Boehm, D. M. Cerchione, et al. ‘Zebrafish as a Model for Apolipoprotein Biology: Comprehensive Expression Analysis and a Role for ApoA-IV in Regulating Food Intake’. *Disease Models & Mechanisms* 8, no. 3 (March 2015): 295–309. https://doi.org/10.1242/dmm.018754.

Pannevis, Marinus C., et Kay E. Earle. ‘Maintenance Energy Requirement of Five Popular Species of Ornamental Fish’. *The Journal of Nutrition* 124, nº suppl_12 (December 1994): 2616S-2618S. https://doi.org/10.1093/jn/124.suppl_12.2616S.

Parichy, David M. ‘Advancing biology through a deeper understanding of zebrafish ecology and evolution’. *eLife* 4. Accessed March 2018. https://doi.org/10.7554/eLife.05635.

Parichy, David M. ‘Advancing biology through a deeper understanding of zebrafish ecology and evolution’. *eLife* 4. Accessed March 2018. https://doi.org/10.7554/eLife.05635.

Parichy, David M. ‘The Natural History of Model Organisms: Advancing Biology through a Deeper Understanding of Zebrafish Ecology and Evolution’. eLife, (Mars 2015). https://doi.org/10.7554/eLife.05635.

Patel, Kevin M., Alanna Strong, Junichiro Tohyama, Xueting Jin, Carlos R. Morales, Jeffery Billheimer, John Millar, Howard Kruth, and Daniel J. Rader. ‘Macrophage Sortilin Promotes LDL Uptake, Foam Cell Formation, and Atherosclerosis’. *Circulation Research* 116, no. 5 (February 2015): 789–96. https://doi.org/10.1161/CIRCRESAHA.116.305811.

Pedroso, Gabriela L., Thais O. Hammes, Thayssa D.C. Escobar, Laisa B. Fracasso, Luiz Felipe Forgiarini, et Themis R. da Silveira. « Blood Collection for Biochemical Analysis in Adult Zebrafish ». *Journal of Visualized Experiments : JoVE*, nº 63 (Mai 2012). https://doi.org/10.3791/3865.

Petersen, Claus M., Morten S. Nielsen, Anders Nykjær, Linda Jacobsen, Niels Tommerup, Hanne H. Rasmussen, Hans Røigaard, Jørgen Gliemann, Peder Madsen, and Søren K. Moestrup. ‘Molecular Identification of a Novel Candidate Sorting Receptor Purified from Human Brain by Receptor-Associated Protein Affinity Chromatography’. *Journal of Biological Chemistry* 272, no. 6 (July 1997): 3599–3605. https://doi.org/10.1074/jbc.272.6.3599.

Poitras, Elyse & Houde, Alain. ‘La PCR en temps réel: Principes et applications’. *Reviews in Biology and Biotechnology*. (2003). 2. 2-11.

Postlethwait, John H., Ian G. Woods, Phuong Ngo-Hazelett, Yi-Lin Yan, Peter D. Kelly, Felicia Chu, Hui Huang, Alicia Hill-Force, et William S. Talbot. ‘Zebrafish Comparative Genomics and the Origins of Vertebrate Chromosomes’. *Genome Research* 10, nº 12 (January 2000): 1890-1902. https://doi.org/10.1101/gr.164800.

Puska, Pekka, Erkki Vartiainen, Tiina Laatikainen, Pekka Jousilahti, and Meri Paavola. *The North Karelia Project: From North Karelia to National Action*. National Institute for Health and Welfare= Terveyden ja hyvinvoinnin laitos (THL), 2009.

Puska, Pekka. ‘Successful Prevention of Non-Communicable Diseases: 25 Year Experiences with North Karelia Project in Finland’. *Public Health Medicine* 4, no. 1 (2002): 5–7.

Quinlivan, Vanessa H., and Steven A. Farber. 'Lipid Uptake, Metabolism, and Transport in the Larval Zebrafish'. *Frontiers in Endocrinology* 8 (November 2017). https://doi.org/10.3389/fendo.2017.00319.

Raab G. and Klagsbrun. 'Heparin-Binding EGF-like Growth Factor. - PubMed – NCBI'. Accessed September 2018. Biochim Biophys Acta. 1997 Dec 9;1333(3):F179-99https://www.ncbi.nlm.nih.gov/pubmed/9426203.

Real-PCR handbook, Life Science Technologies (2012)

Riedel, Claas Sören „Zeitliche Veränderungen der Transkription in menschlicher Monozyten-RNA in Folge eines akuten Myokardinfarktes: Einfluss auf die Monozyten-Adhäsion", Inauguraldisseration Sektion Medizin, Universität zu Lübeck (2011)

Reed, Barney and Jennings, Maggy 'Guidance on the Housing and Care Of Zebrafish Danio Rerio', 2011, Research Animals Department, Science Group, RSPCA, UK

Sager, Hendrik B., Thorsten Kessler, and Heribert Schunkert. 'Monocytes and Macrophages in Cardiac Injury and Repair'. *Journal of Thoracic Disease* 9, no. S1 (March 2017): S30–35. https://doi.org/10.21037/jtd.2016.11.17.

Samani, N. J., et H. Schunkert. « Chromosome 9p21 and Cardiovascular Disease: The Story Unfolds ». *Circulation: Cardiovascular Genetics* 1, nº 2 (December 2008): 81-84. https://doi.org/10.1161/CIRCGENETICS.108.832527.

Samani, Nilesh J., Jeanette Erdmann, Alistair S. Hall, Christian Hengstenberg, Massimo Mangino, Bjoern Mayer, Richard J. Dixon, et al. 'Genomewide Association Analysis of Coronary Artery Disease'. *New England Journal of Medicine* 357, no. 5 (August 2007): 443–53. https://doi.org/10.1056/NEJMoa072366.

Sánchez-Vizcaíno, Elena, Cristina Vehí, Genís Campreciós, César Morcillo, Maria Soley, et Ignasi Ramírez. « Heparin-Binding EGF-like Growth Factor in Human Serum. Association with High Blood Cholesterol and Heart Hypertrophy ». *Growth Factors (Chur, Switzerland)* 28, nº 2 (April 2010): 98-103. https://doi.org/10.3109/08977190903443030.

Sánchez-Vizcaíno, Elena, Cristina Vehí, Genís Campreciós, César Morcillo, Maria Soley, et Ignasi Ramírez. « Heparin-Binding EGF-like Growth Factor in Human Serum. Association with High Blood Cholesterol and Heart Hypertrophy ». *Growth Factors (Chur, Switzerland)* 28, nº 2 (April 2010): 98-103. https://doi.org/10.3109/08977190903443030.

Schlegel, Amnon. « Zebrafish Models for Dyslipidemia and Atherosclerosis Research ». *Frontiers in Endocrinology* 7 (2016): 159. https://doi.org/10.3389/fendo.2016.00159.

Schunkert, H., A. Gotz, P. Braund, R. McGinnis, D.-A. Tregouet, M. Mangino, P. Linsel-Nitschke, et al. 'Repeated Replication and a Prospective Meta-Analysis of the Association Between Chromosome 9p21.3 and Coronary Artery Disease'. *Circulation* 117, no. 13 (March 2008): 1675–84. https://doi.org/10.1161/CIRCULATIONAHA.107.730614.

Schunkert, Heribert, Inke R König, Sekar Kathiresan, Muredach P Reilly, Themistocles L Assimes, Hilma Holm, Michael Preuss, et al. 'Large-Scale Association Analysis Identifies 13 New Susceptibility Loci for Coronary Artery Disease'. *Nature Genetics* 43, no. 4 (March 2011): 333–38. https://doi.org/10.1038/ng.784.

Scuderi, R., S. Travali, P. Castrogiovanni, R. M. Imbesi, V. Mazzone, G. Failla, et A. Failla. « [Immunolocalization of HB-EGF in human atherosclerotic plaques] ». *La Clinica Terapeutica* 160, nº 6 (2009): 435-39.

Shaklee, J. B., J. A. Christiansen, B. D. Sidell, C. L. Prosser, et G. S. Whitt. « Molecular Aspects of Temperature Acclimation in Fish: Contributions of Changes in Enzyme Activities and Isozyme Patterns to Metabolic Reorganization in the Green Sunfish ». *The Journal of Experimental Zoology* 201, nº 1 (July 1977): 1-20. https://doi.org/10.1002/jez.1402010102.

Sheridan, Mark A. « Lipid Dynamics in Fish: Aspects of Absorption, Transportation, Deposition and Mobilization ». *Comparative Biochemistry and Physiology Part B: Comparative Biochemistry* 90, nº 4 (January 1988): 679-90. https://doi.org/10.1016/0305-0491(88)90322-7.

Sobolev, V. V., N. L. Starodubtseva, A. L. Piruzyan, M.T. Minnibaev, M. E. Sautin, V. P. Tumanov, et S. A. Bruskin. « Comparative Study of the Expression of ATF-3 and ATF-4 Genes in Vessels Involved into Atherosclerosis Process and in Psoriatic Skin ». *Bulletin of Experimental Biology and Medicine* 151, nº 6 (October 2011): 713-16. https://doi.org/10.1007/s10517-011-1423-8.

Solin, Staci L., Ying Wang, Joshua Mauldin, Laura E. Schultz, Deborah E. Lincow, Pavel A. Brodskiy, Crystal A. Jones, et al. « Molecular and Cellular Characterization of a Zebrafish Optic Pathway Tumor Line Implicates Glia-Derived Progenitors in Tumorigenesis ». Édité par Joseph Charles Glorioso. *PLoS ONE* 9, nº 12 (December 2014): e114888. https://doi.org/10.1371/journal.pone.0114888.

Solin, Staci L., Ying Wang, Joshua Mauldin, Laura E. Schultz, Deborah E. Lincow, Pavel A. Brodskiy, Crystal A. Jones, et al. 'Molecular and Cellular Characterization of a Zebrafish Optic Pathway Tumor Line Implicates Glia-Derived Progenitors in Tumorigenesis'.*PLoS ONE* 9, nº 12 (December 2014): e114888. https://doi.org/10.1371/journal.pone.0114888.

Song, Youngsup, et Roger D. Cone. 'Creation of a genetic model of obesity in a teleost'. *The FASEB Journal* 21, nº 9 (March 2007): 2042-49. https://doi.org/10.1096/fj.06-7503com.

Spence, R., M. K. Fatema, S. Ellis, Z. F. Ahmed, and C. Smith. 'Diet, Growth and Recruitment of Wild Zebrafish in Bangladesh'. *Journal of Fish Biology* 71, no. 1 (July 2007): 304–9. https://doi.org/10.1111/j.1095-8649.2007.01492.x.

Spence, Rowena, Gabriele Gerlach, Christian Lawrence, et Carl Smith. 'The Behaviour and Ecology of the Zebrafish, Danio Rerio'. *Biological Reviews* 83, nº 1 (February 2008): 13-34. https://doi.org/10.1111/j.1469-185X.2007.00030.x.

Stainier, D, B Fouquet, Jau-Nian Chen, K S Warren, B M Weinstein, Steffen Meiler, M A. P. K. Mohideen, et al. 'Mutations affecting the formation and function of the cardiovascular system in the zebrafish embryo'. *Development (Cambridge, England)* 123 (January 1997): 285-92. https://doi.org/10.5167/uzh-237.

Stainier, Didier Y R, Bernadette Fouquet, Jau-Nian Chen, Kerri S Warren, Brant M Weinstein, Steffen E Meiler, Manzoor-Ali P K Mohideen, et al. 'Mutations Affecting the Formation and Function of the Cardiovascular System in the Zebrafish Embryo', n.d., 8.

Stoletov, K., L. Fang, S.-H. Choi, K. Hartvigsen, L. F. Hansen, C. Hall, J. Pattison, et al. 'Vascular Lipid Accumulation, Lipoprotein Oxidation, and Macrophage Lipid Uptake in Hypercholesterolemic Zebrafish'. *Circulation Research* 104, no. 8 (April 2009): 952–60. https://doi.org/10.1161/CIRCRESAHA.108.189803.

Streisinger, G., C. Walker, N. Dower, D. Knauber, et F. Singer. 'Production of Clones of Homozygous Diploid Zebra Fish (Brachydanio Rerio)'. *Nature* 291, nº 5813 (May 1981): 293-96.

Stylianou, Ioannis M., Robert C. Bauer, Muredach P. Reilly, et Daniel J. Rader. 'Genetic Basis of Atherosclerosis: Insights from Mice and Humans'. *Circulation Research* 110, nº 2 (January 2012): 337-55. https://doi.org/10.1161/CIRCRESAHA.110.230854.

Tanaka, Nobuyoshi, Katsuhiko Masamura, Masahiro Yoshida, Masayuki Kato, Yasuyuki Kawai, et Isamu Miyamori. 'A Role of Heparin-Binding Epidermal Growth Factor-

like Growth Factor in Cardiac Remodeling after Myocardial Infarction'. *Biochemical and Biophysical Research Communications* 297, nº 2 (September 2002): 375-81.

Torpy, Janet M. 'Coronary Heart Disease Risk Factors'. *JAMA* 302, no. 21 (December 2009): 2388. https://doi.org/10.1001/jama.302.21.2388.

Tsai, Chia-Ti, Cho-Kai Wu, Fu-Tien Chiang, Chuen-Den Tseng, Jen-Kuang Lee, Chih-Chieh Yu, Yi-Chih Wang, Ling-Ping Lai, Jiunn-Lee Lin, et Juey-Jen Hwang. 'In-Vitro Recording of Adult Zebrafish Heart Electrocardiogram - a Platform for Pharmacological Testing'. *Clinica Chimica Acta; International Journal of Clinical Chemistry* 412, nº 21-22 (October 2011): 1963-67. https://doi.org/10.1016/j.cca.2011.07.002.

Tveten, Kristian, Thea Bismo Strøm, Jamie Cameron, Knut Erik Berge, and Trond P. Leren. 'Mutations in the SORT1 Gene Are Unlikely to Cause Autosomal Dominant Hypercholesterolemia'. *Atherosclerosis* 225, no. 2 (December 2012): 370–75. https://doi.org/10.1016/j.atherosclerosis.2012.10.026.

Underwood, James C. E., ed. *General and Systematic Pathology*. 5. ed., reprint. Student Consult. Edinburgh: Churchill Livingstone/Elsevier, 2010.

Vastesaeger, M. M., et R. Delcourt. 'The Natural History of Atherosclerosis'. *Circulation* 26 (November 1962): 841-55.

Wang, Annabel Z., Lin Li, Bin Zhang, Gong-Qing Shen, et Qing Kenneth Wang. 'Association of SNP rs17465637 on chromosome 1q41 and rs599839 on 1p13.3 with Myocardial Infarction in an American Caucasian Population'. *Annals of human genetics* 75, nº 4 (July 2011): 475-82. https://doi.org/10.1111/j.1469-1809.2011.00646.x.

Wang, Louis W., Inken G. Huttner, Celine F. Santiago, Scott H. Kesteven, Ze-Yan Yu, Michael P. Feneley, et Diane Fatkin. 'Standardized echocardiographic assessment of cardiac function in normal adult zebrafish and heart disease models'. *Disease Models & Mechanisms* 10, nº 1 (January 2017): 63-76. https://doi.org/10.1242/dmm.026989.
Westerfield, M. The Zebrafish Book. A Guide for the Laboratory Use of Zebrafish (Danio rerio), 5th Edition. University of Oregon Press, Eugene. (2007).

White, Richard Mark, Anna Sessa, Christopher Burke, Teresa Bowman, Jocelyn LeBlanc, Craig Ceol, Caitlin Bourque, et al. 'Transparent Adult Zebrafish as a Tool for In Vivo Transplantation Analysis'. *Cell Stem Cell* 2, nº 2 (February 2008): 183-89. https://doi.org/10.1016/j.stem.2007.11.002.

WHO ‘GlobalCOD_method_2000_2015.Pdf’. Accessed 17 January 2018. http://www.who.int/healthinfo/global_burden_disease/GlobalCOD_method_2000_2015.pdf?ua=1.

WHO Cardiovascular Diseases (CVDs). WHO. Accessed 17 January 2018. http://www.who.int/cardiovascular_diseases/en/.

WHO Integrated Chronic Disease Prevention and Control. WHO. Accessed 16 January 2018. http://www.who.int/chp/about/integrated_cd/index2.html.

WHO Top 10 Causes of Death. WHO. Accessed 17 January 2018. https://doi.org//entity/gho/mortality_burden_disease/causes_death/top_10/en/index.html.

Wixon, Jo. ‘Danio Rerio, the Zebrafish’. *Yeast (Chichester, England)* 17, no. 3 (2000): 225–31. https://doi.org/10.1002/1097-0061(20000930)17:3<225::AID-YEA34>3.0.CO;2-5.

Wolfgang, C D, B P Chen, J L Martindale, N J Holbrook, et T Hai. ‘Gadd153/Chop10, a Potential Target Gene of the Transcriptional Repressor ATF3. ‘ *Molecular and Cellular Biology* 17, nº 11 (November 1997): 6700-6707. https://doi.org/10.1128/MCB.17.11.6700.

Wolpert, Lewis, Cheryll Tickle, et Alfonso Martinez Arias. *Principles of Development*. Fifth Edition. Oxford, New York: Oxford University Press (2015).

Yeh, Kun-Yun, Chi-Yu Lai, Chiu-Ya Lin, Chia-Chun Hsu, Chung-Ping Lo, et Guor Mour Her. ‘ATF4 Overexpression Induces Early Onset of Hyperlipidaemia and Hepatic Steatosis and Enhances Adipogenesis in Zebrafish’. *Scientific Reports* 7, nº 1 (November 2017): 16362. https://doi.org/10.1038/s41598-017-16587-9.

Yoon, Yina, Jihye Yoon, Man-Young Jang, Yirang Na, Youngho Ko, Jae-Hoon Choi, and Seung Hyeok Seok. ‘High Cholesterol Diet Induces IL-1β Expression in Adult but Not Larval Zebrafish’. Edited by Partha Mukhopadhyay. *PLoS ONE* 8, no. 6 (June 2013): e66970. https://doi.org/10.1371/journal.pone.0066970.

9. Posters and publications

1. Deutsches Zentrum für Herz- und Kreislaufforschung (DZHK) Retreat ‚*Zebrafish, a model for Atherosclerosis*'
   Krishan Kumar Vishnolia, **Karim Tarhbalouti**, Phillip Ciba, Zouhair Aherrahrou, Jeanette Erdmann. Institut für Integrative und Experimentelle Genomik (IIEG) und Deutsches Zentrum für Herz- und Kreislaufforschung (DZHK) Universität zu Lübeck, Fraunhofer Einrichtung für Marine Biotechnologien (EMB) Lübeck (January 2015).

2. 10 Jahre Uni im Dialog, Universität zu Lübeck: ‚*Der Zebrabärbling: ein neues Forschungsmodell für Atherosklerose*'
   Karim Tarhbalouti, Krishan Kumar Vishnolia, Phillip Ciba, Charlie Kruse, Zouhair Aherrahrou, Jeanette Erdmann. Institut für Integrative und Experimentelle Genomik (IIEG) und Deutsches Zentrum für Herz- und Kreislaufforschung (DZHK) Universität zu Lübeck, Fraunhofer Einrichtung für Marine Biotechnologien (EMB) Lübeck (June 2015).

3. 82. Jahrestagung der Deutschen Gesellschaft für Kardiologie- Herz und Kreislaufforschung, Mainz ‚*Genetic determinants regulating lipid deposits in different wild type strains of zebrafish using QTL analysis*'
   Krishan Kumar Vishnolia, **Karim Tarhbalouti**, Phillip Ciba, Zouhair Aherrahrou, Jeanette Erdmann. Institut für Integrative und Experimentelle Genomik (IIEG) und Deutsches Zentrum für Herz- und Kreislaufforschung (DZHK) Universität zu Lübeck, Fraunhofer Einrichtung für Marine Biotechnologien (EMB) Lübeck (April 2016).

4. Student Lecture 2.0, Universität zu Lübeck ‚*Zebrafish, a model for Atherosclerosis*' **Karim Tarhbalouti**, Krishan Kumar Vishnolia, Phillip Ciba, Charlie Kruse, Zouhair Aherrahrou, Jeanette Erdmann. Institut für Integrative und Experimentelle Genomik (IIEG) und Deutsches Zentrum für Herz- und Kreislaufforschung (DZHK) Universität zu Lübeck, Fraunhofer Einrichtung für Marine Biotechnologien (EMB) Lübeck (May 2016).

DZHK
DEUTSCHES ZENTRUM FÜR
HERZ-KREISLAUF-FORSCHUNG E.V.

Zebrafish, a model for Atherosclerosis

Krishan Kumar Vishnolia (1,2), Karim Tarhbalouti (1), Phillipp Ciba (2), Zouhair Aherrahrou (1) & Jeanette Erdmann (1)
(1) Institut für Integrative und Experimentelle Genomik und DZHK (Deutsches Zentrum für Herz- und Kreislaufforschung)
(2) Fraunhofer-Einrichtung für Marine Biotechnologie, EMB, Lübeck.

Introduction: Cardiovascular diseases (CVD) and atherosclerosis can be studied using mice or other model organisms after post-mortem. It has been reported that all major nuclear receptors, lipid transporters, apolipoproteins and enzymes involved in lipoprotein metabolism are expressed in zebrafish (Fang *et al.,* 2014). Zebrafish (*Danio rerio*) embryos or larvae until one month remain transparent and the availability of effective genetic manipulation tools together enables *in vivo* monitoring of vascular processes in live fish fed with high fat diet. Therefore, in recent years zebrafish has been successfully used as a model organism for atherosclerosis to investigate different patho-mechanisms.

Aim: We aim to discover the genetic mechanisms for atherosclerosis, using zebrafish as a model organism for novel genes/loci reported in genome-wide association study from Erdmann *et al.,* 2013 and compare those results with mice and human.

Methods: Zebrafish fed with high cholesterol diet, shows early signs of lipid accumulation in the dorsal aorta or caudal vein, with or without any prior genetic manipulation. Atherosclerotic background zebrafish (ldlr-knock down) have shown higher amount of lipid plagues compare to normal (O'Hare *et al.,* 2014). Accumulation of lipid can be monitored in live transgenic zebrafish expressing fluorescent proteins and/or fed a diet supplemented with fluorescent lipid tracers. Using gene knock-out/down or transgene techniques, specific genes/loci associated with atherosclerosis can be elucidated or overexpressed in zebrafish genome for further investigations.

Study design:

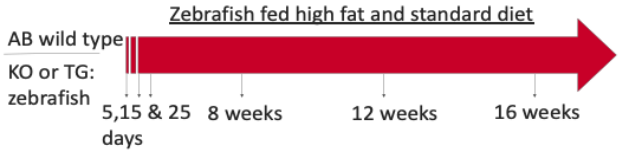

Figure 2: Schematic represents the experimental plan for sample collection at 5, 15 and 25 days initially and later at 8, 12 and 16 weeks from zebrafish fed with standard and high fat diet from different genetic background.

Parameters for analysis: Different parameters have been set in order to confirm the extent of atherosclerosis in zebrafish at different time points such as whole mount Oil Red O (ORO) staining, fluroscence microscopy for lipid deposits, triglycerides measurements, HDL, LDL and VLDL measurements, sectioning and staining for different proteins and gene expression analysis.

Results

Lipid deposits visualised using confocal microscopy

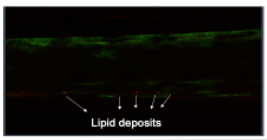

Figure 3: Confocal image zebrafish larve fed with high cholesterol diet supplemented with bodipy dye for oxidised lipid deposits. Green color represents auto fluroscence from zebrafish tissue, red dots represents oxidised lipid deposits in 15 days ppost fertilized zebrafish. Magnification 100X.

Comparision between bodipy fluroscence and ORO staining

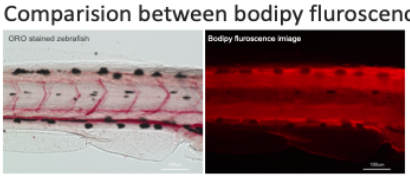

Figure 4: ORO stained and bodipy (dye supplemented in food) fluroscence image for oxidised lipid deposits *in vivo* zebrafish fed with high cholestrol diet for 15 days Magnification 100X.

Oil Red O stained zebrafish larve

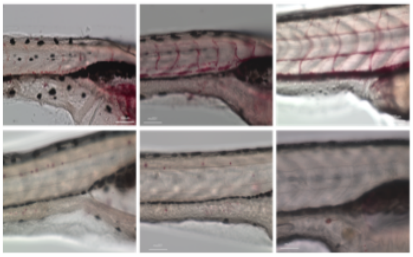

Figure 5: ORO stained images of zebrafish larve; starting from left 5 days old, in middle15 days old and on right 25 days old larve. Top pannel of images are from larve fed high cholesterol diet and lower with control diet. Red dots represents the lipid deposits in DAand CV. Images were captured at 100X magnification for quantification

Quantification of lipid deposits

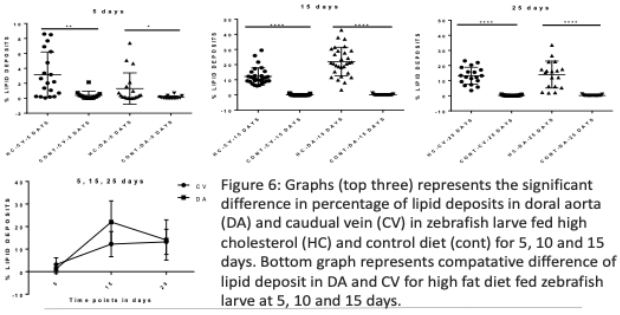

Figure 6: Graphs (top three) represents the significant difference in percentage of lipid deposits in doral aorta (DA) and caudual vein (CV) in zebrafish larve fed high cholesterol (HC) and control diet (cont) for 5, 10 and 15 days. Bottom graph represents compatative difference of lipid deposit in DA and CV for high fat diet fed zebrafish larve at 5, 10 and 15 days.

Total cholestrol and triglycrides measurements

	Total cholestrol (mg/dl)		Triglycerides (mg/dl)	
	Control	HCD 3-months	Control	HCD 3-months
Fang *et al.*, 2014	200	700	150	500
Yoon *et al.*, 2013	280	420	160	500
Our lab	170	NA	130	NA

Figure 7: Comparative analysis of total cholestrol and triglycride values with alrady oublished literature. Data generated in our lab is from wild type zebrafish fed normal diet.

Conclusions

- ✓ Zebrafish as a animal model provides a dynamic and live observation of lipid deposit and vascular inflammation.
- ✓ Significant increase in lipid deposits can be observed both in DA and CV after fed with high cholesterol diets.

CVgenes [at] target
Exzellenzcluster Entzündungsforschung
SEVENTH FRAMEWORK PROGRAMME

UNIVERSITÄT ZU LÜBECK
STIFTUNGSUNIVERSITÄT
SEIT 2015

INSTITUT FÜR INTEGRATIVE UND
EXPERIMENTELLE GENOMIK

Der Zebrabärbling: ein neues Forschungsmodell für Atherosklerose

Institut für Integrative und Experimentelle Genomik

Karim Tarhbalouti* & Krishan Kumar Vishnolia*, Phillip Ciba*˚, Charlie Kruse**
Zouhair Aherrahrou*, Jeanette Erdmann*,
*IIEG Universität zu Lübeck, **Frauenhofer Einrichtung für Marine Biotechnologien Lübeck

Hintergrund

Die Koronare Herzerkrankung (KHK) ist einer der führenden Todesursachen in der westlichen Welt. Hier bildet die Atherosklerose die grundlegende Gefäßveränderung, die zu dieser Erkrankung führt. Im Laufe der Zeit setzen sich dabei in den Wänden der Herzkranzgefäße Lipidablagerung ab, die sich entzünden können. Durch die Verkleinerung des Gefäßdurchmessers verringert sich die Durchblutung. Bei dem Aufbrechen des atherosklerotischen Plaques kann es zu einer völligen Verlegung des Gefäßes mit anschließendem Absterben des versorgten Herzgebietes kommen.(1)

Neben den Hauptrisikofaktoren, wie erhöhten Cholesterinwerten im Blut und Bluthochdruck, spielen auch die Gene bei vielen Patienten eine wichtige Rolle. So konnte das IIEG bisher 46 Risiko-Gene identifizieren, ein Drittel davon werden eng mit Störungen im Fettstoffwechsels in Verbindung gebracht. Die restlichen zwei Drittel jedoch sind Gene die neue Einsichten in den Entstehungsmechanismen der KHK schaffen können.

***Abb. 1**: Bild eines Adulten Zebrabärblinges und einer 5-Tage alten Larve.* Quelle: Wikimedia commons

Der Zebrabärbling

Zebrabärblinge *(Danio Rerio)* sind kleine 3 bis 4cm große Süßwasserfische aus den nördlichen Regionen des indischen Subkontinentes. Zebrabärblinge werden zunehmend für genetische Forschung in Laboren eingesetzt. Sie sind einfach handzuhaben, vermehren sich schnell in großer Zahl und sind einfach genetisch zu manipulieren. Das Herzkreislaufsystem der Zebrabärblinge ist zwar einfach gebaut, besitzt jedoch eine ähnliche Funktionsweise wie beim Menschen. Außerdem ermöglicht es die Transparenz der Embryos, in den ersten 30 Tagen der Entwicklung, Änderungen direkt unter dem Mikroskop zu beobachten. (2)(3)(4)

***Abb. 2**: Aufbau des Fütterunsgsexperiments. Fischlarven wurden unter HCD- und Kontrolldiät gesetzt. Mikroskopiert wurde am 5., 15. und 25. Tag der Fütterung.*

Das Fütterungsexperiment

Nach Befruchtung der Eier werden die Larven der Zebrabärblinge in zwei Gruppen aufgeteilt. Die erste bekommt über 25 Tage lang Fischfutter mit 4% zusätzlichem Cholesterol (HCD). Dies soll die ungesunde Ernährung eines Menschen über einen langen Zeitraum simulieren. Die zweite Gruppe dient als Vergleich und bekommt Fischfutter ohne Cholesterolzusatz. Die Larven werden anschließend nach 5, 15 und 25 Tagen Fütterung mit ORO gefärbt, um die Lipidablagerungen in Rot hervorzuheben und unter dem mikroskopiert gesetzt.

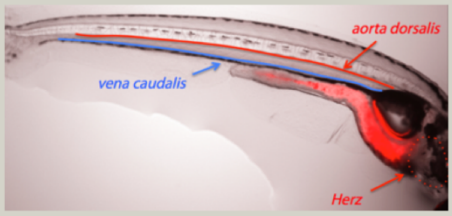

***Abb. 2**: Gefäßanatomie einer 10-Tage alten Zebrabärblingslarve unter dem Mikroskop (x40)*

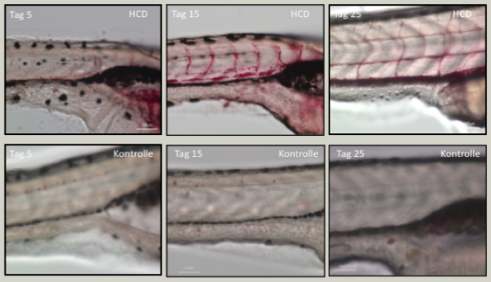

***Abb. 3**: Lipidablagerungen in den großen Gefäßen der Larven am 5., 15. und 25. der Fütterung. Die Larven wurden mit ORO gefärbt um die Ablagerungen in Rot hervorzuheben.*

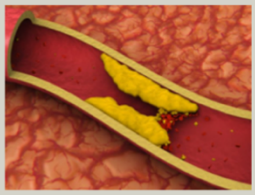

***Abb. 4** Darstellung von Atherosklerose in einem menschlichen Arterie. Gut zu erkennen sind die gestörte Durchblutung durch die Lipidablagerungen bzw. Plaques.* Quelle: eatsmarter.de

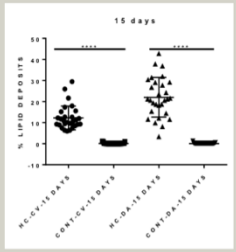

***Abb. 5**: Aufzählung der Lipidablagerungen in den großen Gefäßen der Larven am 5., 15. und 25. der Fütterung.
CV: vena caudalis ; DA: aorta dorsalis ; HC: Cholesteroldiät ; Cont: Kontroldiät*

Ergebnisse

Unter Cholesteroldiät lassen sich bei Larven unter dem Mikroskop und ORO-Färbung deutliche Lipidablagerungen in den Gefäßen erkennen. Im Vergleich zur Kontrollgruppe werden im Schnitt sogar deutlich mehr erkannt.
Ablagerungen nehmen mit der Zeit zu und sind sowohl in der der aorta dorsalis als auch in der vena caudalis zu erkennen.

Konklusion und Ausblick

Zebrabärblinge können als Modell dienen, um die Grundprinzipien der Atherosklerose besser erforschen zu können. Unter einer Fütterung mit Cholesterol lassen sich im Larvenstadium bereits Lipidablagerungen erkennen. Durch Genmanipulation lassen sich Larvenmodelle erschaffen, die in Kombination mit Cholesteroldiäten neue Erkenntnisse in der genetischen Grundlage der Atherosklerose gewonnen werden können.

Quellen
(1)Innere Medizin 2014, Gerd Herold
(2) Vascular lipid accumulation, lipoprotein oxidation, and macrophage lipid uptake in hypercholesterolemic zebrafish; Stoletov, Miller et al.; Circ Res 2009
(3) Emerging applications for zebrafish as a model organism to study oxidative mechanisms and their roles in inflammation and vascular accumulation of oxidized lipids, Longhou Fang, Yury I. Miller, Free Radical Biology and Medicine 2012
(4) Molecular Methods in developmentel Biologu Xenopus and Zebrafish; Matthew Guille; Methods in molecular biology Volume127 Humana Press

IM FOCUS DAS LEBEN

Genetic determinants regulating lipid deposits in different wild type strains of zebrafish using QTL analysis

Krishan Kumar Vishnolia[1,2], Karim Tarhbalouti[1], Phillipp Ciba[2], Charlie Kruse[2], Zouhair Aherrahrou[1] & Jeanette Erdmann[1]

(1) Institut für Integrative und Experimentelle Genomik und DZHK (Deutsches Zentrum für Herz- und Kreislaufforschung), Standort Hamburg/ Lübeck/ Kiel, Universität zu Lübeck, Lübeck.
(2) Fraunhofer-Einrichtung für Marine Biotechnologie, EMB, Lübeck.

Introduction

Zebrafish (*Danio rerio*) has been reported to express remarkable similarities with all major human nuclear receptors, lipid transporters, apolipoproteins and enzymes involved in lipoprotein metabolism. High cholesterol, high fat diet consumption and genetic mutations contribute to dyslipidemia. In contrast to mice, zebrafish show lipoprotein oxidation and dyslipidemia after feeding with high cholesterol diet even without any genetic intervention. Optical transparency of zebrafish larvae after feeding with high cholesterol diets can be used to elucidate novel mechanisms and loci's associated with dyslipidemia in different wild type strains.

Aim

We aim to investigate the genetic factors of lipid metabolism in five different wild type strains of zebrafish i.e. *AB, TL, TU, WIK, LEO* after feeding high cholesterol diets, using classical quantitative trait locus (QTL) analysis at the later stages.

Tabel 1: The five wild-type zebrafish strains used in the preliminary study.

Strain	Description
AB	AB wild type line, originated from Oregon, USA
TU	Tuebingen wild type, originated from Tuebingen, Germany
TL	Tupfel long fin wild type, originated from mating of leo^{t1} and lof^{tl2}
LEO	LEO wild type
WIK	WIK wild type

Methods

Different wild type strains of zebrafish were obtained from European zebrafish resource center (EZRC) and AB*TU line was breed in our won laboratory followed by feeding with high cholesterol (4% added cholesterol) and control diets in isolated groups. After 20 days of feeding with HCD, larvae were collected, anesthetized and whole mount stained for lipid deposits (using ORO stain). Images were captured using inverted microscope and sections of dorsal aorta and caudal vein were cut out from images for analysis of lipid deposits using MATLAB script.

Results

Phase I

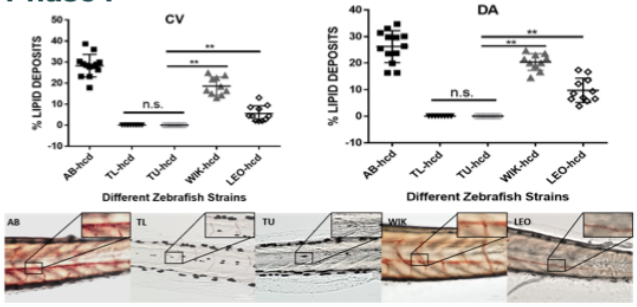

Figure 1: The top panel shows the percentage of lipid deposit in the caudal vein (in left) and dorsal aorta (in right) in all five different wild-type zebrafish strains fed HCD for 20 days (n=10 each group). The bottom panel show representative images from each strain. All images were taken at 100X magnification.

Phase II Study design

To test the hypothesis that certain genetic loci control lipid deposits in the AB (susceptible) and TU (resistant) strains, which showed differential susceptibilities to this phenotype, breeding and characterization of lipid deposits in the F1 and F2 generations needs to be performed. In addition, QTL analysis of a large number (approximately 200) of the F2 progeny will be performed as shown in the schematic below.

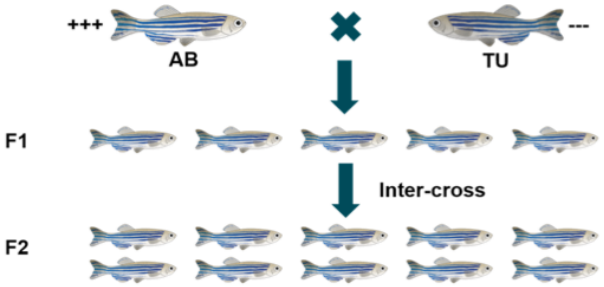

Figure 2: Schematic representation of the work flow for the QTL analysis. The positive and negative symbols indicate susceptibility and resistance to lipid deposits respectively.

Results from F1 generation

As shown in the schematic above a cross between AB (susceptible) and TU (resistant) line was performed, progeny were fed with HCD and control diets along with AB and TU. AB*TU displays intermediate lipid deposits compare to AB and TU, as shown in figure 3 below.

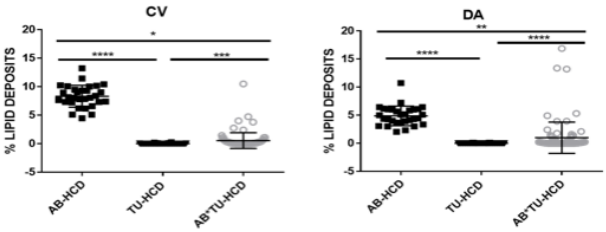

Figure 3: Graphical presentation of percetage of lipid deposits in dorsal aorta and caudual vein of F1 generation, from a cross between AB (suseptiable) and TU (resistant) zebrafish will type line (n=10).

Study plan for QTL analysis in F2 progeny

F2 generation larvae derived from inter-cross of AB*TU line will be fed with HCD and control diets as normal for 20 days. Each larvae will be analysed for both phenotypic and genotypic traits. Due to the small size of zebrafish larvae, after anesthetizing they will be decapitated under microscope in a precise manner to not disturb morphology of remaining larvae.

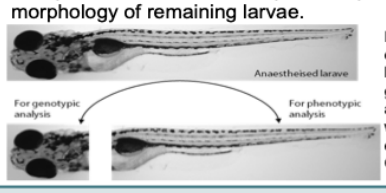

Figure 4: Schematic explaining the overall process of using same larvae for both phenotypic and genotypic analysis during the QTL analysis. Decapitated larvae head will be used for DNA or RNA extraction whereas tail region for ORO staining.

Conclusions

- ✓ Zebrafish as a animal model provides a dynamic and live observation of lipid deposit and vascular inflammation
- ✓ Significant variance in lipid deposits have been observed in different wild type strains of zebrafish after fed with HCD for 20 days
- ✓ Using QTL analysis, we will be able to identify genes or loci associated with resistant or susceptible nature for lipid deposits (early signs for atherosclerosis) in zebrafish, this will help us in developing therapeutic targets

Zebrafish, a model for Atherosclerosis

Karim Tarhbalouti[1], Krishan Vishnolia[1,2], Phillipp Ciba[2], Charli Kruse[2], Zouhair Aherrahrou[1] & Jeanette Erdmann[1]

(1) Institut für Integrative und Experimentelle Genomik und DZHK (Deutsches Zentrum für Herz- und Kreislaufforschung), Standort Hamburg/ Lübeck/ Kiel, Universität zu Lübeck, Lübeck.
(2) Fraunhofer-Einrichtung für Marine Biotechnologie, EMB, Lübeck.

INSTITUTE FOR INTEGRATIVE AND EXPERIMENTAL GENOMICS

Introduction

Cardiovascular diseases (CVD) and atherosclerosis can be studied on mice or other model organisms after post-mortem analysis. It has been reported that all major nuclear receptors, lipid transporters, apo-lipoproteins and enzymes involved in lipoprotein metabolism are expressed in zebrafish[1]. Zebrafish (*Danio rerio*) embryos and larvae remain until the age of one month transparent. The availability of effective genetic manipulation tools enables *in vivo* monitoring of vascular processes in live fish fed with high fat diet[1]. Therefore, in recent years zebrafish has been successfully used as a model organism for atherosclerosis to investigate different patho-mechanisms.

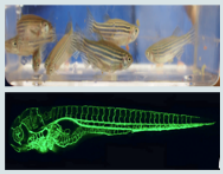

Figure 1: Images of adult zebrafish in the top pannel. In the bottom pannel whole endothelial cells from vasuculture of Tg:Fli1 zebrafish shown by green fluoroscent protein under fluoroscence micrscope. A video for blood ciculation in zebrafish can be view from the QR-code below.

Aim

We aim to discover the genetic mechanisms for atherosclerosis, using zebrafish as a model organism for novel genes/loci reported in genome-wide association study from Erdmann et al., 2013 and compare those results with mice and human[2].

Methods

Zebrafish fed with high cholesterol diet, show early signs of lipid accumulation in the dorsal aorta or caudal vein, with or without any prior genetic manipulation. Accumulation of lipid can be monitored in live transgenic zebrafish expressing fluorescent proteins and/or fed a high cholesterol and control diet supplemented with fluorescent lipid tracers. Using gene knock-out (KO)/down or transgene techniques, specific genes/loci associated with atherosclerosis can be elucidated or overexpressed in zebrafish genome in order to understand the underlying pathomechanisms.

Study design

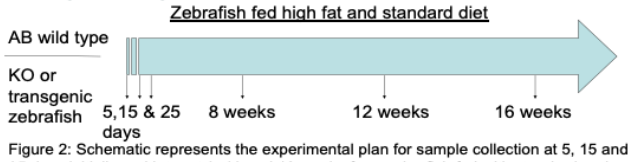

Figure 2: Schematic represents the experimental plan for sample collection at 5, 15 and 25 days initially and later at 8, 12 and 16 weeks from zebrafish fed with standard and high cholesterol diet from wild type and different genetic background.

Parameters for analysis

Different parameters are measured to confirm the extent of atherosclerosis in zebrafish at different time points such as whole mount Oil Red O (ORO) staining, fluroscence microscopy for lipid deposits, triglycerides measurements, HDL, LDL and VLDL measurements, sectioning and staining for different proteins and gene expression analysis.

Results

Oil Red O stained zebrafish larvae

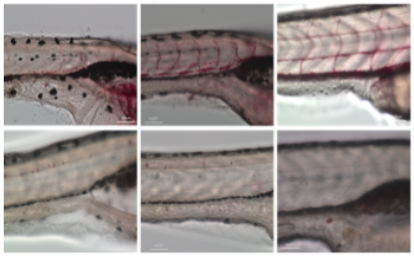

Figure 5: ORO stained bright field images of zebrafish larvae; starting from left 5 days old, in the middle 15 days old and on the right 25 days old larvae. Larvae on the top pannel of images are fed with high cholesterol diet , lower ones with control diet. Red dots represent lipid deposits in The dorsal aorta and caudual vein. Magnification 100X

Quantification of lipid deposits

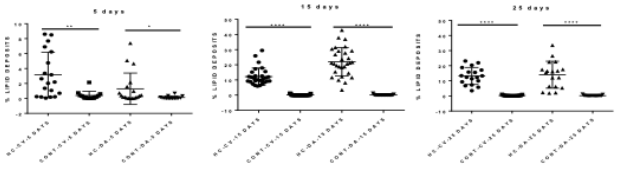

Figure 6: Graphs represent significant difference in percentage of lipid deposits in dorsal aorta (DA) and caudual vein (CV) in zebrafish larvae (n=20) fed high cholesterol (HC) and control diet (cont) for 5, 10 and 15 days.

Genetic determinants controlling lipid deposits in different wild types zebrafish strains

Different wild type strains of zebrafish were obtained from European zebrafish resource center (EZRC) and AB*TU line was bred in our own laboratory. Images were captured using an inverted microscope and analyzed for lipid deposits using MATLAB script.

Table 1: The five wild-type zebrafish strains used in the preliminary study.

Strain	Description
AB	AB wild type line, originated from Oregon, USA
TU	Tuebingen wild type, originated from Tuebingen, Germany
TL	Tupfel long fin wild type, originated from mating of leo^{t1} and lof^{dt2}
LEO	LEO wild type
WIK	WIK wild type

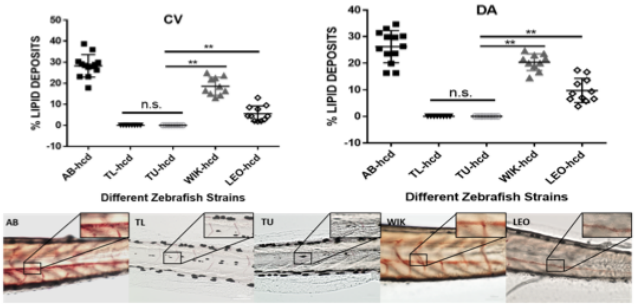

Figure 1: The top panel shows the percentage of lipid deposit in the caudal vein (in left) and dorsal aorta (in right) in all five different wild-type zebrafish strains fed HCD for 20 days (n=20). The bottom panel show representative images from each strain. All images were taken at 100X magnification.

References:
1) Fang *et al.*, Translational Research, 2014 Feb; 163 (2): pp. 99-108. **2)** Erdmann *et al.*, Nature, 2013 Dec 19; 504 (7480): pp. 432-6. **3)** O'Hare *et al.*, Journal of lipid research, 2014 Nov; 55(11): pp. 2242-53.

Conclusions

- ✓ Zebrafish as a animal model provides a dynamic and live observation of lipid deposit and vascular inflammation
- ✓ Differential levels of lipid deposits were observed in different strains of zebrafish after being fed with high cholesterol diets

DZHK DEUTSCHES ZENTRUM FÜR HERZ-KREISLAUFFORSCHUNG E.V.

CVgenes [at] target

Exzellenzcluster Entzündungsforschung

SEVENTH FRAMEWORK PROGRAMME

Abstract

Studies in zebrafish demonstrate that CNNM2 and NT5C2 are most likely the causal genes at the blood pressure-associated locus on human chromosome 10q24.32

Krishan K. Vischnolia, Celine Hoene, **Karim Tarhbalouti**, Julian Revenstorff, Zouhair Aherrahrou, Jeanette Erdmann ; *Frontiers in Cardiovascular Medicine-Hypertension*.

Accepted 30.06.2020

Background: Globally, high blood pressure (BP) is the most important risk factor for cardiovascular disease. Several genome-wide association studies (GWAS) have identified variants associated with BP traits at more than 535 chromosomal loci with genome-wide significance. The post-GWAS challenge is to annotate the most likely causal gene(s) at each locus. Chromosome 10q24.32 is a locus associated with BP that encompasses five genes: CYP17A1, BORCS7, AS3MT, CNNM2, and NT5C2 and warrants investigation to determine the specific gene or genes responsible for the phenotype.
Aim: To identify the most likely causal gene(s) associated with BP at the 10q24.32 locus using zebrafish as an animal model.
Results: We report significantly higher blood flow, increased arterial pulse, and elevated linear velocity in zebrafish larvae with cnnm2 and nt5c2 knocked down using gene specific splice modification transcriptional morpholinos, compared with controls. No differences in blood flow parameters were observed after as3mt, borcs7 or cyp17a1 knockdown. There was no effect on vessel diameter in animals with any of the four genes knocked down.
At the molecular level, expression of hypertension markers (crp and ace) was significantly increased in cnnm2 and nt5c2 knockdown larvae. Further, the results obtained by morpholino knockdown were validated using zebrafish knockout (KO) lines with cnnm2 and nt5c2 deficiency again resulting in higher blood flow, increased arterial pulse, and elevated linear velocity.
Analysis of nt5c2a KO larvae demonstrated that lack of this gene resulted in reduced expression of cnnm2a, with reciprocal downregulation of nt5c2a in cnnm2a KO larvae. Staining of whole blood smears from nt5c2 mutants revealed that KO of this gene might be associated with an acute lymphoblastic leukemia phenotype, consistent with literature reports. Additional experiments were designed based on previous literature on cnnm2a mutant zebrafish revealed impaired renal function, high levels of renin, and significantly increased expression of the ren gene, leading us to hypothesize that the observed elevated blood flow parameters may be attributable to triggering of the renin-angiotensin-aldosterone signaling pathway.
Conclusion: Our zebrafish data establish CNNM2 and NT5C2 as the most likely causal genes at the 10q24.32 BP locus, and indicate that they trigger separate downstream mechanistic pathways.

10. Acknowledgments

This thesis was written and prepared at the Institute for Cardiogenetics, formerly known as Institute for Integrative and Experimental Genomics (IIEG), of the University of Lübeck.

My sincere acknowledgments go to my thesis supervisor and institute director Prof. Jeanette Erdmann for granting me the opportunity to produce this work.

My deep appreciations go to my advisor Dr. Zouhair Aherrahrou for having diligently provided me qualified guidance and moral support all along this journey.

Special gratitude goes to Dr. Krishan Vishnolia for sharing advice and support thanks to his expertise in Zebrafish methods. His assistance has been indispensable to the realisation of this work.

Many thanks go to our collaborators Charlie Kruse and Philipp Ciba at the Fraunhofer Institute for Marine Biotechnology EMB Lübeck for having provided us zebrafish husbandry facilities and technical support.

Acknowledgments are also directed to the scholarship program “Exzellenzmedizin” of the University of Lübeck for granting the honour of sponsorship of this thesis.

Gratitude is directed to Prof. Al-Hasani. This work wouldn’t have been possible without his kind referral to this institute many years ago. I would especially also like to thank Dr. Jaafar Al-Hasani, Dr. Redouane Aherrahrou and Dr. Maria Segura for having opened me this research group’s gates, taken me under their wings in the project’s very early phases and provided me with invaluable support all along.

I would like to thank our trustworthy lab technicians for having assisted and helped me troubleshooting countless intricate details throughout this experimental work: Maren Behrensen, Sandra Wrobel, Petra Bruse, Anette Liebers and Sabine Stark.

Great appreciation is for my fellow doctorate students: Felix, Caroline, Celine, Till, Janis, Victor, Marlon, Anja, Beatrice, Elisa, Sogol. Thank you for having contributed to an encouraging, cheerful and productive atmosphere in our lab. This extends to all members of the Institute during the time I wrote my thesis there.

Finally, my most profound gratitude goes towards my parents and partner for having bestowed me with inexhaustible support and encouragements throughout my years of study and writing this thesis. Thank you.

11. Curriculum Vitae (Deutsch)

Persönliche Angaben

Name	TARHBALOUTI
Vornamen	Karim Heinz Frederic
Jahrgang	1991
Geburtsort	Guangzhou, V.R. China

Studium, Promotion und berufliche Tätigkeit

Seit 2019	Assistenzarzt an der Klinik für Allgemein-, Viszeral- und Gefäßchirurgie Schön Klinik Neustadt in Holstein
2014 – 2021	Promotion am Institut für Kardiogenetik der Universität zu Lübeck "*Expression of Human CAD-Associated Risk Genes in Blood of Hypercholesterolemic Zebrafish (Danio rerio)"* Doktormutter: Prof. Jeanette Erdmann Bewertung: 1,0 *summa cum laude* Stipendiat „*Lübecker Exzellenzmedizin*" der Universität zu Lübeck
2010 – 2017	Studium der Humanmedizin an der Universität zu Lübeck 3. Staatsexamen der Humanmedizin
2016 – 2017	Praktisches Jahr: Klinik für Orthopädie und Unfallchirurgie am UKSH Campus Lübeck Klinik für Chirurgie am Haukeland Universitetsjukehus Bergen (Norwegen) Klinik für Innere Medizin und Kardiologie am der Schön Klinik Neustadt in Holstein

Zivildienst

2009 – 2010	Diakonie-Klinikum Schwäbisch Hall

Schulbildung

2009	Baccalauréat Général Scientifique, Französisches Abitur